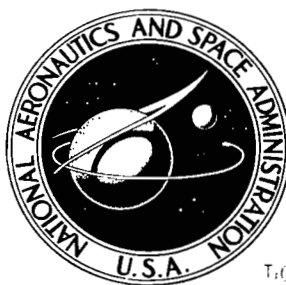


NASA TECHNICAL NOTE



NASA TN D-5781

c.1

LOAN COPY: RETURN TO  
AFAG (WFO)  
KIRKLAND AFB, TEX

0132512



TECH LIBRARY KAFB, NM

NASA TN D-5781

# FLIGHT AND SIMULATION INVESTIGATION OF METHODS FOR IMPLEMENTING NOISE-ABATEMENT LANDING APPROACHES

by  
*Hervey C. Quigley, C. Thomas Snyder, Emmett B. Fry,  
Leo J. Power, and Robert C. Innis*

*Ames Research Center*

*and*

*W. Latham Copeland  
Langley Research Center*



NATIONAL AERONAUTICS AND SPACE ADMINISTRATION • WASHINGTON, D. C. • MAY 1970



0132512

1. Report No. NASA TN D-5781		2. Government Accession No.		3. Recipient's Catalog No.	
4. Title and Subtitle FLIGHT AND SIMULATION INVESTIGATION OF METHODS FOR IMPLEMENTING NOISE-ABATEMENT LANDING APPROACHES		5. Report Date May 1970		6. Performing Organization Code	
7. Author(s) : Hervey C. Quigley, C. Thomas Snyder, Emmett B. Fry, Leo J. Power, and Robert C. Innis (ARC); and W. Latham Copeland (LRC)		8. Performing Organization Report No. A-3080		10. Work Unit No. 733-02-00-01-00-21	
9. Performing Organization Name and Address NASA Ames Research Center Moffett Field, Calif. 94035		11. Contract or Grant No.		13. Type of Report and Period Covered Technical Note	
12. Sponsoring Agency Name and Address National Aeronautics and Space Administration Washington, D. C. 20546		14. Sponsoring Agency Code			
15. Supplementary Notes					
16. Abstract  A flight and simulator investigation has been conducted to determine methods for implementing steep two-segment and decelerating landing approaches. For the research jet transport used in the study a reduction in noise of approximately 11 PNdB (9 EPNdB) at a point 1.1 nautical miles from the runway threshold was achieved with a two-segment approach with an upper segment of 6° and a lower segment of 2.65° which intercepted at an altitude of 250 feet. The two-segment profiles with an intercept of 400 feet reduced noise about 10 PNdB at a point 1.5 nautical miles and 13 PNdB (11 EPNdB) at a point 3.4 nautical miles from the threshold. Decelerating approaches on a normal approach angle (2.65°) reduced noise only moderately 3 to 4 PNdB, but combining decelerating with steeper or two-segment approaches reduced noise 11 PNdB (9 EPNdB) at a point 1.1 nautical miles from the runway threshold.  The noise abatement landing approach profiles evaluated in this program could be flown in a modified jet transport with the same precision as conventional instrument landing approaches without a significant increase in pilot workload. The pilots preferred two-segment approach profiles with an intercept altitude of 400 feet. The research airplane had improvements over current jet transports including a flight director modified for noise abatement profiles, an autothrottle, and stability augmentation that improved longitudinal and lateral directional handling qualities. The evaluation flights were flown under simulated instrument conditions in daylight and in near-ideal weather. Further research is needed to examine the requirements and operational limitations of two-segment approaches in an environment more representative of airline operations.					
17. Key Words Suggested by Author(s) Landing approach Approach noise abatement Operating procedures Noise measurements		18. Distribution Statement  Unclassified - Unlimited			
19. Security Classif. (of this report) Unclassified	20. Security Classif. (of this page) Unclassified	21. No. of Pages 125	22. Price* \$ 3.00		

\*For sale by the Clearinghouse for Federal Scientific and Technical Information  
Springfield, Virginia 22151



## TABLE OF CONTENTS

	<u>Page</u>
SYMBOLS AND ABBREVIATIONS . . . . .	v
SUMMARY . . . . .	1
INTRODUCTION . . . . .	1
EQUIPMENT . . . . .	3
Research Airplane . . . . .	3
Simulator . . . . .	6
Approach Radar System . . . . .	7
TEST PROCEDURES . . . . .	8
Profiles and Guidance . . . . .	8
Test Procedure . . . . .	9
RESULTS AND DISCUSSION . . . . .	10
Single-Segment Approach Profiles . . . . .	10
Two-Segment Approach Profiles . . . . .	12
Decelerating Approaches . . . . .	22
CONCLUSIONS . . . . .	26
APPENDIX A - GROUND NOISE MEASUREMENTS . . . . .	28
INTRODUCTION. . . . .	28
METHODS AND PROCEDURES . . . . .	28
RESULTS . . . . .	32
DISCUSSION . . . . .	34
SUMMARY OF RESULTS . . . . .	35
APPENDIX B - AIRPLANE SYSTEMS . . . . .	37
SYSTEMS TO IMPROVE GUIDANCE AND DISPLACE INFORMATION . . . . .	37
SYSTEMS TO IMPROVE FLIGHT-PATH CONTROL AND TO REDUCE PILOT WORKLOAD . . . . .	40
REFERENCES . . . . .	44
TABLES . . . . .	46
FIGURES . . . . .	61



# SYMBOLS AND ABBREVIATIONS

$A_z$	normal acceleration, ft/sec <sup>2</sup> or g
$b$	wing span, ft
$\bar{c}$	wing mean aerodynamic chord, ft
$C_D$	drag coefficient, $\frac{\text{drag force}}{q_0 S}$
$C_L$	lift coefficient, $\frac{\text{lift force}}{q_0 S}$
$C_l$	rolling-moment coefficient, $\frac{\text{rolling moment}}{q_0 S b}$
$C_m$	pitching-moment coefficient, $\frac{\text{pitching moment}}{q_0 S \bar{c}}$
$C_{m_0}$	$C_m$ at zero angle of attack
$C_n$	yawing-moment coefficient, $\frac{\text{yawing moment}}{q_0 S b}$
$C_T$	thrust coefficient, $\frac{\text{thrust force}}{q_0 S}$
$C_{T_{INBD}}$	$\frac{\text{thrust of inboard engines}}{q_0 S}$
$C_{T_{OTBD}}$	$\frac{\text{thrust of outboard engines}}{q_0 S}$
$C_y$	side-force coefficient, $\frac{\text{side force}}{q_0 S}$
$F_G$	gross thrust of all engines, lb
$h$	altitude, ft
$i_H$	horizontal stabilizer angle of incidence, rad
$N_2$	percent maximum RPM of engine
$p$	roll angular velocity, rad/sec
$q$	pitch angular velocity, rad/sec

$q_o$	dynamic pressure, lb/sq ft
$r$	yaw angular velocity, rad/sec
$R$	range from runway threshold, ft or nmi
$S$	wing reference area, ft <sup>2</sup> , or Laplace operator
$T$	thrust, lb
$V$	airspeed, ft/sec, knots
$V_{APP}$	approach speed, knots
$V_{ref}$	reference speed, knots
$V_S$	stall speed, knots
$W$	airplane weight, lb
$y$	lateral error from ILS localizer centerline, ft
$\alpha$	angle of attack, rad
$\beta$	angle of sideslip, rad
$\gamma$	flight-path angle, rad or deg
$\gamma_{GS}$	glide-slope angle, rad or deg
$\delta_a$	average aileron deflection, rad
$\delta_c$	column deflection, in.
$\delta_e$	elevator deflection, rad
$\delta_F$	flap deflection, rad or deg
$\delta_{F_{aux}}$	auxiliary flap deflection, rad or deg
$\delta_r$	rudder deflection, rad
$\Delta( )$	deviation from reference
$\eta$	$\Delta\delta_{F_{aux}} C_{T_{INBD}}$
$\epsilon$	error from glide slope of ILS
$\epsilon_{LOC}$	error from localizer of ILS
$\theta$	airplane pitch attitude, rad
$v_i$	

$\theta_c$	flight director pitch attitude command, deg
$\phi$	roll angle, deg
$\phi_c$	flight director bank angle command, deg
$\psi$	heading angle, deg
ADI	attitude director indicator
BLC	boundary-layer control
DFG	diode function generator
DLC	direct lift control
EADI	electronic attitude director indicator
EPNdB	effective perceived noise, dB
EPNL	effective perceived noise level
HSI	horizontal situation indicator
IFR	instrument flight rules
ILS	instrument landing system
PNdB	perceived noise, dB
PNL	perceived noise level
MDA	minimum decision altitude
SAS	stability augmentation system
TV	television
VFR	visual flight rules



FLIGHT AND SIMULATION INVESTIGATION OF METHODS FOR  
IMPLEMENTING NOISE-ABATEMENT LANDING APPROACHES

Hervey C. Quigley, C. Thomas Snyder,  
Emmett B. Fry, Leo J. Power,  
and Robert C. Innis

Ames Research Center

and

W. Latham Copeland

Langley Research Center

SUMMARY

A flight and simulator investigation has been conducted to determine methods for implementing steep two-segment and decelerating landing approaches. For the research jet transport used in the study a reduction in noise of approximately 11 PNdB (9EPNdB) at a point 1.1 nautical miles from the runway threshold was achieved with a two-segment approach with an upper segment of  $6^\circ$  and a lower segment of  $2.65^\circ$  which intercepted at an altitude of 250 feet. The two-segment profiles with an intercept at 400 feet reduced noise about 10 PNdB at a point 1.5 nautical miles and 13 PNdB (11 EPNdB) at a point 3.4 nautical miles from the threshold. Decelerating approaches on a normal approach angle ( $2.65^\circ$ ) reduced noise only moderately 3 to 4 PNdB, but combining decelerating with steeper or two-segment approaches reduced noise 11 PNdB (9 EPNdB) at a point 1.1 nautical miles from the runway threshold.

The noise abatement landing approach profiles evaluated in this program could be flown in a modified jet transport with the same precision as conventional instrument landing approaches without a significant increase in pilot workload. The pilots preferred two-segment approach profiles with an intercept altitude of 400 feet. The research airplane had improvements over current jet transports including a flight director modified for noise abatement profiles, an autothrottle, and stability augmentation that improved longitudinal and lateral directional handling qualities. The evaluation flights were flown under simulated instrument conditions in daylight and in near-ideal weather. Further research is needed to examine the requirements and operational limitations of two-segment approaches in an environment more representative of airline operations.

INTRODUCTION

Investigations of methods of reducing the noise of jet transport airplanes during take-off and landing have been the subject of extensive NASA

research. The recent progress of NASA research efforts in various fields of noise alleviation of large subsonic jet transports is summarized in reference 1. For noise abatement in the landing approach, much of the effort has been concentrated on the use of modified landing approach profiles and techniques. Reference 2 has shown that the use of increased approach angles is a feasible operational method for decreasing the noise on landing. With a steep approach the noise is reduced in two ways. First, a steep approach permits a reduction in engine thrust, and second, a steep approach places the airplane at a higher altitude above the ground at a given distance from the runway. Measurements of noise of jet transports (ref. 3) have shown that the combination of reduced thrust and higher altitude can result in a significant reduction in noise. Reference 4 pointed out some of the problems of the steep approach that must be solved before it could be considered operationally acceptable.

Decelerating landing approaches are another means of reducing noise. A decelerating approach starts at high speed, the engine thrust is reduced to a low value, and the airplane decelerates to the landing speed at a point near the runway. The decelerating technique can be combined with normal, steep, or various two-segment profiles. The noise reduction will depend on the amount of engine thrust reduction used during the decelerating period.

A combined flight and simulator investigation was conducted to determine what would be required in a jet transport to enable pilots to fly steep or decelerating noise abatement landing approaches with the precision common to normal instrument landing approaches without a significant increase in pilot workload. This investigation was limited to the study of the basic problems of noise abatement approaches and, therefore, did not include the effects on pilot opinion of airplane or guidance system failures or adverse weather conditions. Airplane systems were studied that would provide the pilot with improved guidance, adequate flight path control, and a reduced workload. The systems and profiles were developed and initially evaluated on the simulator before being evaluated in flight. The flight investigation was conducted in a four-engine jet transport under simulated instrument conditions. The results of the pilot's evaluation of the profiles and the airplane systems to alleviate the problems of flying noise abatement approaches are reported herein. The measured reduction in noise with the various noise abatement approach profiles is discussed in appendix A. A detailed discussion of the development of the systems used on the airplane is presented in reference 5 and further discussed in appendix B.

A summary of the investigation has been prepared as an NASA Technical Film. The 23-minute, 16-mm sound film entitled "Landing Noise Reduction, A Study in Abatement of Noise From Multi-Engined Aircraft Through Modification of Approach Path," Film No. AT-137, is available for loan from the Film Library, Ames Research Center, Moffett Field, California, 94035.

## EQUIPMENT

### Research Airplane

The Boeing 367-80 (707/KC-135 prototype) four-engine turbo fan jet engine airplane, shown in figure 1, was used in the investigation. The airplane control system, described in reference 5, was the fly-by-wire type, and pilot controller inputs were processed by on-board analog computers. The airplane was flown as an in-flight simulator for initial studies of single segment steep approaches, as described in reference 6. For two-segment and deceleration approaches, the airplane was configured for variable control systems, which are described in reference 5.

The following paragraphs describe briefly, with simplified block diagrams, the aircraft systems that were essential to the program.

Basic longitudinal control system- The evaluation pilot flew from the right seat, as shown in figure 2. Mechanical characteristics of the evaluation pilot's control column are shown in the force/displacement plot of figure 3. The fly-by-wire control system elements consisted of an electrical signal from a column-mounted position transducer, analog computers to process the signals, and electrohydraulic servoactuators to position the elevators. For the basic airplane control system, column inputs were geared directly to the elevator servos as shown in the block diagram of figure 4. Direct lift control (DLC) could be interconnected through the column, as shown in figure 4. Proportional elevator deflection was provided to compensate for pitching moments due to deflection of the auxiliary flaps.

An automatic trim system (fig. 4) realigned the stabilizer with the elevator whenever a set threshold value was exceeded. Although essentially an open-loop servosystem, it performed as a zero-force trimmer with the pilot acting as a follow-up.

Rate-command/attitude-hold system- In this system, aircraft pitching rate was commanded as a function of column deflection. With zero-column deflection, zero pitch rate and a constant attitude were commanded, resulting in an attitude-hold feature. Thus, the airplane pitch attitude was stabilized against all external disturbances, such as atmospheric turbulence or airplane configuration changes, and responded only to the pilot's inputs. The system is further described in reference 5, and a simplified block diagram is shown in figure 5. Bank angle compensation was incorporated to command the airplane pitch rate that accompanies bank angle in a steady turn. The "downspring" loop provided a force gradient to the control system of 0.6 pound per knot below reference speed. The  $\Delta V$  dead zone was included, with no force change from 0 to 1.7 knots below reference speed.

Flap system- The boundary-layer control (BLC) flaps, previously installed on the airplane (ref. 7), were modified to provide a controllable aft flap (auxiliary flap) for direct lift control (DLC). See figure 6. Design details of the flaps are discussed in reference 8, and the aerodynamic characteristics are presented in references 9 and 10.

The auxiliary flaps operated at a deflection rate of  $29^\circ/\text{sec}$ , which is comparable to that of other primary flight control surfaces. The neutral position of the auxiliary flap was  $10^\circ$  down relative to the main flap. This position permitted auxiliary flap deflections of  $\pm 20^\circ$  from neutral for DLC, which gave a response of approximately  $\pm 0.1$  g normal acceleration at landing approach speeds.

The modified BLC flap permitted a wide range of landing approach speeds. With a trim setting of  $40^\circ$  for the main flaps and  $10^\circ$  additional deflection for the auxiliary flaps ( $40^\circ/10^\circ$ ), a landing approach speed range of 110 to 122 knots was possible with the engine thrust levels used for the noise abatement approaches. These speeds corresponded to about  $1.25 V_S$  for the low engine thrust required for the steep approach segment, and  $1.35 V_S$  at power required for the normal approach angle. A  $30^\circ/10^\circ$  flap setting was used for approach speeds between 130 and 145 knots, which gave a stall margin greater than  $1.3 V_S$ .

Direct lift control- Direct lift control (DLC) was provided by the deflection of the auxiliary flaps (fig. 6). The block diagrams of the DLC system as used with the basic control system and the rate command control system are shown in figures 4 and 5, respectively. The diagrams show that there were two methods by which the pilots could control DLC. The primary method was by deflecting the auxiliary flaps in proportion to control column input; the gearing and other characteristics are presented in reference 5. The other method was by deflecting the flaps in proportion to the deflection of the thumb controller, which was the same as a trim switch. It was mounted on the right side of the evaluation pilot's control wheel.

Lateral-directional stability augmentation system- Airplane lateral-directional handling qualities were improved by augmentation which is described in reference 5. The lateral-directional augmentation system provided turn coordination, reduced dihedral effect, increased  $\beta$  damping, increased roll damping, and increased spiral stability.

Autothrottle system- A simplified block diagram of the autothrottle system is shown in figure 7. Airplane pitch attitude was used to provide lead information to the system. All four throttle levers were mechanically servo driven, and the pilot had the option of manual override. The system automatically maintained a preselected reference speed except during deceleration approaches when the reference approach speed was programmed to change as a function of commanded auxiliary flap position.

Electronic attitude director indicator (EADI)- The EADI is an advanced cathode-ray tube type of attitude director display. The philosophy behind the design and development of the EADI is discussed in reference 11. Figure 8 is a photograph of the cockpit installation, and figure 9 is a sketch of the instrument face with the symbols identified. The display had exposed dimensions of 5.4 by 7.2 inches, and could accommodate a maximum of 11 items of symbolic information. The symbols were superimposed over a video scene from a closed-circuit television camera. The TV camera installation under the nose of the airplane is shown in figure 10.

Information displayed on the EADI (fig. 9), but not normally found on conventional attitude director indicators, included the following:

1. Digital radio altitude
2. Flight-path angle
3. Potential flight-path angle (longitudinal acceleration scaled to indicate the steady-state flight-path angle which would result if speed and engine thrust were held constant)
4. Error from the ILS beam, displayed by a unique method
5. Television picture of the real world

The television camera had a zoom lens set at a focal length of approximately 21 mm. This gave a horizontal field of view of about  $37^\circ$ , and a 0.7 magnification of the real world perspective when the pilot's head was in normal position. The central portion of the vertical video field was suppressed above the horizon to give the symbols additional uncluttered space above the horizon. The camera was aimed  $3.5^\circ$  down from the aircraft waterline reference.

The video picture and many of the symbols could be switched on or off to permit evaluation of various combinations. An additional feature of the display was the ability to choose black, white, or shades of gray for the color of the command bars, speed error, flight-path angle, and potential flight-path angle.

The large size of the instrument permitted a pitch attitude scaling of  $4.8^\circ/\text{in.}$ , whereas the scaling was about  $30^\circ/\text{in.}$  for the electromechanical unit which was used for comparison. The rectangular symbol representing error from the ILS beam was scaled so that  $\pm 0.35^\circ$  vertical error put the reference airplane wings on the upper or lower bar, and  $\pm 0.33^\circ$  lateral error put the center of the fixed airplane symbol on the right or left bar of the rectangle.

Electromechanical attitude director indicator (ADI)- An electromechanical ADI was used for the initial phase of the program, and was mounted in the central position of the evaluation pilot's instrument panel, as shown in figure 11(a). When the electronic attitude director indicator (EADI) was installed, the electromechanical ADI was mounted at the lower left corner of the EADI, as shown in figure 8. Figure 11(b) is a sketch of the ADI with the features identified. The instrument was driven by the same signals as the EADI, but with different scaling.

Flight director computations- Flight director pitch commands were computed by the airborne analog computers to provide guidance for the various noise abatement landing approach profiles.

Simplified block diagrams of the pitch flight director are shown in figures 12(a) and 12(b). The flight director computations and logic provided

guidance to capture and track steep single beam and two-segment approaches with the precision of normal approaches. The pitch command bar sensitivity was  $1^\circ$  of corrective pitch attitude change for each 15 feet of altitude error from the beam.

For lateral guidance, a commercially available flight director computer, designed for category I weather minimum operation, was used. Figure 13 is a block diagram of the system. The unit permitted localizer capture angles up to  $45^\circ$  in the heading mode, and would automatically switch to the tracking mode when the beam error was within  $\pm 2^\circ$ .

### Simulator

Cockpit- The external shape of the simulator cab (fig. 14) was originally designed to represent a supersonic transport. The cockpit, however, was configured to represent the controls and instrumentation of the evaluation pilot's station in the Boeing 367-80 airplane (fig. 15).

The column, wheel, and rudder pedals were powered by hydraulic control loaders, giving the control force and deflection characteristics shown in figure 3. Throttle levers for inboard and outboard engine control (not shown in fig. 15) were installed on the left side of the cockpit because the evaluation pilot was seated on the right in the airplane. The throttle location necessitated that the longitudinal and lateral trim button be located on the right side of the control wheel. The DLC thumb controller was also located on the right side of the wheel.

The cockpit instruments, shown in figure 15, were similar to the primary flight and navigation instruments of the airplane and included the EADI. Several items on the instrument panel were used only for the simulation, and included landing gear touchdown lights and a flare warning light.

Motion system- Hydraulic servoactuators move the simulator  $\pm 9^\circ$  in roll,  $+14^\circ$  to  $-6^\circ$  in pitch, and  $\pm 1.0$  foot in vertical translation. The motion commands were washed-out toward zero position to prevent the cab from striking the limit stops when the displacement signals exceeded the motion capability. The motion equipment included a pneumatic seat which provided a subtle cue of vertical acceleration.

Simulator motions were particularly useful in subjecting the pilot to moderate turbulence and touchdown landing reactions.

Visual system- The visual system, described in detail in reference 6, was a color television projection system which provided six-degrees-of-motion freedom. The scene was a daylight view of a typical runway with provision for an in-the-clouds scene and breakout to visual flight at an altitude of 100 feet. The field of view was  $38^\circ$  vertically by  $46^\circ$  horizontally, and gave unity magnification. For this program the scale of the visual scene model was 1:600, which resulted in runway dimensions of 8050 feet long by 150 feet wide.

Sound generator- A sound generator simulated jet engine and aerodynamic noise, but no attempt was made to reproduce the actual noise level of the airplane cockpit.

Computations- The basic six-degrees-of-freedom airplane equations of motion used in the simulation are given in reference 12. Dimensionless aerodynamic derivatives for the Boeing 367-80 airplane are given for 115 and 135 knot speeds and airplane physical characteristics are given in table 1. Airplane weight was set at a midrange value of 150,000 lb. The equations for the special systems used in this study are given in table 2.

Continuous computations were made of perceived noise level (PNdB) on the ground directly under the airplane. The curves for the variation of noise with thrust and altitude shown in figure 16 were derived from noise measurements of a similar fan-jet equipped aircraft.

The thrust response characteristics of each fan-jet engine to throttle steps was programmed to give the time response curves shown in figure 17. These curves were prepared from measured response of a similar fan-jet engine. Maximum thrust of each engine was 14,000 lb without BLC, and 11,200 lb with BLC.

Inboard engine thrust impingement effects on the auxiliary flaps were computed and the derivatives are included in table 1. The simplified block diagrams of the various airplane systems in figures 4, 5, 7, 12, and 13 apply for the simulation except as noted on the diagrams. In figure 5, for example, the bank angle compensation loop was not required for the simulation.

### Approach Radar System

Flight-path guidance for the 367-80 airplane was provided by a radar landing approach system. The system was programmed specifically for this investigation, and used in conjunction with the Instrument Landing System (ILS) at the Oakland International Airport. Figure 18 is a photograph of the installation. The system was programmed to simulate the beam of the ILS, but had the additional capability of generating nonstandard linear and nonlinear approach paths. The system, shown schematically in figure 19, used the precise tracking radar to determine elevation and azimuth angles and slant range of the aircraft, and this information was processed by an analog computer to determine the aircraft position in space coordinates. The computed aircraft position was compared with a programmed flight path to determine vertical and lateral linear displacement errors, and these signals were converted and then multiplied by a sensitivity factor (a function of range) to convert to angular ILS glide-slope and localizer errors. The error signals were encoded as 90 and 150 Hz modulations on separate carrier wavelengths, which were distinct from the Oakland ILS, and transmitted to the aircraft's ILS receiver. They were received as conventional ILS error signals in the airplane.

A variety of approach paths could be generated, and the ones used during this program are described in detail in the Profiles and Guidance section.

Two-segment, two-beam profiles were formed by combining a steep approach path from the approach radar system with the normal Oakland  $2.65^\circ$  glide slope. The airplane carried two ILS receivers to monitor both approach radar and Oakland frequencies, and switching logic to permit automatic changeover from one source to the other. The single beam curved profiles were wholly generated by the approach radar system.

Two audio-tones, 2200 and 3000 Hz, were carried on the approach radar localizer frequency. The lower frequency was used to transmit timing pulses to the airplane for time correlation of airborne oscillograph data. The higher tone was used to trigger at a specific range the switching logic of the airborne flight director computer to identify the start of the nonlinear portion of the curved profile.

Another important function of the approach radar facility was to record the altitude-range profile of each aircraft approach.

As indicated above, the Oakland ILS was used for the lower beam of the two-beam profiles. The ILS was also used for lateral (localizer) guidance.

## TESTS AND PROCEDURES

### Profiles and Guidance

All the noise abatement approach profiles which were evaluated on both the simulator and in flight are listed in table 3. They can best be described by category: single-segment, two-segment, and deceleration approaches.

Single-segment approaches- Figure 20 illustrates the five different single-segment approaches that were evaluated. The  $2.65^\circ$  beam intersected the runway 1230 feet from the threshold, and the higher angle beams intersected the ground 500 feet from the threshold.

Guidance for the higher angle beams was the same as for the standard  $2.65^\circ$  beam. A beam error of  $\pm 0.7^\circ$  gave maximum deflection of the glide-slope pointer on the electromechanical ADI.

Two-segment approaches- Two variations of two-segment approach profile geometry were investigated. As shown in figure 21, the  $6^\circ$  high beam was made to intersect a  $2.65^\circ$  low beam at either 250 or 400 feet altitude.

In addition to the variations of intercept altitude, two types of guidance systems were evaluated: (1) one consisted of two separate ILS glide-slope beams; and (2) one consisting of a glide-slope beam with a curvilinear transition. Figure 22 shows details of the two-beam guidance system for both intercept altitudes. The approach radar system formed the high beam, and the Oakland ILS served as the low beam. Virtually, the transmitter for the high beam was located underground to keep the angular error sensitivity the same as for the low beam at the intersection altitude.



Details of the guidance for the single-beam system with curvilinear transition are shown in figure 23. This beam was generated by the approach radar system which computed straight-line segments for the high and low beams which were joined by a parabolic curve. The equations and tangent points for the curve are shown on figure 23(b). For the simulation, the transition was a circular arc with radius of 40,200 feet and tangent points at 124 feet above and 62 feet below the intercept altitude of 400 and 250 feet. Curvature of the beam was selected to give a rate change of flight-path angle of about  $0.29^\circ/\text{sec}$  at 115 knots approach speed.

Deceleration approaches- Three decelerating approach profiles were used in the flight investigation. Two of these combined the two-segment and the decelerating approaches, and the third used a single-segment  $4^\circ$  approach.

Figure 24 shows the three profiles. Profiles M and N included a  $5^\circ$  upper segment and  $2.65^\circ$  lower segment. Intercept altitudes of the upper segment with the lower segments were 500 feet and 800 feet for M and N, respectively. Deceleration was initiated at 670 feet for M, 970 feet for N, and 1400 feet for L. Deceleration continued until touchdown for M, but ended at 300-feet altitude for N and L. Nominal flap rates and deceleration rates were  $0.37^\circ/\text{sec}$  and  $0.59 \text{ knot/sec}$  for profiles M and N, and  $0.31^\circ/\text{sec}$  and  $0.49 \text{ knot/sec}$  for profile L.

Configuration K, listed on table 3 and also shown in figure 24, is a decelerating approach on a normal  $2.65^\circ$  approach angle and was evaluated only on the simulator.

#### Test Procedure

The various landing approach profiles selected for noise abatement and the systems incorporated into the airplane to alleviate the problem areas of these approaches were evaluated by the pilots both on the simulator and in flight. The simulator was used in three ways: (1) to develop the required airplane systems and evaluate them prior to flight; (2) to study the noise reduction potential of various profiles; and (3) to familiarize the participating pilots with the instrumentation, displays, airplane configurations, and approach profiles before flight. The primary objective of the evaluation was to determine the airplane systems (guidance, control system, etc.) that would enable the pilot to fly the approaches with the precision similar to that required for category II weather minimum (ref. 13) without an increase in pilot workload. Table 5 lists desired precision in this investigation. The profiles evaluated are listed in table 3, and the airplane configuration in table 4.

The evaluation was of a research nature; the pilots were asked not to consider operational conditions such as equipment failure, adverse weather, night operations, or traffic control in their evaluation. This is not to imply they did not consider the operational problem important, but the purpose of this investigation was to study requirements for guidance, flight-path control, and low pilot workload on noise abatement approaches. Additional

tests will be necessary to investigate all of the operational problems associated with noise abatement approaches.

Three NASA pilots participated in the evaluation of the single-segment approaches. Eleven pilots, one commercial airline, four NASA, and six FAA, participated in the evaluation of the two-segment and decelerating approaches. Two of the NASA pilots were project pilots and flew about 50 approaches each while the other pilots flew about 20 approaches each. The comments and opinions of the pilots were obtained from their evaluation both on the simulator and in flight; no attempt was made to separate the comments and opinions in this report unless they seemed pertinent.

Three types of noise abatement profiles were studied in this investigation: (1) single-segment profiles with approach angles between  $2.65^\circ$  and  $6^\circ$ , (2) two-segment profiles with a steep upper approach angle of  $6^\circ$  and a lower approach angle of  $2.65^\circ$ , (3) decelerating approaches on several types of profiles. The noise reduction potential, problems, methods for alleviating the problems, and pilot evaluation of each type of noise abatement approach are discussed separately in the following sections.

## RESULTS AND DISCUSSION

### Single-Segment Approach Profiles

Noise reduction potential- The noise reduction that can be achieved with a change in landing approach profile or technique will depend mainly on: (1) the amount of thrust reduction possible during the approach and (2) the increase in height above the ground at any point. The engine thrust required on an approach depends on the aerodynamic characteristics of the airplane and the approach angle. The following simplified equation shows the relationship:

$$T = W[(C_D/C_L) + \gamma]$$

where  $\gamma$  is the flight-path angle (negative for descent). The thrust can, therefore, be reduced by either steepening the approach angle or reducing drag (i.e.,  $C_D$ ). It is difficult to achieve a significant reduction in drag without a change in airspeed (i.e.,  $C_L$ ), but steepening the approach angle will both decrease thrust and increase height above the ground. The variation of thrust, altitude, and the computed reduction in noise for the test airplane as the approach angle is steepened is shown in figure 25 for an approach speed of 115 knots at a point 2 nautical miles from the runway threshold. The noise in a standard  $2.65^\circ$  approach was used for comparison of the noise reduction. These calculations show that noise reduction of about 18 PNdB is possible when the approach angle is steepened to  $6^\circ$ . An approach angle of  $6^\circ$  is near the maximum that can be considered for most current jet transports at minimum approach speeds when allowances are considered for overshoot of  $1.5^\circ$  to  $2^\circ$  from the  $6^\circ$  approach.

Problem areas- In the initial phase of the program, the problem of high rate of descent with steep approaches was the primary problem studied on the ground-based simulator and in flight. The variation in rate of descent with approach angle for three approach speeds is shown in figure 26. Current jet transport landing approach speeds are between 115 and 150 knots, and the rates of descent on normal  $2.5^\circ$  to  $3^\circ$  instrument approaches are between 500 and 800 ft/min. The data points show the approach angles investigated. From the results of the pilots' evaluation of these steep approaches, it was determined that rates of descent greater than 900 to 1000 ft/min were unsatisfactory because of the problem of accurately judging the progress of the flare. With this rate of descent as a boundary, the approach angle at an approach speed of 150 knots can only be steepened about  $1^\circ$  (from  $2.65^\circ$  to  $3.5^\circ$ ) with a resulting reduction in noise of only 5 PNdB. Of course, as approach speed is reduced, the approach angle goes up for a rate of descent that is below the boundary. A  $6^\circ$  approach would take, as shown in figure 26, an approach speed of 90 knots. Approach speeds as low as 90 knots would likely require powered lift which would necessitate some increase in thrust above that shown in figure 25 with consequent higher noise.

Pilots' evaluation- The initial phase of the investigation concentrated on the evaluations of steep single-segment approaches to examine the problem of high rate of descent near the ground. Approach angles of  $2.65^\circ$ ,  $4.5^\circ$ ,  $5^\circ$ ,  $5.5^\circ$ , and  $6.0^\circ$  (see fig. 20 and table 3) were flown on both the simulator and in the test airplane at 115 knots. The procedure used was to have the pilot intercept the ILS at between 2000 and 2500 feet altitude under simulated instrument conditions (a hood was used in flight) and go visual (remove hood) at between 100 and 200 feet altitude. Only three NASA pilots participated in this phase of the investigation.

The pilots first made a series of approaches on the standard  $2.65^\circ$  ILS at the Oakland International Airport for a basis of comparison of the later steep approaches. Normal  $2.65^\circ$  instrument approaches could be flown comfortably at 115 knots with the required precision and at a satisfactory workload level. Although the flight director and the autothrottle reduced the workload and made the approach easier to fly, they were not considered essential for a satisfactory normal approach.

Steepening the approach angle to  $4.5^\circ$  increased the rate of descent from 540 to 910 ft/min. The increased rate of descent was readily apparent to the pilot as was the difference in the pilot's view of the runway when the hood was removed at 200 feet. One of the problems was found to be associated with the position of the intersection of  $4.5^\circ$  glide-slope beam of the ILS with the runway. At first the intersection point was the same as for the  $2.65^\circ$  (1230 ft from threshold) but with this intercept point the pilot could not readily see the runway threshold when the hood was removed at 200 feet altitude. The intercept point was then moved to 500 feet from the threshold which greatly aided the pilot in judging the flare and touchdown point. Also, moving the intersection to 500 feet made the touchdown point on the runway about the same as for a normal landing because a greater distance was required for the flare on a  $4.5^\circ$  approach angle. The altitude for the initiation of the flare was usually less than 50 feet for a  $2.65^\circ$  approach, but was between 75 and 100 feet for  $4.5^\circ$ .

The need to reduce the workload became more apparent to the pilot with steeper approach paths. The management of thrust is more critical as is the monitoring of the approach to determine the airplane position relative to the ground near minimum decision altitude (MDA). Also, the lateral alignment of the airplane with the runway at MDA is more critical. When the hood-off altitude was less than 200 feet, the pilot did not have time to make large lateral corrections and then perform a flare and touchdown. A good lateral flight director was found to be required to restrict the localizer and heading errors to acceptable limits with the minimum of pilot effort.

The next step was to increase the approach angle first to  $5^\circ$  and then to  $6^\circ$  which increased the rate of descent to 1200 ft/min. It was immediately evident to the pilot that this rate of descent would be unacceptably high unless the hood-off altitude was raised above 200 feet. It was usual, on the  $5^\circ$  to  $6^\circ$  approaches, for the pilot first to reduce the rate of descent to less than 500 ft/min and then perform a more normal flare and touchdown. On these landings there tended to be two distinct flares. After accomplishing several steep approaches, the pilots were able to bring the two flares together, but the task became more critical. Figure 27 presents time histories of two  $6^\circ$  landings illustrating the two flare techniques used.

The use of DLC to quicken the vertical response of the airplane for flight-path control was examined to determine if better response would assist the pilots on steep approaches. On  $4.5^\circ$  approaches where the rate of descent is about 900 ft/min, DLC increased the pilot's sense of security because he could reduce the rate of descent more quickly and with less change in pitch attitude. Rates of descent over 1000 ft/min ( $5^\circ$  to  $6^\circ$  approach angles) were excessive and the quickening provided by the DLC, although very much appreciated by the pilot, did little to make the rates of descent more acceptable.

### Two-Segment Approach Profiles

Noise reduction potential- Two-segment landing approach profiles were introduced in earlier tests (refs. 2 and 4) to reduce the high rate of descent near the ground. Figure 28(a) is a multiple exposure photograph of a typical two-segment approach at the Oakland International Airport. Figure 28(b) illustrates a typical two-segment profile and shows the computed reduction in noise. The noise reduction for a straight  $6^\circ$  approach is also shown for comparison. The two-segment approaches considered in this program had an upper segment approach angle of  $6^\circ$  and a lower segment approach angle of  $2.65^\circ$ . With a two-segment approach, the advantages of the steep approach (i.e., reduced thrust and increased height above the ground) are achieved on the upper segment while the rate of descent at the flare or minimum decision altitude (MDA) is unchanged from a normal approach. The noise reduction is, of course, not so great as for a straight  $6^\circ$  approach because the airplane is not so high above the ground on the  $6^\circ$  segment (see fig. 28(b)). Also, at the intercept point, engine thrust must be brought up to the value for a normal approach, and since altitude is the same, no reduction in noise is possible beyond this point. The noise reduction of a two-segment approach is determined, therefore, by the altitude of the intercept. When the intercept

altitude is low, the noise reduction is high, but the high rate of descent must be continued closer to the ground. The altitude for the intercept was, therefore, one of the variables in the program.

The two-segment approach profiles are shown in figure 28(c) along with the corresponding computed noise reductions. The intercept altitudes are 250 and 400 feet. The 250-foot intercept altitude was chosen to give a computed noise reduction of about 10 PNdB 1 nautical mile from the runway threshold and beyond. The second profile with the intercept at 400 feet was chosen to give about 10 PNdB noise reduction 1.5 nautical miles from the threshold and beyond. These two intercept altitudes also provided the pilots with an opportunity to evaluate a low and a moderately high intercept altitude on two-segment approaches.

The computed noise reductions presented in figure 28(c) were verified by measurements of noise during two of the evaluation flights of the airplane. The methods and results of the measurements are presented in appendix A. The data show good correlation between computed and measured noise reduction for the two-segment approach. The noise data in appendix A are also presented in terms of the effective perceived noise level (EPNL) which is being recommended by reference 14 as the noise measurement criterion.

Problem areas- The use of two-segment approaches to help solve the problem of high rate of descent near the ground created new problems because of the nonlinearity in the glide path toward the end of the approach. The results of previous tests (ref. 4) and the initial phase of the flight and simulation investigation of the present program identified the following problems of two-segment approaches when flown with a standard jet transport:

1. Inadequate guidance and display information
2. High pilot workload
3. Lack of precise control in flight path
4. Poor engine response

All of these problems are interrelated. Figure 29(a) shows a typical path of the airplane as measured by radar (solid line) when the pilot is flying a two-segment approach (dotted line) using instrumentation common to current jet transports. Primarily because of inadequate guidance, the flight path at transition goes below the glide slope of the ILS. The correction of the resulting deviation is a demanding flight-path control task that greatly increases the pilot's workload. This is illustrated by time histories in figure 29(b) of the control activity, pitch attitude, and errors from the ILS glide slope during the transition portion of the approach. (The range and time can be used to correlate figures 29(a) and 29(b).) The pilot is busy keeping the airspeed error as low as possible by the control of thrust as the flight-path angle changes and controlling height error with airplane pitch attitude changes. Since this difficult control problem and the large increase in workload occurs only seconds before the flare, the pilots rated the task unacceptable.

Another problem that concerns the pilot in two-segment or any steep approaches is the engine response time. Jet engines traditionally respond slowly to throttle command, particularly at low thrust. Figure 17 shows the engine response characteristics used in the simulator. They approximate those of the JT3D-1 engines used on the airplane. The data from figure 17 have been cross-plotted on figure 30 to show the time from approach power to maximum thrust. It can be seen from these data that a  $6.0^\circ$  approach almost doubles the time to maximum thrust, 6.2 seconds compared to 3.6 for a normal  $2.65^\circ$  approach. The lag in thrust with the application of the throttle requires the pilot to lead with the throttle; otherwise airspeed will decrease during the transition. Since there is insufficient lead information for the pilot, the pilot gets behind and requires a large application of thrust. This can be seen by the throttle position time history of figure 29(b). Such large thrust changes, approaching maximum thrust, actually increase the noise level of a two-segment approach.

From a review of their problems, it is obvious that two-segment approaches must be flown with precise guidance to smooth the transition from the steep upper segment to the lower segment so that low rate changes in flight-path angle and thrust are assured. As attempts were made to solve each problem discussed in the preceding section, it was recognized that there may be several ways of alleviating them. The simulator and flight studies in this program used the variable stability and on-board computer capabilities of the test airplane. The methods used to provide adequate guidance and situation information, to assure adequate flight-path control, to reduce pilot workload, and to eliminate the requirement for rapid engine response are discussed in the sections following.

Methods to provide adequate guidance and display information- A guidance system was required for an instrument landing task. Provisions had to be made, therefore, for the necessary ground-based guidance systems for two-segment profiles. The basic guidance considered was an adaptation of current instrument landing systems (ILS). Since the glide slope of present ILS is set at an angle of  $2.5^\circ$  to  $3^\circ$ , changes had to be made to the ILS. Two systems were considered as described in an earlier section and illustrated in figures 22 and 23. One system (fig. 22) involved the establishment of a second glide slope of  $6^\circ$  at an airport presently equipped with a  $2.65^\circ$  glide slope. The other system (fig. 23) was a single beam with curved transition ILS. This type of system would require either a radar and computer on the ground to generate such an ILS, or some form of on-board computer based on precision distance measuring equipment. The two-beam ILS would apparently be easier to implement without extensive development. For this investigation, a research radar system, described in the Equipment section and illustrated on figures 18 and 19, was used that could readily be changed to any desired profile.

The primary guidance information for the pilot was provided by a flight director. Most current flight directors used in airline and military operations present to the pilot the command attitude changes which are computed as a function of the angular errors from the ILS. The pitch flight director computations for current systems are designed for only linear low-angle

instrument landing approaches. The computations must, therefore, be modified for the nonlinear, steep, two-segment approaches which consist of either two separate ILS beams (fig. 22) or a curved beam (fig. 23). The modified flight director computations are described in the Equipment section and block diagrams of the system are shown on figure 12. The output of the flight director computer is displayed on an attitude director indicator (ADI) in the cockpit. Two types of ADI were used - an electromechanical system (fig. 11(b)) and an electronic ADI (fig. 9). The flight director is discussed further in appendix B.

The situation information required by the pilot to determine airplane position during a two-segment approach is somewhat different and more critical than that for a normal approach. Pilots normally determine their position on a standard Category II flight director ILS approach from the altitude, the ILS error indications, the roll and pitch attitude, and marker beacon annunciators. This information is the minimum needed for instrument approaches. To study the advantages that might be gained by including other situation information, an electronic ADI was used that could present situation information along with the flight director on a cathode-ray tube mounted in the cockpit. This display, EADI, is described in the Equipment section and, as illustrated in figures 8 and 9, included some additional information not normally available to assist the pilot in flying the approach. (1) The radio altitude was presented digitally at altitudes below 700 feet. (2) The flight-path angle of the airplane was indicated by a symbol which enabled the pilot to monitor the progress of the approach from the upper-segment capture through the transition to the lower segment. (3) The potential flight-path angle was indicated by another symbol that showed the potential steady-state flight path if the thrust were maintained; that is, the longitudinal acceleration calibrated in terms of potential flight-path angle. This symbol assisted the pilot in monitoring the thrust changes in two-segment approaches. (4) Another addition on the EADI display was a television picture from a camera on the nose of the airplane (fig. 10). For these tests, the television display was used for evaluating the benefits of a real-world type of display to assist the pilot in determining the progress of the approach. The television display was considered a simulation of a real-world pictorial display that could possibly be developed in the foreseeable future. The television picture enabled the pilot to relate the flight-director guidance to a real-world runway picture. The television was also evaluated as an aid for the pilot in the transition from instrument flight condition (hood-on) to visual flying (hood-off).

Methods to assure adequate flight-path control- When the pilot is provided with adequate guidance, a precise instrument approach can be flown only if the airplane has adequate flight-path control capability. Flight-path control involves two responses of the airplane to a control-column input. First, pitch response must be such that precise changes in pitch attitude can be made without excessive overshoots in either pitch rate or control inputs. Second, the vertical response of the airplane to longitudinal control must provide precise control of rate changes of flight-path angle. Several longitudinal handling-qualities criteria include both of the required responses. Reference 15 is an example of such a criterion. To study methods of improving

the pitch and vertical response of transport airplanes, the Boeing 367-80 was provided with a longitudinal-stability augmentation system and direct-lift control.

The pitch stability augmentation system, SAS, chosen for this investigation was a pitch-rate command with attitude hold control system. This system is described in detail in reference 5 and discussed in the Equipment section (fig. 5). This particular control system was chosen not only to assure that the test airplane had satisfactory pitch response but to study the application of such a system for future jet transport airplanes.

An important feature of the SAS is the automatic trim capability inherent in such a system. Since pitch rate will be held to zero as long as the pilot does not move the control column, any trim change due to thrust, flap extension, ground effect, or change in airspeed will be compensated. The lack of speed stability (trim change with speed) and the lack of trim change in ground effect required some change in piloting technique in the flare and touchdown task.

A direct lift control (DLC) system was also included to assure adequate vertical response. The DLC system used in this investigation is discussed in the Equipment section and is illustrated in figures 4 and 5. Direct lift control provides a means of changing the lift, and therefore, the vertical acceleration of the airplane, without changing angle of attack. DLC systems have been successfully tested on both fighter (ref. 16) and transport (ref. 17) airplanes, and the tests have demonstrated that quickened vertical response with DLC can improve the pilot's control of the flight path.

Methods of reducing pilot workload- The pilot's workload in any instrument approach is high not because of the difficulty of the various tasks but because of their number. For example, the pilot must control the position of the airplane center of gravity in two axes while keeping the airplane attitudes (roll, pitch, and yaw) within acceptable limits. He must also control airspeed to within  $\pm 5$  knots, monitor the condition of the airplane systems, avoid other airplanes, and listen for instructions from air traffic control. Introducing any complication or addition to these tasks, such as steep or nonlinear noise abatement landing approach profiles, makes the workload totally unacceptable.

To enable him, therefore, to cope with the added concerns of the noise abatement approaches, his workload was reduced in three ways: First, he was provided with guidance and displays that were easy to use; second, satisfactory handling qualities were provided; third, automatic devices were added for performing some of the tasks.

The control of engine thrust is one task that can be turned over to an automatic device. Ordinarily, the task requires much pilot attention, particularly on a two-segment approach where a large ( $6^\circ$ ) change in flight-path angle is made initially and another change ( $3.35^\circ$ ) to the lower segment is made late in the approach. Whenever the flight-path angle is changed, the engine thrust must be changed to keep the airspeed from changing. An



autothrottle relieves the pilot of continually adjusting engine thrust. However, he must still monitor the airspeed to assure himself that it is within acceptable limits but the airspeed error symbol on the EADI (fig. 9) facilitates this task.

The mechanization of the autothrottle is discussed in the Equipment section and is illustrated in figure 7. The system was not necessarily the best system for two-segment approaches but did prove satisfactory for the tests.

Another task that can be performed by an automatic device to reduce pilot workload is trimming the airplane for moments due to thrust changes, configuration changes, or speed changes. On the two-segment approaches, particularly with an autothrottle, the trim change with engine thrust can greatly increase the pilot workload. The attitude hold feature of the rate command control system provided the required automatic trim because the airplane attitude will not change except at the pilot's command. Attitude hold also reduces the pilot's workload in gusty conditions by keeping the airplane attitude from being disturbed by the gusts.

Autotrim was also provided with the basic control system (SAS off) to reduce the pilot workload. The autotrim is described in the Equipment section and is illustrated on figure 4. The trim changes were not eliminated by the autotrim as in the attitude hold system. When an out-of-trim moment occurred, the pilot initially made a control input to compensate for the trim change, and then the control input would be slowly reduced to zero. The pilot was relieved of the task of manipulating the trim switch to eliminate the control forces due to out-of-trim moments. The autotrim was slower, however, than the manual trim.

Lateral-directional stability augmentation- Although the primary task in this investigation was to fly a precise flight path in the vertical plane, the control of the airplane laterally could not be ignored. In fact, poor lateral-directional handling qualities can make the pilot workload on the approach unacceptably high. The lateral-directional characteristics were, therefore, augmented to give very good lateral-directional handling qualities. The augmentation, described in reference 5, consisted of sideslip-rate directional damping, increased roll damping, reduced dihedral effect, and roll-rate turn coordination. With the augmentation the pilot workload associated with lateral-directional control was much less than on most current jet transports.

Methods to eliminate the requirement for rapid engine response- Rapid thrust response to the application of the throttle is a desirable characteristic in any landing approach. But, the response characteristics of an engine cannot be readily changed. However, the early simulator results showed that when the airplane was flown precisely during the transition on the two-segment approaches, rapid-thrust changes were not required. Adequate guidance, good flight-path-control capability, and an autothrottle that helped solve other problems of two-segment approaches, also reduced the requirement for rapid engine response. On the two-segment approach, power is brought up slowly as the airplane flight-path angle changes from  $6^\circ$  to  $2.65^\circ$ , and the airplane has

normal approach power soon after transition. The two-segment approaches eliminated the problem of low thrust near the ground on steep approaches where a wave-off or go-around might be required.

Evaluation conditions- Various flight conditions were evaluated to determine the combination of profile, guidance, and airplane systems that would best fulfill the objectives of the program. Table 3 lists the noise abatement profiles and table 4 tabulates the airplane configurations and equipment used with each profile. In general, the evaluation involved two different intercept altitudes, two different guidance schemes, and two different landing approach speed ranges. Each approach was flown with either the basic control system with autotrim or with the pitch rate command-attitude hold control system and with and without DLC and autothrottle. The displays used were either an electromechanical ADI or the electronic ADI (EADI) with the television either on or off.

Guidance schemes- The two guidance schemes for two-segment approaches consisted of (1) two ILS glide-slope beams, figure 22, and (2) a single bent ILS glide-slope beam with a curvilinear transition, figure 23. These two types of guidance gave the pilot an opportunity to evaluate two methods for making the transition from the upper  $6^\circ$  segment to the lower  $2.65^\circ$ . The primary differences from the pilot's point of view were pitch rates and control required in the transition, and the situation information to determine error from the glide slope during transition. A comparison of the time histories of typical two-segment approaches with curvilinear and two-beam transition is shown in figure 31. The difference in control is quite evident from these data for the curvilinear transition, the pitch attitude changes slowly, whereas, for the two-beam transition it changes quicker. The more rapid pitch attitude change causes a faster thrust increase (see fig. 31), shifting the point at which the noise reduction goes to zero (fig. 28(c)) by about 0.1 nautical mile.

Figure 32 presents statistical data on 125 two-segment approach transitions. These bar graphs show the pitch rate of the airplane and the maximum errors from the ILS glide slope during the two-beam and curved transitions; the data for a few standard approaches are also shown for comparison. The ILS error for the two-beam guidance is the maximum error after intercept of the low segment or the maximum error after ILS intercept altitude. These errors for the most part are, therefore, undershoots of the lower beam. In figure 33(a) typical tracks of the airplane as measured by radar are compared to the ILS glide slope of a two-beam profile. Figures 33(b) and 33(c) present time histories showing glide-slope and localizer errors for both types of guidance. The tracking of the linear portion of either segment of the approach was little different from that of a normal ILS approach. With a flight director that gave good guidance for the capture of the upper segment from level flight and the transition to the lower segment, the pilot had little difficulty tracking the ILS glide slope to the precision of a normal approach. Figure 32 shows that over 80 percent of the approaches with two-beam guidance had angular errors from the ILS of less than  $\pm 0.15^\circ$  at transition which corresponds to an altitude error of about 20 feet at the 400-foot intercept altitude and 15 feet at the 250-foot intercept. These errors compare favorably

with those in a normal approach at altitudes between 200 and 300 feet. The transitions with the single curvilinear beam had a higher percentage of errors over  $\pm 0.15^\circ$ . Curved transitions required a little more pilot attention to keep the flight director bar centered and achieve minimum error. The pilot preferred to fly these transitions, therefore, without tightening the control, thus a small percentage of the approaches had greater errors than the two-beam transitions. Less than 10 percent of all the transitions had errors greater than desired by the criteria of table 5. Figure 34 shows the lateral and vertical error at an altitude of 200 feet for most of the evaluation approaches flown. At this altitude transition is complete and the airplane is usually fairly well stabilized. The errors from the ILS for most of the approaches were within a window of  $\pm 12$  feet vertically and  $\pm 100$  feet laterally. The lateral flight director computations were not to category II standards and the lateral errors are, therefore, higher than desired; a better lateral flight director would be required for low weather minimum.

The pilots stated that either type of guidance for the transition gave acceptable tracking performance for the approach, but their opinions were mixed on which type lessened the workload most. The NASA pilots preferred the two-beam transitions because they could be accomplished in a shorter period of time (see fig. 31) than curved transitions. Also, they felt that displaying the ILS glide-slope error of the lower segment rectangle on EADI (fig. 9) gave them situation information which was not available on the curved transition. Other pilots, however, preferred the curved transitions which seemed less abrupt because they required lower overall pitch rates. These pilots felt that the curved transitions required about the same workload or situation information as a standard approach. The peak pitch rates were low (see fig. 32) with over 90 percent of the transitions less than  $2^\circ/\text{sec}$ . The peak pitch rates were only slightly higher than experienced during normal approaches.

Intercept altitude- Two different intercept altitudes were evaluated with the two types of guidance discussed in the preceding section. The four profiles are illustrated on figures 22 and 23; the intercept altitude is defined as the point where the ILS glide slope of the  $6^\circ$  segment crosses the  $2.65^\circ$  lower segment (extended tangents for single beam with curved transition); the two intercept points were 250 and 400 feet. The precision of tracking the glide slope and the pilot's workload to control the airplane were about the same for either intercept altitude. It cannot be said, however, that the pilots total workload was the same. At the lower intercept altitude the pilot is more concerned about the high rate of descent and about anticipating the flare.

The pilots were quite conscious of the time to ground impact on the steep upper segment and the time from transition to minimum decision altitude (MDA) on the lower segment. Figures 35(a) and 35(b) present the variation, with altitude, of computed time to ground impact with two-segment curvilinear transition approaches with intercept altitudes of 250 and 400 feet at 115 and 135 knots. Figure 35(a), the time for the 115-knot approach, shows that at the start of transition (370 ft) the airplane is 18 seconds from ground impact on a 250-foot intercept profile, whereas on the 400-foot profile the time is increased to 25 seconds (510 ft). Figure 35(b) shows that increased approach

speed reduces these times to 15 and 21 seconds, respectively. Most of the pilots felt that the lower 250-foot intercept would be marginal if problems developed during transition. Another important time that can be determined from figure 35 is the time available to the pilot after transition for assessing the progress of the approach and becoming stabilized before an MDA of 100 feet altitude. At 115 knots approach speed the pilot had only 11 seconds for the 250-foot intercept profile, whereas for the 400-foot profile he had 28 seconds from the completion of the transition to an MDA. Here again, the pilots felt the time on the linear portion of the lower segment for the 250-foot intercept was low but the 400-foot intercept gave sufficient time to become stabilized. The minimum time required, however, would have to be determined from operational evaluation which was beyond the scope of this investigation.

The pilots concluded that their ability to fly the two-segment approach with either type of guidance was the same for the two intercept altitudes. But, the 250-foot intercept brought the high rate of descent of the 6° upper segment too close to the ground and gave a marginal amount of time between the end of transition and MDA.

Landing approach speed- The two-segment approach profiles were evaluated at two nominal speeds, 115 and 135 knots. In flight the airspeed depended on gross weight; an airspeed range from 112 to 122 was used with a main flap setting of 40°, and airspeeds from 144 to 135 knots were used with a main flap setting of 30°. These two ranges gave the pilots an opportunity to evaluate the effects of a reduced speed on two-segment approaches. The pilots found that airspeed had little effect on their precision or workload in flying the approaches. The lower airspeed did give slightly more time for transition, as well as an increase in the time between the completion of transition and MDA (see fig. 35). The increase in times at the lower speed was appreciated by the pilots on the 250-foot intercept, but the difference in time was hardly noticeable at the higher intercept altitude of 400 feet.

As shown on figure 26, the rate of descent is reduced by a reduction in approach speed. The rate of descent on the 6° upper segment was reduced from 1530 ft/min at the highest approach speed (144 knots) to 1180 ft/min at the lowest approach speed (112 knots). The pilots appreciated any reduction in rate of descent on the upper segment, particularly with the lower intercept profile.

System requirements- The pilots were asked to evaluate the importance of the various systems incorporated to alleviate the problems in flying two-segment landing approaches in the Boeing 367-80 airplane. The following list showing the relative importance of each system is based on a summary of pilot opinion. In addition to the following, the airplane had satisfactory handling qualities and was equipped with instrumentation required for normal category II landing weather minimums (ref. 13).

#### Essential

1. Guidance system for two-segment profile
2. Flight director modified for two-segment profile

3. Autothrottle
4. Autotrim

#### Desirable

1. Electronic attitude director indicator
2. Rate command-attitude hold control system
3. Direct lift control

The pilot needed the items listed as essential in order to fly two-segment landing approach profiles with the same precision as normal approaches without a significant increase in his workload. The guidance system included the necessary ground-based equipment to generate a two-segment instrument landing system as well as the equipment in the airplane to receive and display the guidance information. The modified flight director system provided computations and logic compatible with the guidance system and included good lateral guidance. The situation information, particularly radio altitude and errors from the guidance system, was readily available to the pilot and easily used with the flight director. In order to maintain a low pilot workload, an autothrottle was required to maintain nearly constant airspeed. Autotrim also was necessary to reduce workload because the airplane trim changed appreciably with thrust changes.

Although the items listed as desirable contributed some improvement and made the approaches more comfortable to fly, the majority of the pilots did not consider them essential. The advanced cathode-ray tube display of the general type used in this program, EADI, was recognized by the pilots as having the potential of achieving some of the much needed improvements in pilot cockpit display for landing approach. The digital readout of radio altitude and the indication of flight-path angle on the EADI provided information that some of the pilots felt might be essential for two-segment approaches in an adverse operational environment.

Because the pitch response of the test airplane without the rate command control system was considered satisfactory, the two-segment approaches could be flown with or without the SAS without significant change in performance or pilot workload. It should be pointed out, however, that good pitch response is essential and improvements in pitch response characteristics with SAS systems, such as a rate-command system, will probably be required for some current and future jet transports for satisfactory flight-path control in two-segment approaches.

The direct-lift control did not significantly improve the flight-path control during the approach above MDA for a well-executed two-segment approach, because the vertical response of the airplane without DLC was satisfactory. The benefits of the quickened vertical response were appreciated, however, by the pilot in the flare and touchdown task. The quickened vertical response with DLC also gave the pilot the capability of rapidly reducing rate of descent in an emergency or during wave-off from steep approaches.

Additional research is required to define handling qualities improvements possible with DLC in other tasks and with other airplane configurations.

### Decelerating Approaches

Noise reduction potential- Another means of reducing the ground-level noise is to allow the aircraft to decelerate during the landing approach. During deceleration thrust levels are lower than normal and less noise is emitted. Therefore, studies were included to investigate the noise-reduction potential, and the problems and methods of solution associated with decelerating approaches. The methods considered in this study were dictated by the capability and limitations of the Boeing 367-80 airplane.

It was determined early in the simulator program that the noise reduction obtainable from deceleration on a normal  $2.65^\circ$  approach path was only 3 to 4 PNdB. In order to realize a sizable reduction in noise, it was decided to combine the deceleration with steepened approach angles. A number of decelerating approach profiles were investigated on the analog simulator which provided a computation of the ground-level noise. The three profiles chosen for complete evaluation are listed on table 3 and illustrated in figure 24. The noise reduction for the three profiles as determined from representative approaches on the simulator and measured in flight are shown in figure 36. The noise from a normal constant-speed  $2.65^\circ$  approach was used as a reference. The two-segment ( $5^\circ$  to  $2.65^\circ$ ) profile with deceleration to the runway, profile M, and the  $4^\circ$  deceleration approach, profile L, reduced the peak noise level at ranges less than 1 mile from the runway. Measurements of the noise reduction obtained with the various decelerating approach profiles are included in appendix A.

Guidelines for decelerating approaches- The general guidelines used for implementing decelerating approaches are listed below. Since the Boeing 367-80 airplane in the fly-by-wire mode as used in these tests has a maximum safe airspeed of only 160 knots and a minimum approach speed of between 118 and 125 knots (dependent on gross weight), the airspeed range for deceleration was limited to about 35 knots. This airspeed range is recognized to be somewhat shorter than would be considered for operation, but the range is considered to be sufficiently long for studying the problems associated with decelerating approaches.

1. Flight director guidance must insure a level of ILS tracking precision equal to that for standard instrument approaches. This may be difficult to achieve with the varying flight conditions of the decelerating approach because variations in trim angle of attack can "confuse" conventional flight director computations.
2. The pilot workload should be no greater than for a normal instrument approach without automatic devices.
3. A sufficient airspeed margin above the stall must be maintained at all times during the deceleration period.

4. Thrust level should be high enough that reducing thrust nearly to idle can steepen the flight path by at least  $1\text{-}1/2^\circ$  as a general maneuvering requirement. Also, thrust level should be high enough to insure adequate thrust response in the event of a wave-off or emergency.

5. The deceleration level must be low enough to avoid passenger and crew discomfort from kinesthetic effects.

6. Implementation should be accomplished with a minimum of system complexity.

Methods used to implement decelerating approaches- In addition to the improvements incorporated into the airplane for the segmented approaches (e.g., autothrottle, improved guidance, stability augmentation), other changes had to be made for the decelerating approach task.

Initial calculations indicated the feasibility of using the auxiliary flaps (fig. 6), which were controllable by the on-board computer, to maintain the stall margin during the decelerating phase. Thus a nearly constant angle of attack and a constant reference attitude were provided during the 155 to 120 knot deceleration without having to modify the flight director computations. The variation of the lift-to-drag ratio (with auxiliary flap deflection and speed changes) was small. With the exception of initiating and halting deceleration, little additional demand was placed on the autothrottle.

Selection of deceleration level- For maximum noise reduction, the deceleration levels were as high as considered practical to keep engine thrust low, but sufficient thrust was maintained for maneuvering and engine response time considerations. Because the engine-response transport lag becomes large at near-idle thrust (as shown in fig. 17), combinations of deceleration level and flight-path angle requiring extremely low thrust levels were avoided. The variation of transport lag with thrust setting has been plotted in figure 37 from data shown on figure 17. Also shown is a boundary corresponding to the minimum thrust level that would provide a  $1\text{-}1/2^\circ$  steepened flight path when thrust was reduced to idle. This shows that satisfying the maneuvering thrust margin criterion also avoids the region of very poor engine response.

The selection of 0.59 knot/sec deceleration for the segmented approaches was based on these thrust level considerations as shown in figure 37 by the band identifying the thrust-level operating range for profiles A and B. Simulator runs with this same deceleration level on the  $4^\circ$  approach (profile C) reduced thrust levels 10 to 15 percent, occasionally approaching idle. The deceleration was decreased, therefore, to 0.49 knot/sec for this approach angle, providing a satisfactory operating level of thrust for profile C. At the end of the deceleration, 300 feet altitude, the thrust level was increased.

Method for determining flap schedule- The simulator was used to determine the flap schedule. This required establishing the appropriate flap position variation with time for the chosen deceleration level. In order to

approximate the form of this schedule, a run was "flown" on the simulator in which thrust was reduced to produce the desired deceleration, pitch attitude was held constant by the SAS, and the auxiliary flap position was varied to maintain the desired flight-path angle. Upon completion of this run, it was apparent that the recorded auxiliary flap position varied almost linearly with time, and the deceleration remained relatively constant. This finding made it possible to use a simple constant-rate flap drive during the deceleration. A sketch for the system programming is shown in figure 38.

Because accurate on-board range information was lacking, deceleration was triggered at a preset radio altitude. The trigger altitude was computed from the speed schedule and the point deceleration was to end. The deceleration ended when the flap reached a preset deflection which stopped the changing  $V_{ref}$ . One of the objectives of this study was to evaluate the acceptability of decelerating to touchdown, as compared to stopping deceleration at approximately 300 feet. When deceleration was programmed to continue until near touchdown, the pilot would simply override the autothrottle to avoid an increase in thrust when the end-of-deceleration point was reached just prior to touchdown.

Effect on pilot task- The piloting task for the decelerating approaches was essentially the same as for the constant-speed approaches. Deceleration was initiated automatically (see fig. 38) and was called out to the pilot by a test engineer when the flaps started down. Thrust was reduced automatically by the autothrottle (see fig. 7); for the two-segment approaches, initiation of deceleration and transition to the lower segment were matched so as to require little autothrottle activity.

From the cockpit, the deceleration was difficult to discern. It was not apparent from the kinesthetic cues; there was no noticeable effect on pitch attitude; and the airspeed error indication (on the EADI) remained near zero. The engines were quieter than usual, however, and of course, the instrument indications of airspeed, vertical velocity, and auxiliary flap position reflected the changing flight condition.

Figures 39(a) and 39(b) show recorded time histories of two of the first decelerating approaches flown in the program. The first of these is a  $4^\circ$  approach (profile C) with airspeed reducing from 151 to about 121 knots between 1350 and 320 feet altitude. Note that pitch attitude is essentially unchanged by the changing airplane configuration and flight condition. Glide-slope tracking throughout the run is good, with angular displacements from the beam within category II limits. A minimum amount of pilot effort is shown by the control column trace, with no greater effort nor change in technique on the decelerating portion of the approach. Demands on the autothrottle were low, and when final speed was reached, power increased automatically allowing about 1 knot of overshoot. Figure 39(b) shows a time history of a segmented decelerating approach (profile M) with the deceleration occurring from 650 feet altitude to 400 feet. At this point the flaps stopped but the pilot allowed the speed to continue to decrease during the flare; touchdown occurred at about 112 knots. Control column activity was again low with pitch attitude relatively constant except during transition from the upper segment



to the lower segment. Tracking precision on the ILS during the deceleration was little different from the constant speed approaches.

Pilots evaluation of decelerating approaches- It was the general feeling of the evaluating pilots that the tracking task presented by the decelerating approach in these tests was no more difficult than flying a normal approach, but they expressed reluctance to accept a "sliding reference scale" and flap angle change late in the approach, for they felt these required additional monitoring. In extrapolating to an operational environment, pilots also expressed some concern over the low power setting at altitudes less than 200 feet in adverse atmospheric conditions.

With a precise deceleration schedule and adequate engine response for wave-off, the pilots did not consider it difficult to continue the deceleration to touchdown, although the deceleration schedule might have to be adjusted for the prevailing wind.

With the aid of the speed-error bar on the integrated flight display (EADI) indicating errors from the airspeed schedule, decelerating approaches were also flown without the assistance of the autothrottle. The pilot workload was slightly greater, but not significantly greater than for a constant speed manual-throttle approach.

System requirements- Because the tasks presented by the decelerating approach and the constant speed approaches are similar, the same devices are essential and desirable to both types of approaches. The following additional items are essential to the decelerating approach to guarantee no degradation in tracking precision nor increase in pilot workload from that of conventional landing approaches.

1. Programmed flap and airspeed schedule
2. Accurate radio altitude or range equipment for flap/speed program logic.
3. Display for indicating errors from flap/airspeed schedule.
4. Flight director compensation for angle-of-attack variability, if flap speed schedule utilizes a varying angle of attack.

Although the conditions of this research did not show wind compensation to be an essential element, it certainly appears to be desirable. It becomes increasingly important to the deceleration schedule (1) as wind conditions become stronger, of course; (2) as the deceleration time interval is increased; and (3) as the deceleration is programmed to continue nearer to touchdown. The use of precision distance measurement equipment, in place of time, to schedule airspeed would be one way of compensating for wind.

## CONCLUSIONS

The following conclusions can be drawn from the flight and simulator investigation of the problems associated with flying single-segment, two-segment, and decelerating landing approaches for jet transport noise abatement. The methods of alleviating the problems were initially studied and evaluated on the simulator. The evaluation flights were flown in a modified jet transport airplane under simulated instrument conditions in daylight and in nearly ideal weather.

1. Increasing the single-segment approach angle from  $2.65^\circ$  to  $6^\circ$  reduced noise about 5 PNdB per degree increase in approach angle at a point 2 nautical miles from the runway threshold. The increase in the rate of descent that is associated with an increase in approach angle limited the angle that the evaluating NASA pilots considered acceptable. The pilots considered rates of descent greater than 900 ft/min unacceptable for normal operation at altitudes below 200 feet. At landing approach speeds of 115 knots, an approach angle of  $4.5^\circ$  was considered acceptable in an airplane with satisfactory handling qualities and adequate guidance.

2. Two-segment noise abatement approaches minimized the problem of high rates of descent near the ground while providing significant noise reduction. The reduction in noise with the two-segment approach profile with an upper segment of  $6^\circ$  which intercepts a lower segment of  $2.65^\circ$  at 250 feet, was approximately 11 PNdB (9 EPNdB) at a point 1.1 nautical miles from the runway threshold. Two-segment approaches with a 400-foot intercept gave no noise reduction at 1 mile, but at least a 10 PNdB reduction could be expected 1.5 nautical miles from the threshold and beyond. The noise reduction with either intercept altitude was 13 PNdB (11 EPNdB) or greater at a point 3.4 miles from the threshold.

3. The two-segment profiles could be flown in a modified jet transport (Boeing 367-80) with the same precision as a conventional instrument approach without a significant increase in pilot's workload. The essential additions to the airplane beyond those required for normal category II instrument approaches were: (1) a flight director system compatible with the two-segment guidance system; and (2) an autothrottle and automatic trim capability to reduce pilot workload. Advanced cockpit displays, improved flight control systems, and direct-lift control were desirable but not essential additions to the airplane.

4. On two-segment approaches with an intercept altitude of 250 feet, the pilots considered the time between the completion of transition and minimum decision altitude too short for coping with any adverse condition. An intercept altitude of 400 feet was considered acceptable when flown in the environmental conditions encountered during the flights.

5. Deceleration approaches gave relatively small reductions in noise level (3 to 4 PNdB) on a standard  $2.65^\circ$  approach. But when deceleration was combined with two-segment approach paths with  $5^\circ$  upper segment which

intercepted a normal approach angle at 500 feet altitude, or a steepened approach angle of 4°, noise reductions as high as 11 PNdB or 9 EPNdB were measured 1.1 nautical miles from the runway threshold.

6. Decelerating approaches were flown with no reduction in tracking precision nor observable increase in pilot workload over that experienced in the two-segment approaches. Deceleration was accomplished by utilizing a programmed rate change of airspeed and flap position schedule. The pilots were reluctant to accept a "sliding reference scale" and changing flap position during the final phases of the landing approach.

7. The flight evaluation of noise abatement approaches was made under ideal weather conditions in a research jet transport and with a safety pilot in command of the airplane. A complete evaluation of noise abatement approaches under adverse operational conditions was not made. Further tests will be needed to examine the requirements and operational limitations of noise abatement landing approaches in an environment more representative of airline operations and under conditions of combined adverse weather and airplane equipment or guidance failures.

Ames Research Center  
National Aeronautics and Space Administration  
Moffett Field, Calif., 94035, Dec. 24, 1969



## APPENDIX A

### GROUND NOISE MEASUREMENTS

#### INTRODUCTION

In order to determine the noise reductions possible with noise abatement approach profiles, noise was measured for some of the flight profiles used during the investigation. However, experiments have shown that a simple measurement of the intensity or loudness of a sound may not always be an accurate indication of its offensiveness to the public (ref. 18).

In recent years a number of parameters have been proposed that attempt to estimate the subjective offensiveness to the public of certain noises, including airplane flyover noise. For anyone unfamiliar with the subject of acoustics, a brief description of some of the more widely used of these parameters is presented.

Flyover noise data are then presented in terms of all the parameters described. Averaged noise reductions achieved by the various noise abatement approaches are then given in terms of tone corrected perceived noise level and integrated effective perceived noise level.

#### METHODS AND PROCEDURES

##### Noise Measurement Stations

Acoustic noise data were obtained at three noise measurement stations along the ground track under the approach path. The stations (designated 1, 2, and 3) were located along the ground track centerline at approximately 6,520, 20,770, and 30,770 feet (respectively) from the runway threshold. Figure 40 is a chart of the vicinity of Oakland Airport showing the locations of the stations.

As can be seen from the chart, the number of possible satisfactory sites was restricted by the topography of the area. Although a small amount of background noise was present at station 2 and some radio interference was encountered at station 3 making these sites less than ideal, the sound pressure level of these interfering signals was low relative to the aircraft flyover noise being measured and could be ignored. Station 1, situated on a boat in the San Leandro channel, was almost completely free of background noise or radio interference.

## Meteorological Considerations

Since the object of our investigation was to determine the relative noisiness of the various approaches, no attempt was made to gather meteorological data. However, in order to minimize the meteorological effects, all noise data for an airspeed of approximately 115 knots were taken on one day and all noise data for an airspeed of approximately 135 knots and for the decelerating approaches were taken on the other.

## Airplane Characteristics

The test airplane used for this investigation is a Boeing model 367-80 (707 prototype) with four Pratt and Whitney model JT3D-1 prototype turbofan jet engines. The maximum gross weight of this airplane is 175,000 pounds. However, because of the high drag associated with its experimental flap system, the thrust required for trimmed flight was higher than one would normally expect for a similar airplane of the same weight, and the noise levels were correspondingly higher. All approaches were made with landing gear extended.

## Test Procedures

Noise measurements were made during 20 approaches. The various approach profiles used and the relative positions of the noise measurement stations are shown in table 6 along with a description of the approach profiles and airspeed, weight, and flap configuration data.

## Noise Measurement Methods

Each noise measurement station was equipped with three microphones and a multichannel tape recorder. The microphones were located about 5 feet above the ground and were shielded from the wind. The entire sound measuring system was calibrated in the field before and after the flight measurements. The outputs of the microphones were recorded on separate channels of the tape recorder which were played back later resulting in data in the form of time histories of overall sound pressure level, OASPL.

## Data Reduction Methods

"It has been found that, for sound having about equal meaning to a group of people, the intensity, bandwidth, spectral content, and duration of the sounds determine in a systematic and consistent way, the subjectively judged unwantedness of a sound" (ref. 18). The judged perceived noise level of a given sound is a measure, in decibels, of the subjectively judged unwantedness of the given sound based on an experimentally developed scale.

The judged perceived noise level of a given sound, as would be determined by subjective tests, can be estimated approximately by physical

measurements, or by calculations performed on data obtained by a spectral analysis of the sound (refs. 18 and 19).

A one-third octave band frequency analysis of the data was performed resulting in instantaneous values of sound pressure level  $SPL(i)$ ,  $i = 1, \dots, 24$  for each of the 24, one-third octave frequency bands from 50 to 10,000 Hz at intervals of one-half second. These data then were the basis for the various computational schemes used to calculate the various estimates of judged perceived noise level which have been suggested to approximate the subjectively judged unwantedness of a sound (refs. 18 and 19).

Some of the most commonly used estimates (not in order of importance) with a brief description are listed below (ref. 19).

Symbols	Units	Description
$SPL(i)$	dB	Sound-pressure level - the sound pressure level at a given instant of time that occurs in the $i$ th one-third octave frequency band
$OASPL(k)$	dB	Overall sound pressure level - the sound pressure level that occurs at the $k$ th increment of time over all of the 24 one-third octave frequency bands from 50 to 10,000 Hz
$dB(c)$	dB	An approximation to the judged perceived noise level of a sound determined by weighting sound frequencies by a "C" network (sound level meter - ref. 20)
$PNL(k)$	PNdB	Perceived noise level at the $k$ th increment of time calculated from the 24 instantaneous values of $SPL(i)$
$PNLT(k)$	PNdB	tone corrected perceived noise level - the value of $PNL$ adjusted for the presence of discrete frequencies that occur at the $k$ th increment of time
$MAX$ $dB(c)$	dB	The maximum value of $dB(c)$ that occurs during the airplane flyover
$PNLP$	PNdB	Peak perceived noise level - the perceived noise level computed from the highest level reached in each of the one-third octave frequency bands irrespective of time
$PNLM$	PNdB	Maximum perceived noise level - the maximum value of $PNL(k)$ that occurs during the airplane flyover
$PNLTM$	PNdB	Maximum tone corrected perceived noise level - the maximum value of $PNLT(k)$ that occurs during the airplane flyover
$EPNL$	EPNdB	Effective perceived noise level - the perceived noise level adjusted for both the presence of discrete frequencies and the time history

Symbols	Units	Description
(i)	---	Frequency band index - the numerical indicator denoting any one of the 24 one-third octave frequency bands from 50 to 10,000 Hz
(k)	---	Time increment index - the numerical index denoting the number of equal time increments that have elapsed from a reference zero

The overall sound pressure level as a function of time is obtained directly from the tape recording of the flyover. It is a measure of the overall intensity of the sound. It has been found, however, that the subjectively judged unwantedness of a sound depends not only on its intensity but also on its spectral content, bandwidth, and duration (ref. 18).

One of the simplest methods of estimating the judged perceived noise level of a sound which attempts to account for the spectral content involves the use of a frequency weighting network in conjunction with a sound level meter. Several such networks have been developed (ref. 20). Data for dB(c) shall be presented here because it is representative of what one would read with a sound level meter, and, since the frequency response of the "C" network is relatively flat in the frequency range from 50 to 10,000 Hz, it can be considered as an approximation to the overall sound pressure level.

A more effective estimate that accounts for the spectral content of a sound is perceived noise level. The instantaneous perceived noise level PNL(k) is obtained by weighting instantaneous sound pressure levels SPL(i) for each of the 24 one-third octave frequency bands according to a subjectively derived table and then using the results to obtain values of perceived noise level according to a prescribed formula (ref. 19). A comparison of perceived noise level, PNL, with dB(c) for a typical flyover, figure 41, shows PNL to be higher than dB(c).

Tests have shown that for sounds of equal overall energy, those which contain some relatively intense steady-state tones have higher judged perceived noise levels than those which do not (ref. 18). Aircraft with turbofan engines generally have such tones in their noise signatures, for example, compressor whine. Figure 42, a plot of sound pressure level SPL versus frequency at the time of maximum tone corrected perceived noise level for a typical flyover of the Boeing 367-80B airplane, shows the nature of a noise spectrum with tones. Two of the most widely used methods of estimating the judged perceived noise level of a sound while taking into account the occurrence of pure tones in the frequency spectrum are those proposed by Kryter and Pearsons (refs. 18 and 21) and the Federal Aviation Administration (ref. 19). Both schemes require considerable computation. The Kryter and Pearsons method is somewhat simpler and is based on corrections to the sound pressure levels SPL(i) before the computations for the instantaneous perceived noise levels PNL(k) are made. The FAA method is based on corrections to the instantaneous perceived noise levels, PNL(k), (computed in the standard way) derived from a series of computations on the sound pressure levels SPL(i).

The results of both schemes are presented in table 7 so they may be compared. However, where not otherwise specified, all of the remaining data given are calculated according to the FAA method. A comparison of the tone corrected perceived noise level (FAA method) with the perceived noise level for the flyover with frequency characteristics given in figure 42 is shown in figure 43.

The judged perceived noise level of a sound also varies with the duration of the sound. For sounds of equal overall energy, those of long duration are more "unwanted" than those of short duration (ref. 18). The effective perceived noise level, EPNL, is an estimate of judged perceived noise level which attempts to account for duration effects. Both an integral (or, more properly, summation) and an approximate method of computing effective perceived noise level have been proposed (ref. 19). The integral method makes use of the instantaneous tone corrected perceived noise level,  $PNLT(k)$ , and the duration  $d$ , while the approximate method makes use of only the maximum tone corrected perceived noise level,  $PNLTM$ , and the duration  $d$ . The duration used in this report is the continuous increment of time which begins when the tone corrected perceived noise level exceeds 10 PNdB below  $PNLTM$  and remains above this level until  $PNLTM$  and ends when the tone corrected perceived noise level falls below 10 PNdB below  $PNLTM$  for the first time after  $PNLTM$  (refer to fig. 43). Values of effective perceived noise level calculated from tone corrected perceived noise level data computed by both the Kryter-Pearsons and Federal Aviation Administration (FAA) methods are presented for comparison in table 7.

## RESULTS

### Spatial Coordinates and Engine Characteristics at Flyover

Altitude, lateral displacement, airspeed, total gross thrust (FG), and percent of maximum RPM ( $N_2$ ) for each flyover are given in table 8.

### Noise Measurement Data at Flyover

Effective perceived noise level (EPNL), maximum tone corrected perceived noise level ( $PNLTM$ ), maximum perceived noise level ( $PNLM$ ), peak perceived noise level ( $PNLP$ ), and the maximum dB(c) level for the various flight profiles and runs at stations 1, 2, and 3 are given in tables 7(a), 7(b), and 7(c), respectively. Also, column 10 in these tables shows the difference between maximum tone corrected perceived noise level and maximum perceived noise level (tone correction factor), column 11 shows the duration  $d$  of the flyover, and column 12 shows the difference between effective perceived noise level and maximum tone corrected perceived noise level (duration correction factor).

Table 9 shows the difference for each flight profile at each noise measurement station between approximated and integrated EPNL and between the FAA and Kryter-Pearsons methods of calculating EPNL.



Table 10 shows the averaged values of the data presented in table 7 (FAA calculations only) for each flight profile at each noise measurement station along with the difference between the high and low values of integrated effective perceived noise level (integrated EPNL variation).

Table 11 shows the averaged noise reductions for each flight profile at each noise measurement station. Profile A was the reference level used for profiles G, I, H, M, and L. For profiles G-1 and I-1, profile A-1 was the reference level.

#### Data Evaluation

For the purpose of comparing the noise measured in flight for the various flight profiles with the noise predicted by the simulator, a number of runs had to be disregarded as unrepresentative for various reasons. For example, during profile A, run 1, the radar sent erroneous commands to the aircraft, causing it to fly an erratic course.

Comparison with raw OASPL shows that errors were made in processing the data for profile G, run 1 at station 1 and for profile M, run 1 at station 1.

During profile L, run 1, station 3, the aircraft was higher and had less thrust than normal.

The data for the runs discussed above were disregarded while computing the averages shown in tables 10 and 11.

#### Data Variation

Some variation in the perceived noise level of an airplane can be expected to occur even under controlled constant altitude and constant power conditions as a result of instrument instability, meteorological conditions, slant range variations, and trim power variations due to weight changes (ref. 1). However, large variations can also occur as a result of:

1. Throttle activity to perform capture tasks when the transition occurs near the noise measurement station
2. Unequal thrust levels of various engines, and
3. Throttle activity to correct for tracking errors.

Data taken during unsteady throttle activity are indicated by footnotes in tables 8 and 10.

## DISCUSSION

### General Method Comparison

Comparison of the FAA and Kryter-Pearsons columns for PNLT and EPNL in table 7 shows that, in general, there is not a great deal of difference between the estimates derived by either method. Table 9 shows that the average difference between the FAA and Kryter-Pearsons methods of calculating EPNL over all runs was -0.38 EPNdB at station 1, +1.03 EPNdB at station 2, and +0.84 EPNdB at station 3.

Column 10 in table 7 shows that the effect of the steady-state tones associated with the JT3D-1 prototype turbofan jet engines is to raise the perceived noise level approximately 5 PNdB.

Column 12 in table 7 shows that flyover duration effects can vary the effective perceived noise level by as much as 10 EPNdB. However, examination of column 11 shows a wide variation in duration for different runs in the same flight profile. This is due to the definition used for the duration  $d$  which makes it very sensitive to the shape of the peak of the PNLT(k) curve. This also accounts for some of the data variation observed in column 12 and in integrated and approximated EPNL.

Table 9 also shows that the approximated EPNL was, on the average, about 1.7 EPNdB higher than the integrated EPNL at stations 1 and 2 and approximately 2.6 EPNdB higher at station 3.

### Comparison With Simulator

Simulator PNLM versus range curves for the various flight profiles are shown in figure 44 with measured PNLM points plotted at ranges corresponding to the noise measurement stations. As can be seen from these figures, there was generally good agreement between predicted and measured values of PNLM at ranges corresponding to the noise measurement stations.

### Comparison of PNLT Time Histories for Various Flight Profiles

Figures 45, 46, and 47 show time histories of tone corrected perceived noise level for examples of the various noise abatement approaches used during the investigation.

Examination of figures 45(a), 46(a), and 47(a) indicates that, of the flight profiles studied, only profiles H and L hold promise of a substantial noise reduction at station 1. This is not surprising since, for all other profiles, by the time of station 1 flyover the aircraft is approaching trimmed flight on a  $2.65^\circ$  glide slope. However, table 11 shows that noise reductions in excess of 11 and 9 EPNdB were achieved with profiles H and L.

Examination of figures 45(b), 46(b), and 47(b) indicates that substantial noise reductions were achieved at station 2 with all of the noise abatement profiles studied. According to table 11, the greatest noise reductions, approximately 17 PNdB and 18 EPNdB, were achieved with profiles G-1 and I-1. Profiles G, H, and M reduced noise in excess of 11 PNdB and 12 EPNdB. Profiles I and L, although reducing noise in excess of 10 PNdB in terms of maximum tone corrected perceived noise level, actually reduced noise less in terms of effective perceived noise level because of the long duration of these flyovers.

Examination of figures 45(c), 46(c), and 47(c) indicates that only a small reduction of noise can be expected at station 3. The sketches in table 8 show that although some reduction in noise can be expected from the increased altitude, the thrust level is higher than for the normal approach because the aircraft is in level flight. The greatest noise reductions occurred with profiles G-1 and I-1 which reduced noise in excess of 6 PNdB and 5 EPNdB (see table 11). However, if greater noise reductions are required at this range, it would only be necessary to increase the altitude of the high beam capture so that at station 3 the aircraft would be higher and on a 6° approach angle.

#### SUMMARY OF RESULTS

The acquisition and reduction of ground noise data for the Boeing 367-80 aircraft during noise abatement approaches, led to the following conclusions.

1. Of the flight profiles studied, only profile H (two-segment with 250-ft transition altitude) and profile L (4° decelerating approach) hold promise of a substantial noise reduction at 1 nautical mile from the runway threshold. Profile H resulted in a reduction in average maximum tone corrected perceived noise level (PNLTM) of approximately 13 PNdB and a reduction in average integrated effective perceived noise level (EPNL) of approximately 11 EPNdB while profile L resulted in an average PNLTM reduction of approximately 11 PNdB and an average EPNL reduction of approximately 9 EPNdB at a range of 1.09 nautical miles from the runway threshold.

2. Profiles G-1 and I-1 (two segment with 400-ft transition altitude) resulted in average PNLTM reductions of approximately 17 PNdB and average EPNL reductions of approximately 18 EPNdB at a range of 3.46 nautical miles from the runway threshold. The most effective decelerating approach at this range was profile M (two segment) which resulted in an average PNLTM reduction of approximately 11 PNdB and an average EPNL reduction of approximately 12 EPNdB.

3. At a range of 5.13 nautical miles from the runway threshold, profiles G-1 and I-1 (two segment with 400-ft transition altitude) resulted in average PNLTM reductions of approximately 6 and 8 PNdB, respectively, and average EPNL reductions of approximately 6 and 5 EPNdB, respectively. However, greater noise reductions at this range could be achieved simply by increasing the altitude of the high beam capture. The most effective decelerating

approach at this range was profile L ( $4^\circ$ ) which resulted in an average PNLTm reduction of approximately 6 PNdB and an average EPNL reduction of approximately 3 EPNdB.

4. The effect of the steady-state tones associated with the JT3D-1 prototype turbofan engines was to raise the perceived noise level approximately 5 PNdB.

5. The approximated values of EPNL were, on the average, about 1.7 EPNdB higher than the integrated values of EPNL at 1.09 and 3.46 nautical miles from the runway threshold and about 2.6 EPNdB higher at a range of 5.13 nautical miles from the runway threshold.

## APPENDIX B

### AIRPLANE SYSTEMS

#### SYSTEMS TO IMPROVE GUIDANCE AND DISPLAY INFORMATION

##### Flight Director

The modified pitch flight director (fig. 12) provided the pilot with adequate guidance on the various noise abatement approaches. Figures 32 and 34 present the errors from the ILS measured at transition and at 200-feet altitude, respectively, on the two-segment approaches. The data show that a high percentage of the approaches had errors less than 12 feet which is well within the accuracy required for category II (ref. 13). There was a relationship, however, between the pilots workload and precision of tracking with the flight director. With a high sensitivity (a large flight director displacement for small errors), the precision of tracking improved but the pilot had to change the pitch attitude constantly to keep the flight director zeroed which increased his workload. The sensitivity used, therefore, was a compromise determined by the pilots on the simulator. With the EADI display (fig. 9), 0.25-inch deflection of the pitch command flight director bar gave an indication of 15-feet altitude error from the glide slope and was a command for a  $1^\circ$  pitch attitude change. With the small electromechanical ADI (fig. 11), the scaling was much less - about 0.08 inch for similar error and command. But the resolution on the ADI and comparable tracking could be accomplished with either. The two pilots who flew both instruments preferred the expanded scale of the EADI because the ease of reading it reduced the workload somewhat.

##### Situation Displays

From situation display information the pilot must determine as accurately as possible: (1) his position in space relative to the airport, (2) the airplane's attitude, and (3) the vertical and horizontal and lateral flight paths. On two-segment approaches, situation information becomes more critical because of the change in glide-slope angle late in the approach. The primary items of situation information which the pilot requires for a flight director guided instrument approach are airplane roll and pitch attitudes, heading, airspeed, or error from a referenced airspeed, pressure and radio altitude, angular errors from the ILS (both glide slope and localizer), and marker beacon annunciators which indicate a specific range from the runway threshold. Much of the primary information is currently provided on the ADI to reduce the number of instruments the pilot must scan for the information. On the electromechanical ADI used for some of the approaches, this information is presented on a small 4-inch instrument. This instrument had all the required primary information listed above except radio altitude and heading which were on adjacent instruments. The pilots felt the information was adequate for two-segment approaches but certainly not an optimum method of display.

For the majority of the approaches, the EADI was used (see figs. 8 and 9). This instrument which was a 5.4 by 7.2 inch cathode ray tube included all of the primary information except heading, plus some additional information not found on other ADI's to assist the pilot in determining his position and assessing his situation.

Since the EADI was a new type of cockpit display, the pilots were given an indoctrination in the simulator before using the display in flight. The pilots were able to adapt quickly to the new display. Although some pilots considered the display somewhat cluttered, they had no difficulty using the primary information. The pitch and roll attitude, the flight director bars, and the airspeed error indicator differed little from current instrumentation except for their position on the display and the enlarged scale. With enlarged scale of pitch and roll attitude, attitude control on instruments was easier. One of the pilots commented that the attitude information was similar to real world with a narrow field of view. This comment was probably prompted by his ability to detect small attitude angle changes and low angular rates.

The airspeed error symbol was prominently positioned on the fixed airplane symbol close to the flight director bars and scaled to show small airspeed errors. The pilots considered this method of displaying airspeed very easy to use, particularly when monitoring the autothrottle operation.

The radio altitude was presented digitally on the face of the display. The pilots considered the digital readout an improvement over the current method of displaying radio altitude on a 4-inch dial instrument. In these tests the indicated digital radio altitude changed every 10 feet down to 200-foot altitude and every 2 feet from 200 feet to touchdown. The 10-foot scaling avoided the rapid flickering of the display early on the approach, and the 2-foot scaling gave the pilot precise height information as he approached the runway.

The errors from the ILS were indicated on the EADI by the rectangle in the middle of the display shown on figure 9. The rectangle moved vertically on the face of the tube to indicate glide-slope errors and horizontally to indicate localizer errors. The rectangle was referenced to the same position on the display as the flight director bars - the small black square on figure 9. Having the same reference enabled the pilot to easily determine the adequacy of the flight director for maintaining small ILS errors. The symbol was scaled so that as long as the small square remained inside the rectangle, the errors were within the desired accuracy shown in table 5. The pilots found this symbol on the display easy to use. Two of the pilots tried flying a normal  $2.65^\circ$  approach on the simulator using only the ILS error symbol for guidance (without flight director) and found some difficulty. Further study of this method of displaying ILS error is, therefore, required for use without a flight director.

The flight-path angle symbol on the EADI provided the pilot with a new type of situation information. The symbol had the same scaling as the pitch angle lines, the artificial horizon being zero flight-path angle. The pilots considered the symbol helpful and used it much the same way that they use the

rate of climb instrument. In two-segment approaches the symbol gave the pilot the situation information to monitor the progress of the capture of the upper segment and the transition to the lower segment. Some of the pilots had difficulty using the symbol effectively. The pilots felt the difficulty was due either to the limited time available for learning to use a new piece of information or to the method of presentation.

The potential flight-path angle symbol on the EADI could be used in two ways: (1) to indicate a change in either thrust or drag, and (2) to indicate the approximate steady-state flight-path angle for the speed and engine thrust at that moment. This symbol indicated essentially the acceleration along the flight path and was scaled the same as the flight-path symbol. In steady flight the potential flight-path symbol is always in line with the flight-path angle symbol. This symbol was used by some of the pilots in approaches without the autothrottle to assist in determining the thrust level required. For example, when intercepting the upper  $6^{\circ}$  segment, the pilot would keep the potential flight-path symbol aligned with the flight-path angle symbol by reducing the engine thrust as flight path was changed from  $0^{\circ}$  to  $6^{\circ}$ . Other pilots felt that the extra attention required in tracking these symbols increased their workload too much. Most pilots were able to use the symbol, however, to help monitor the operation of the autothrottle.

Another unique feature of the EADI display was the television picture of the runway (see fig. 9). This feature was evaluated to determine the benefits of a pictorial type situation display showing the real world. Initial evaluations were made with the television "on" for the complete approach, but the pilots got little useful information from the picture to assist them until the altitude was low. The pilots tend to use the picture as a backup for the information normally used on the approach. The pilots felt the pictorial type of display was particularly helpful when going from IFR (instrument flight rules) to VFR (visual flight rules) at hood-off altitude. With the TV picture, the pilot had a good indication of what his situation would be when he removed the hood and viewed the runway. On several occasions the pilots flew the airplane using primarily the TV and flight-path angle symbol to altitudes less than 50 feet under the hood and had no problem completing the landing visually.

There was occasionally a problem when the TV picture obscured some of the other symbols on the display. When there was a lot of contrast between sky and ground, and the flight path was changing, the pilots could momentarily lose the flight director or flight-path angle symbol on the display.

The pilots felt that the pictorial display provided an independent backup of situation information for the ILS. In instrument approaches the ILS provides the main input to the flight director as well as the situation information. The pilot is dependent, therefore, on the ILS to guarantee a safe landing. An independent display that provides the extra insurance can make instrument approaches more comfortable for the pilot. Although the television display as used in this program for research purposes may not be very effective under actual instrument weather conditions, the development of an independent situation display merits attention.

## SYSTEMS TO IMPROVE FLIGHT-PATH CONTROL AND TO REDUCE PILOT WORKLOAD

### Rate Command With Attitude Hold Control System

The pitch rate command with attitude hold control system, referred to as simply SAS, is described in the Equipment section. Figure 5 is a block diagram of the system.

One of the most important characteristics that pilots desire for good flight-path control is precise control of the pitch attitude of the airplane. When maneuvering, pilots like to command pitch rate with control column inputs; and with no control inputs, they do not want pitch attitude to change. These two characteristics were readily apparent with SAS and provided a satisfactory control system for flying any of the noise abatement profiles. The system provided some reduction in pilot workload because of its inherent attitude stability. Noise abatement approaches were being "flown" on the simulator with and without mild turbulence with little change in pilot workload. A few of the pilots encountered light turbulence in flight and noted that with the SAS the workload was not significantly different than in calm air.

Figure 48 illustrates a  $5^\circ$  attitude change performed with the SAS. Since the SAS commands pitch rate in proportion to control column input, the pilot entered essentially a step column input to establish a pitch rate and returned the control to neutral when the desired attitude was reached. The system had good response characteristics in that pitch rate followed the control input quite closely. When the control column was returned to neutral, pitch rate was commanded to zero and the attitude was held at the value reached at that time. The pitch rate to column gearing was  $0.9^\circ/\text{sec}/\text{in.}$  of column. The gearing was not necessarily an optimum value but was considered satisfactory by the pilots.

Much of the workload reduction that was attributed to the attitude stability feature resulted from the inherent characteristic of eliminating trim change due to thrust, flaps, ground effect, etc. The pitching moments due to angle-of-attack changes are also automatically compensated; the airplane has, therefore, no speed stability. The term "speed stability" as used here refers to control force changes with changes in airspeed. The pilots felt that in the absence of speed stability, an autothrottle was desirable for better control of airspeed.

Although all the pilots considered the SAS a very good system for controlling flight path on the approach, the unusual characteristics of the system in flare and touchdown created some problems. These unusual characteristics and the use of a "downspring" to help eliminate the problem are discussed in reference 5.

### Basic Control System With Autotrim

The basic control system with autotrim (fig. 4), described in the Equipment section, also provided a satisfactory control system for the



profiles evaluated in this program. The pilot considered the basic control system to be much better than most conventional control systems on current transports. The inherent advantages of the fly-by-wire mode reduces many of the undesirable mechanical characteristics of a control system, and the control sensitivity and forces could be set to a near optimum value for the landing approach task.

The autotrim system did not completely eliminate trim changes as did the SAS. It performed the trimming function much the same as a pilot, but automatically; for example, when the flaps were lowered the pilot had to put in a control force to trim the pitching moments due to the flaps. After several seconds, however, the trim forces would be reduced to zero. The automatic trim rate was slower than with manual trim, but the pilot considered the system an acceptable method of reducing the workload on the approach. The autotrim had little effect on the pilot evaluation in the flare and touchdown. Because of the slow trim rates, the control forces were only slightly reduced in the flare and touchdown task.

#### Direct Lift Control

The direct lift control (DLC) was used with both the SAS and basic control system. The implementation of the system is described in the Equipment section and is shown on the block diagrams of figures 4 and 5.

Preliminary studies of methods of incorporating DLC into the control system of a transport airplane were made on the simulator and in the initial phase of the flight tests. The results of the brief study indicated that integrating the DLC into the longitudinal (pitch) controls of the airplane for the approach task was more desirable than having a separate controller. The response of the airplane to a step column input with the rate command system with and without DLC is shown in figure 49. The time histories show that with DLC the time required to change the vertical acceleration,  $A_z$ , has been reduced. This quickened vertical response of the airplane to control column inputs enables the pilot to change the flight-path angle or rate of descent faster.

A separate controller, a thumb switch similar to a trim switch on the control wheel, was also provided. Approaches were made by some of the pilots using primarily the thumb controller for flight-path control. DLC was used for small changes but pitch attitude still had to be controlled and changed during intercept and transition on two-segment approaches. The pilot felt that during the approach the addition of another control in the cockpit increased the pilot workload.

The evaluation of the DLC on the two-segment approaches showed that there was little difference in the pilot's ability to control flight path with or without DLC. The airplane with either control system had good (vertical) response, and with the tight guidance provided by the flight director the ILS errors could be kept small. The transitions were also performed relatively slowly and did not require an increase in vertical response of the airplane.

The pilot did recognize, however, the potential advantage of DLC in steep approaches to help arrest the high rate of descent quickly in case of an emergency.

The pilot appreciated the quickened vertical response of the DLC in the flare and touchdown task. More precise control of the flare and touchdown was possible and smaller changes in pitch attitude were required for vertical acceleration control. Some of the pilots used the separate thumb DLC controller for precise control in the touchdown task.

### Autothrottle

The autothrottle system was designed to keep the airspeed within  $\pm 5$  knots on the two-segment approaches. For these approaches an airplane attitude term was found to be required in addition to the velocity terms in the throttle command computations (see fig. 7) because of the large flight-path angle changes on the two-segment approaches. The autothrottle provided a commanded thrust change which tended to follow the airplane flight-path angle changes, reducing the excursions in airspeed and thrust.

The pilots considered the autothrottle satisfactory for the noise abatement task as flown in this program. It was the opinion of all the evaluating pilots that the autothrottle was the most important system added to the airplane to assist the pilot in flying two-segment approaches with an acceptable workload. Without an autothrottle, controlling thrust to keep airspeed within  $\pm 5$  knots is a time-consuming task for the pilot. In two-segment approaches where both thrust and airplane attitude changes must be made simultaneously and late in the approach, the pilot workload becomes unacceptably high.

### Engine Thrust Response

The effects of the slow engine thrust response to throttle inputs at low values of engine thrust as shown in figures 17 and 30 were examined during transition from the steep to the shallow approach angle. A time history of airplane track, throttle position, and thrust of No. 2 engine and airspeed during transition with two-beam guidance is shown in figure 50. This particular time history was chosen because at the time of transition the pilot was correcting a slightly high condition that momentarily steepened flight-path angle to about  $7.0^\circ$ . Because of the increased angle, the autothrottle had decreased engine thrust nearly to idle. The increased angle and low engine thrust condition would tend to amplify any thrust response problem.

At transition the autothrottle commands (thrust command on fig. 49) an increase in thrust. Since the engine is slow to respond, the thrust lags the throttle position for several seconds. The maximum time lag is, however, only 2 seconds. The lag in thrust results in a bleed-off in airspeed of 4.5 knots, but within 10 seconds the airspeed has returned to the proper value. This example illustrates approximately the maximum airspeed error

experienced with satisfactory guidance and an autothrottle. The pilots considered the engine response satisfactory for the transition task. Airspeed errors of  $\pm 5$  knots were within the band normally expected during the approach. No flight-path control problems were associated with the engine response characteristic.

Some approaches were conducted on the simulator with mild turbulence of  $\pm 5$  knots about all three axes and windshears of up to 6 knots per 100 feet starting at 300-foot altitude. The autothrottle was able to keep the airspeed acceptable limits under these conditions.

Because of the restriction on landing with gross weights greater than 165,000 pounds, wave-offs starting at altitudes below 100 feet were made routinely with gross weights between 165,000 and 175,000 pounds. The wave-offs from the lower segment were, therefore, no different than from a normal approach. Several missed approaches from the 6° segment were made with wave-off initiated at altitudes as low as 300 feet, but the pilot did not have to perform a minimum altitude loss wave-off to maintain a safe altitude. The engine response was, therefore, not critical. Further tests are required to examine the operational problems of thrust response in missed steep approaches at lower altitudes.

## REFERENCES

1. Conference on Progress of NASA Research Relating to Noise Alleviation of Large Subsonic Jet Aircraft, Oct. 8-10, 1968. NASA SP-189, 1968.
2. Zalovcik, John A.; and Schaefer, William T., Jr.: NASA Research on Noise-Abatement Approach Profiles for Multiengine Jet Transport Aircraft. NASA TN D-4044, 1967.
3. Zalovcik, John A.: Effect of Thrust and Altitude in Steep Approaches on Ground Track Noise. NASA TN D-4241, 1967.
4. Sawyer, Richard A.; and Schaefer, William T., Jr.: Operational Limitations in Flying Engine Noise Abatement Approaches. NASA TN D-5497, 1969.
5. Flora, Clarence C.; Kriechbaum, Gerhard, K. L.; and Willich, Wayne: A Flight Investigation of Systems Developed for Reducing Pilot Workload and Improving Tracking Accuracy During Noise-Abatement Landing Approaches. NASA CR-1427, 1969.
6. Condit, Philip M.; Kimbrel, Laddie G.; and Root, Robert S.: In-Flight and Ground-Based Simulation of Handling Qualities of Very Large Airplanes in Landing Approach. NASA CR-635, 1966.
7. Gratzner, L. B.; and O'Donnell, Thomas J.: Development of a BLC High-Lift System for High Speed Airplanes. J. Aircraft, vol. 2, no. 6, Nov.-Dec. 1965, pp. 472-484.
8. Model 367-80 Project Engineering Group: Detail Design and Installation of a Direct Lift Control Flap for the Boeing 367-80 Airplane. NASA CR-73292, 1969.
9. Taylor, Charles R.: Flight Test Results of a Trailing Edge Flap Designed for Direct Lift Control. NASA CR-1426, 1969.
10. Rolls, L. Stewart; Cook, Anthony M.; and Innis, Robert C.: Flight-Determined Aerodynamic Properties of a Jet-Augmented, Auxiliary-Flap, Direct-Lift-Control System Including Correlation With Wind-Tunnel Results. NASA TN D-5128, 1969.
11. Gannett, James R.: Flight Management Concepts. Proc. Air Line Pilots Association, Fifteenth Air Safety Forum, Seattle, Washington, July 9-11, 1968.
12. Jackson, Charles T., Jr.; and Snyder, C. Thomas: Validation of a Research Simulator for Investigating Jet Transport Handling Qualities and Airworthiness Criteria During Take-Off. NASA TN D-3565, 1966.
13. Anon.: Criteria for Approval of Category II Landing Weather Minima. FAA Advisory Circular AC No. 120-20, 6-6-66.

14. Sperry, William C.: Aircraft Noise Evaluation. FAA-NO-68-34, Sept. 1968.
15. Tobie, H. N.; Elliott, E. M.; Malcom, L. G.: A New Longitudinal Handling Qualities Criterion. 1966 Proc. 18th Annual Natl. Aerosp. Electronic Conf., Dayton, Ohio. Inst. Elec. and Electron. Engrs., May 16-18, 1966, pp. 93-99.
16. Stickle, Joseph W.; Patton, James M.; Henry, Robert C.: Flight Tests of a Direct Lift Control System During Approach and Landing. NASA TN D-4854, 1968.
17. Jansen, George R.: Flight Evaluation of Direct Lift Control on the DC-8 Super 63. Proc. Soc. of Exptl. Test Pilots, Twelfth Symp., Beverly Hills, Calif., Sept. 26-28, 1968, Tech. Rev., vol. 9, no. 2, 1968, pp. 117-127.
18. Kryter, K. D.: Concepts of Perceived Noisiness, Their Implementation and Application. J. Acoust. Soc. Am., vol. 43, no. 2, Feb. 1968, pp. 344-361.
19. Sperry, William C.: Aircraft Noise Evaluation. Rep. FAA-NO-68-34, D.O.T., Federal Aviation Administration, Sept. 1968.
20. Anon.: General Purpose Sound Level Meters. ASA S1.4-1961 (U.S.A. Stand. Inst., N. Y., 1961).
21. Kryter, K. D.; and Pearsons, K. S.: Judged Noisiness of a Band of Random Noise Containing an Audible Pure-Tone. J. Acoust. Soc. Am., vol. 38, no. 1, July 1965, pp. 106-112.
22. Hilton, David A.; and Henderson, Herbert: Variability in Airplane Noise Measurements. Conf. on Progress of NASA Research Relating to Noise Alleviation of Large Subsonic Jet Aircraft, NASA SP-189, 1968.

TABLE 1.- BOEING 367-80 AIRPLANE CHARACTERISTICS FOR GROUND-BASED SIMULATION

Characteristics	Low Approach Speed	High Approach Speed and Decelerating Approaches
W	150,000 lb	
S	2,821 ft <sup>2</sup>	
b	130 ft	
$\bar{c}$	20.05 ft	
I <sub>xx</sub>	2,560,000 slug-ft <sup>2</sup>	
I <sub>yy</sub>	2,250,000 slug-ft <sup>2</sup>	
I <sub>zz</sub>	4,730,000 slug-ft <sup>2</sup>	
V <sub>I</sub> <sup>*</sup>	115 knots	135-150 knots
$\delta_f$	40/10	30/10
$\partial C_D / \partial \alpha$	Nonlinear (0.315 at $\alpha_0$ )	Nonlinear (0.425 at $\alpha_0$ )
$\partial C_D / \partial \delta_{FAUX}$	Nonlinear (0.1645 at $\delta_{FAUX} = 10$ )	0.11
$\partial C_D / \partial C_{TINBD}$	-0.115	-0.321
$\partial C_D / \partial C_{TOTBD}$	-0.9	-0.98
$\partial C_D / \partial \eta$	0	0.1152
C <sub>L</sub> <sup>*</sup>	1.2	0.86
$\partial C_L / \partial \alpha$	Nonlinear (5.12 at $\alpha_0$ )	Nonlinear (5.15 at $\alpha_0$ )
$\partial C_L / \partial \delta_e$	0.279	0.279
$\partial C_L / \partial \delta_{FAUX}$	0.495	Nonlinear (0.70 at $\delta_{FAUX} = 0$ )
$\partial C_L / \partial C_{TINBD}$	2.37	1.45
$\partial C_L / \partial C_{TOTBD}$	0.192	0.192
$\partial C_L / \partial \eta$	0	0.341
$\partial C_L / \partial \beta$	-0.0707 <sup>†</sup>	-0.0603 <sup>†</sup>
$\partial C_L / [\partial \dot{\beta}(b/2V)]$	-0.0417 <sup>†</sup>	-0.1380 <sup>†</sup>
$\partial C_L / [\partial p(b/2V)]$	-0.897 <sup>†</sup>	-1.02 <sup>†</sup>

\*See footnote p. 47.

<sup>†</sup>See footnote p. 47.

TABLE 1.- BOEING 367-80 AIRPLANE CHARACTERISTICS FOR GROUND-BASED  
SIMULATION - Concluded

Characteristics	Low Approach Speed	High Approach Speed and Decelerating Approaches
$\partial C_L / [\partial r(b/2V)]$	0.2050	-0.0196
$\partial C_L / \partial \delta_a$	0.16	0.194
$\partial C_L / \partial \delta_r$	-0.0206	-0.0179
$C_{mI}^*$	0	0
$\partial C_m / \partial \alpha$	-1.11	-1.11
$\partial C_m / \partial \delta_e$	-0.802	-0.802
$\partial C_m / \partial \delta_{FAUX}$	Nonlinear (-0.154 at $\delta_{FAUX} = 10$ )	-0.142
$\partial C_m / \partial C_{TINBD}$	-0.53	-0.5
$\partial C_m / \partial C_{TOTBD}$	0.0796	0.0796
$\partial C_m / [\partial q(\bar{c}/2V)]$	-13.7	-13.6
$\partial C_m / [\partial \dot{\alpha}(\bar{c}/2V)]$	-5.25	-5.33
$\partial C_m / \partial \eta$	0	-0.20
$\partial C_n / \partial \beta$	0.0611 <sup>†</sup>	0.0929 <sup>†</sup>
$\partial C_n / [\partial \dot{\beta}(b/2V)]$	0.157 <sup>†</sup>	0.556 <sup>†</sup>
$\partial C_n / [\partial p(b/2V)]$	0.0340 <sup>†</sup>	0.100 <sup>†</sup>
$\partial C_n / [\partial r(b/2V)]$	-0.2170	-0.252
$\partial C_n / \partial \delta_a$	0.0112	0.0265
$\partial C_n / \partial \delta_r$	0.0777	0.0724
$C_{TI}^*$	0.271	0.159
$\partial C_y / \partial \beta$	-0.773	-0.829
$\partial C_y / [\partial \dot{\beta}(b/2V)]$	-0.404 <sup>†</sup>	-1.314 <sup>†</sup>
$\partial C_y / \partial \delta_r$	0	-0.171

\*Subscript "I" indicates initial trim value.

<sup>†</sup>Augmented value.

TABLE 2.- SIMULATION EQUATIONS OF AIRPLANE SYSTEMS

Basic airplane pitch control with direct lift control

$$\delta_e = \frac{2.54\delta_c + 0.215 \Delta\delta F_{aux}}{(0.1S + 1)}$$

$$\delta_{e_{max}} = \pm 20^\circ$$

$$\dot{\delta}_{e_{max}} = \pm 23^\circ/\text{sec}$$

$$\Delta\delta F_{aux} = -5.33\delta_c$$

$$\Delta\delta F_{aux_{max}} = \pm 20^\circ$$

$$\Delta\dot{\delta} F_{aux_{max}} = \begin{matrix} +20^\circ/\text{sec} \\ -30^\circ/\text{sec} \end{matrix}$$

Pitch rate-command system with direct lift control

$$\delta_e = \frac{2.66(q - \dot{\theta}_c) + 3.75[\theta - (\dot{\theta}_c/S)]}{(0.1S + 1)}$$

$$\delta_{e_{max}} = \pm 20^\circ$$

$$\dot{\delta}_{e_{max}} = \pm 23^\circ/\text{sec}$$

$$\dot{\theta}_c = -0.0157\delta_c + (0.103 \Delta V)^*$$

$$\Delta\delta F_{aux} = -0.0173\delta_c$$

$$\Delta\delta F_{aux_{max}} = \pm 20^\circ$$

$$\Delta\dot{\delta} F_{aux_{max}} = \begin{matrix} +20^\circ/\text{sec} \\ -30^\circ/\text{sec} \end{matrix}$$

Autothrottle

$$C_T = 0.00352 \left[ \left( \frac{0.075}{S} + \frac{0.225}{S + 0.5} \right) (V - V_{ref}) - 210 \Delta\theta \right] \left( \frac{3.88}{S + 3.88} \right)$$

$$\dot{V}_{max} = \pm 0.845 \text{ ft/sec}^2 \text{ except for decelerating approaches}$$

NOTE: Autothrottle goes into "hold" when  $h \lesssim 50 \text{ ft.}$

\*Downspring operative when  $\Delta V \lesssim 2.87 \text{ ft/sec.}$



TABLE 2.- SIMULATION EQUATIONS OF AIRPLANE SYSTEMS - Continued

Pitch flight director

$$\theta_c = - \frac{S}{S + 0.08} \left( \Delta\theta - \theta_{\text{bias}} + 25.4 \Delta C_T + 0.147 \Delta V \right) - 0.0688 h_e$$

$\theta_{\text{bias}}$  = pitch attitude change commanded at glide-slope capture, deg

$h_e$  = error from ILS glide slope, ft

Altitude hold mode:

$$\theta_{\text{bias}} = 0$$

$$h_e = 5.2(h - h_{\text{ref}})$$

Glide-slope capture and tracking mode:

$$\theta_{\text{bias}} = \frac{\Delta\gamma}{0.63}$$

$$h_e = \left( \frac{h - h_{\text{bias}}}{\gamma_{\text{GS}}} \right) \epsilon, \text{ ft}$$

$h_{\text{bias}}$  = virtual location of ILS glide-slope transmitter; negative is below runway level

$$h_{\text{bias}} = \sin \gamma_{\text{GSUS}} \left( \frac{h_{\text{INT}}}{\tan \gamma_{\text{GSLS}}} \right)$$

TABLE 2.- SIMULATION EQUATIONS OF AIRPLANE SYSTEMS - Concluded

Type of noise abatement approach (see Table 3)	$\theta_{\text{bias}}$ , deg		$\theta_{\text{bias}}$ at $h_e$ insertion, ft		$h_{\text{bias}}$ , ft	
Profile	Upper segment	Lower segment	Upper segment	Lower segment	Upper segment	Lower segment
A	---	-4.35	---	-77	---	0
B	---	-7.4	---	-131	---	0
C	---	-7.4	---	-131	---	0
D	---	-8.2	---	-146	---	0
E	---	-9.05	---	-160	---	0
F	---	-9.85	---	-175	---	0
G	-9.85	5.2	-175	83	-505	0
H	-9.85	5.2	-175	83	-315	0
I	-9.85	3.05*	-175	(+)	---	0
J	-9.85	3.05*	-175	(+)	---	0
K	---	-4.35	---	-77	---	0
L	---	-6.57	---	117	---	0
M	-8.2	3.64	-146	58	-442	0
N	-8.2	3.64	-146	58	-707	0

Lateral flight director

$$\phi_c = -0.47\phi - 4.36\epsilon_{\text{LOC}} - \left( \frac{2S}{4S^2 + 6S + 1} \right) (1.467\psi + 0.155\phi + 28.10\epsilon_{\text{LOC}})$$

\* $\theta_{\text{bias}}$  input as ramp;  $\dot{\theta}_{\text{bias}} = 0.33^\circ/\text{sec}$ .

+ $\theta_{\text{bias}}$  inserted at beginning of transition.

TABLE 3.- NOISE ABATEMENT PROFILES

Profile	Type of noise abatement approach	Glide-slope angle, deg		Type of guidance	Intercept altitude, ft	Distance from runway threshold to glide-slope intersection, ft
		Upper segment	Lower segment			
A	Single segment ↓	---	-2.65	Single ILS beam ↓	---	-1230
B		---	-4.5		---	-1230
C		---	-4.5		---	-500
D		---	-5.0		---	↓
E		---	-5.5		---	↓
F		---	-6.0		---	↓
G	Two segment ↓	-6.0	-2.65	Two ILS beams	400	-1230
H		↓	↓	↓	250	-1230
I		↓	↓	Single ILS beam	400	-1130
J		↓	↓	curved transition	250	-1110
K	Deceleration ↓	---	-2.65	Single ILS beam ↓	---	-1230
L		---	-4.0		---	↓
M		-5.0	-2.65		500	↓
N		-5.0	-2.65		800	↓

TABLE 4.- AIRPLANE CONFIGURATIONS

Evaluation phase	Profile	Approach speeds, knots		Flaps main/aux., deg	Pitch rate-command control system	Direct lift control	Auto-throttle	EADI television	Type attitude director indicator
		Simulator	Flight						
Single segment ↓	A-2			50/10 BLC off	Not used	On/Off	On/Off	Not used	Electromechanical
	B	115	115	↓	↓	↓	↓	↓	↓
	C								
	D								
	E								
↓	F			↓	↓			↓	↓
	A	115	112-122	40/10 BLC on	On/Off			On/Off	Electronic
	A-1	135	135-144	30/10 BLC off	On/Off	↓	↓	On/Off	Electronic
Two segment ↓	G	115	112 to 122	40/10 BLC on	On/Off	On/Off	On/Off	On/Off	Electromechanical and electronic
	H								
	I	135	135 to 144	30/10 BLC off	On/Off	On/Off	On/Off	On/Off	Electromechanical and electronic
	J								
Deceleration ↓	K	150	155	30/-10 to 30/10 BLC on	On	On/Off	On/Off	On/Off	Electronic
	L	↓	↓		↓	↓	↓	↓	↓
	M	↓	↓						
	N	112	120		↓	↓	↓	↓	↓

TABLE 5.- DESIRED ILS TRACKING PERFORMANCE  
[Derived from reference 13]

	Altitude, ft	Maximum deviation
Glide slope	700 to 100	$\pm 0.16^\circ \epsilon$
	200	$\pm 12$ ft
Localizer	700 to 100	$\pm 0.35^\circ \epsilon$
	200	$\pm 100$ ft
Airspeed	2500 to 50	$\pm 5$ knot from $V_{ref}$

TABLE 6.- AIRPLANE AND FLIGHT CONFIGURATION DATA

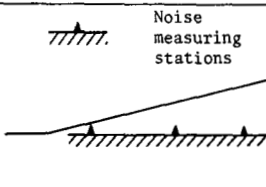
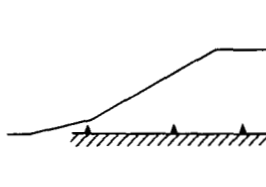
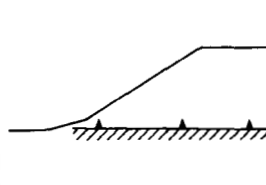
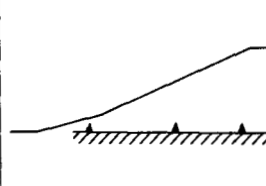
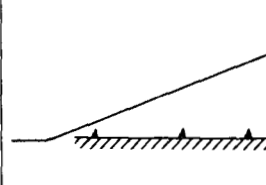
TABLE 5. AIR DATA AND FLIGHT CONFIGURATION DATA										
Profile	Profile	Run	Glide-slope angle, deg		Transition altitude, ft	Type of guidance	Flap setting, deg	Average approach velocity, knots	Airplane weight	
			Initial	Final			Main/auxiliary		Initial	Final
 Noise measuring stations	A	1 2 3	-2.65	-2.65	---	Single beam	40/10	117.5 118.5 118.5	175,200 172,000 168,900	174,400 171,200 168,100
	A-1	1 2 3					30/10	141 141.5 140.5	176,200 173,600 170,300	175,600 172,900 169,600
	G	1 2	-6.0	-2.65	400	Two segment, two beam	40/10	116.5 114	166,200 161,700	165,400 161,100
	G-1	1 2					30/10	138.5 137.5	165,200 163,300	164,600 162,700
	Single curved beam	I				1 2	40/10	114.0 107.5	159,600 154,600	159,000 148,500
		I-1				1	30/10	135	160,700	160,000
	H	1 2 3	-6.0	-2.65	250	Two segment, two beam	40/10	112.5 110 110	157,000 154,600 151,700	156,200 153,800 150,900
	M	1 2	-5.0	-2.65	500	Two segment, two beam	30/(-8.1 + 10) 30/(-9.4 + 10)	150 + 112 151 + 113.5	158,000 155,700	157,300 155,100
	L	1 2	-4.0	-4.0	---	Single beam	30/(-9.4 + 10)	150 + 114 151 + 114	153,300 150,800	152,700 150,100

TABLE 7.- FLYOVER NOISE MEASUREMENT DATA

		①	②	③	④		⑤	⑥		⑦	⑧		⑨	⑩	⑪	⑫	
Profile	Run	Max dB(c), dB	PNLP, PNdB	PNLM, PNdB	PNLTM		Kryter- Pearson, PNdB	FAA, PNdB	Kryter-Pearson		EPNL		FAA		Tone correction factor, ⑤ - ③, PNdB	Duration time, d, sec	Duration correction factor, ⑧ - ⑤, EPNdB
					Integrated, EPNdB	Approximated, EPNdB			Integrated, EPNdB	Approximated, EPNdB	Integrated, EPNdB	Approximated, EPNdB					
(a) Station 1																	
A	1*	103.4	120.4	117.9	123.9	122.2	118.4	120.3	119.1	121.1	4.3	11.5	-3.2				
	2	107.6	123.2	122.2	127.8	126.4	121.8	123.0	120.7	122.1	4.2	5.5	-5.7				
	3	105.3	121.7	119.7	125.9	124.6	119.9	121.6	119.3	121.3	4.9	7.0	-5.3				
A-1	1	105.9	120.8	119.9	123.4	122.9	117.1	117.6	117.0	118.1	3.0	5.0	-5.9				
	2	107.3	125.0	121.2	127.2	125.6	118.3	119.4	118.7	120.3	4.4	4.5	-6.9				
	3	106.5	122.2	120.9	126.3	125.2	118.6	120.6	117.9	119.5	4.3	4.0	-7.3				
G	1*	95.4	110.8	109.5	113.1	112.9	105.6	106.1	106.1	107.2	3.4	4.0	-6.8				
	2	104.1	118.9	117.9	120.9	121.4	114.8	117.3	115.5	117.4	3.5	6.0	-5.9				
G-1	1	107.6	122.8	122.0	128.0	126.8	120.2	120.2	120.0	121.6	4.8	4.5	-6.8				
	2	108.9	123.6	122.9	129.1	127.6	121.4	122.8	120.0	121.3	4.7	3.5	-7.6				
I	1	106.4	120.9	120.5	126.0	125.4	120.3	122.0	119.4	121.0	4.9	5.5	-6.0				
	2	106.9	123.1	120.6	127.5	126.4	121.2	123.5	121.3	122.8	5.8	6.5	-5.1				
I-1	1	106.7	121.8	120.6	125.3	124.1	119.0	120.9	118.5	119.8	3.5	5.5	-5.6				
H	1	92.3	109.5	105.4	112.9	110.4	107.8	109.2	107.8	110.3	5.0	14.5	-2.6				
	2	96.1	111.8	108.8	116.3	114.8	113.4	113.9	112.6	114.5	6.0	14.0	-2.2				
	3	93.2	109.0	104.9	114.3	111.6	105.8	107.3	105.2	107.6	6.7	6.0	-6.4				
M	1*	97.9	113.1	112.5	117.9	116.5	109.2	110.9	109.7	111.8	4.0	5.0	-6.8				
	2	103.1	118.6	117.2	121.7	120.2	118.0	119.0	116.6	117.4	3.0	8.0	-3.6				
L	1	95.1	111.3	108.8	115.5	113.8	110.7	111.9	111.1	112.5	5.0	11.0	-2.7				
	2	95.4	111.5	107.6	115.5	114.2	110.0	111.9	110.3	113.1	6.6	11.5	-3.9				
Average														4.6			
(b) Station 2																	
A	1*	93.1	109.8	107.8	113.6	112.1	111.7	113.1	111.3	111.7	4.3	13.5	-0.8				
	2	93.9	109.8	108.4	114.0	113.8	110.1	110.7	111.1	112.8	5.4	13.5	-2.7				
	3	95.1	111.0	109.6	116.6	114.7	111.0	113.3	111.6	114.1	5.1	13.0	-3.1				
A-1	1	95.6	111.9	110.4	117.3	115.6	111.5	111.6	111.3	113.2	5.2	8.5	-4.3				
	2	92.1	107.6	105.4	111.6	110.7	106.8	107.6	108.5	109.8	5.3	12.0	-2.2				
	3	90.3	107.5	104.8	111.0	109.5	101.6	104.0	108.0	109.1	4.7	13.5	-1.5				
G	1	85.3	99.0	97.6	103.1	102.8	99.1	99.8	98.7	100.6	5.2	9.0	-4.1				
	2	82.7	96.1	91.2	98.5	97.9	93.0	94.9	91.7	94.3	6.7	6.5	-6.2				
G-1	1	76.4	90.6	86.5	93.9	92.8	89.8	91.2	89.0	90.0	6.3	8.0	-3.8				
	2	77.0	93.2	89.6	97.9	96.1	93.0	95.1	92.3	94.1	6.5	9.5	-3.8				
I	1	83.9	97.5	96.0	101.4	100.6	100.6	101.1	101.1	100.9	4.6	16.0	-5				
	2	83.4	97.5	95.2	101.1	100.4	100.7	101.2	100.9	102.1	5.2	22.0	.5				
I-1	1	76.5	93.0	89.1	95.9	94.7	86.3	85.9	90.8	92.5	5.6	9.0	-3.9				
H	1	82.0	97.2	93.8	100.6	100.4	94.8	95.4	96.3	98.0	6.6	8.5	-4.1				
	2	81.3	98.3	94.9	102.5	101.6	96.8	98.1	95.6	97.2	6.7	5.5	-6.0				
	3	81.9	95.7	93.4	97.8	98.3	94.6	97.2	95.4	97.7	4.9	13.0	-2.9				
M	1	82.9	99.8	96.4	102.4	101.4	97.5	98.0	100.4	102.0	5.0	17.5	-1.0				
	2	83.4	99.8	97.1	105.2	103.8	99.2	101.9	97.4	99.8	6.7	6.0	-6.4				
L	1	85.0	101.6	98.3	105.3	104.1	99.8	101.0	102.6	104.5	5.8	16.5	-1.5				
	2	85.5	101.8	99.0	104.9	104.2	99.6	100.9	102.6	104.8	5.2	17.5	-1.6				
Average														5.6			
(c) Station 3																	
A	1*	84.5	101.3	98.7	103.9	102.6	103.0	104.7	102.5	103.4	3.9	18.0	-0.1				
	2	88.7	104.5	102.0	110.3	108.2	104.7	107.3	104.0	105.7	6.2	8.5	-4.2				
	3	86.6	102.2	100.5	105.7	105.2	101.5	103.2	102.4	104.7	4.7	13.5	-2.8				
A-1	1	88.0	104.2	102.0	109.2	108.5	102.6	104.4	101.8	104.1	6.5	5.5	-6.7				
	2	89.7	104.3	103.7	110.0	108.8	100.7	103.1	99.5	101.9	5.1	3.0	-9.3				
	3	85.6	102.5	99.7	106.6	105.5	99.7	101.3	101.1	103.5	5.8	9.5	-4.4				
G	1	84.1	96.9	95.3	100.6	100.1	98.0	99.4	99.8	101.6	4.8	21.5	-3				
	2	85.3	97.7	95.4	100.8	102.1	96.7	99.8	99.2	102.0	6.7	14.5	-2.9				
G-1	1	84.5	97.3	96.7	101.5	103.4	94.2	98.2	93.1	95.6	6.7	2.5	-10.3				
	2	83.2	95.5	93.7	99.6	99.6	95.4	97.4	96.6	98.8	5.9	12.5	-3.0				
I	1	85.5	98.4	96.5	104.5	103.2	96.7	100.5	97.0	101.0	6.7	9.0	-6.2				
	2	83.7	97.2	95.7	101.2	101.1	97.7	100.4	96.8	99.8	5.4	11.0	-4.3				
I-1	1	82.2	94.1	92.8	98.9	99.4	94.6	96.5	95.7	98.6	6.6	12.5	-3.7				
H	1	86.8	98.9	97.7	103.8	104.2	97.8	99.8	100.8	104.1	6.5	14.5	-3.4				
	2	84.8	97.9	95.2	101.0	101.9	96.2	98.5	96.0	99.5	6.7	8.5	-5.9				
	3	85.3	97.3	95.9	100.7	102.3	92.2	95.0	94.1	97.1	6.4	4.5	-8.2				
M	1	86.0	100.4	99.1	105.7	104.6	101.1	102.4	101.9	104.4	5.5	14.5	-2.7				
	2	86.8	100.8	99.6	104.8	105.6	97.5	98.5	99.7	103.1	6.0	8.5	-5.9				
L	1*	80.9†	95.6	93.6	101.4	100.0	93.8	96.2	94.3	97.2	6.4	8.0	-5.7				
	2	83.8	98.3	96.4	101.7	100.6	98.9	99.3	99.8	100.8	4.2	15.5	-.8				
Average														5.8			

\*Disregarded in computing averages.  
†OASPL data not available.

TABLE 8.- SPATIAL COORDINATES AND ENGINE CHARACTERISTICS AT FLYOVER

Profile	Run	Station 1					Station 2					Station 3				
		Altitude, ft	Airspeed, knots,	FG, lb	N <sub>2</sub> , percent <sup>1</sup>	Lateral displace- ment, ft	Altitude, ft	Airspeed, knots	FG, lb	N <sub>2</sub> , percent <sup>1</sup>	Lateral displace- ment, ft	Altitude, ft	Airspeed, knots	FG, lb	N <sub>2</sub> , percent <sup>1</sup>	Lateral displace- ment, ft
A	1	340	118	23,500	86.5	8	1,000	118	25,000 <sup>2</sup>	88 <sup>2</sup>	120	(3)	(3)	(3)	(3)	20
	2	350	118	25,000	87.5	30	1,030	118	24,000	87.0	70	1,490	118.5	23,500	88	120
	3	360	118	23,000	86.0	35	1,030	118.5	25,000	87.5	70	1,500	119	21,000	86.7	60
A-1	1	360	141	22,800	83.5	10	1,020	140	33,000 <sup>2</sup>	87.3 <sup>2</sup>	40	1,510	141	25,500	85.5	200
	2	370	141	25,000	84.3	3	1,030	141	17,000 <sup>4</sup>	82.0 <sup>4</sup>	100	1,460	140	22,500 <sup>4</sup>	84.0 <sup>4</sup>	570
	3	360	(3)	(3)	(3)	20	1,040	140	23,400	84.0	35	1,500	140.5	21,000	83.2	140
G	1	320	110	16,000 <sup>4</sup>	84 <sup>4</sup>	55	1,780	116	8,000 <sup>4</sup>	73 <sup>4</sup>	50	2,400 <sup>5</sup>	112.5	32,000 <sup>5</sup>	92 <sup>5</sup>	10
	2	330	106.5	18,000 <sup>4</sup>	85 <sup>4</sup>	50	1,800	116	4,000 <sup>4</sup>	69 <sup>4</sup>	30	2,390	108	31,500	92	80
G-1	1	340	135	29,000	85	45	1,820	138	5,000	62	30	2,415	138	31,000	88.5	110
	2	340	134.5	28,000	85	20	1,850	140	4,900	60	40	2,340	136	31,800	88.4	270
I	1	310	112.5	15,500 <sup>4</sup>	81 <sup>4</sup>	70	1,760	112	13,500	82	70	2,400	110.5	32,300	92	20
	2	340	104	22,000 <sup>4</sup>	85.2 <sup>4</sup>	40	1,740	106.5	13,700	81	30	2,600	107	26,500	89.6	150
I-1	1	370	133	22,000 <sup>4</sup>	82.0	10	1,820	136.5	4,500	60	35	2,360	134.5	29,900	87.8	10
H	1	475	112.5	6,000	66.5 <sup>2</sup>	10	2,000	111.5	6,500	70.5 <sup>4</sup>	10	2,400	109.5	33,000	90.5	125
	2	480	110	7,300	70.0	25	2,030	111	11,400	79.3	25	2,420	109.5	26,000 <sup>2</sup>	89.0	70
	3	480	110.5	4,100	59.0	30	1,970	108.5	7,000	72.0 <sup>4</sup>	60	2,590	105.5	32,200	92.5	60
M	1	310	133	20,000	84.5	50	1,460	152	11,500	79.0	80	1,850	150.5	31,000	88.0	160
	2	350	135	13,500	79.0	5	1,450	151	6,900	69.0	30	2,090	150	32,000	91.5	165
L	1	550	127	8,300	75.0	70	1,540	151.5	15,000	81.5	30	2,090	151	23,500	88.0	60
	2	540	126.5	7,000	71.4	30	1,540	150	14,500	81.8	60	1,970	150	27,500	89.5	130

<sup>1</sup>100 percent N<sub>2</sub> = 9,655 RPM.<sup>2</sup>Power coming off.<sup>3</sup>Data not available.<sup>4</sup>Power coming on.<sup>5</sup>Exact data not available.



TABLE 9.- COMPARISON OF APPROXIMATED AND INTEGRATED EPNL, AND OF FAA AND KRYTER-PEARSONS EPNL

Profile	Run	Approximated minus integrated EPNL (9) - (8)			FAA minus Kryter-Pearsons EPNL (8) - (6)		
		Station 1	Station 2	Station 3	Station 1	Station 2	Station 3
A	1	---	---	---	---	---	---
	2	1.4	1.7	1.7	-1.1	1.0	-0.7
	3	2.0	2.5	2.3	-.6	.6	.9
A-1	1	1.1	1.9	2.3	-.1	-.2	-.8
	2	1.6	1.3	2.4	.4	1.7	-1.2
	3	1.6	1.1	2.4	-.7	6.4	3.4
G	1	---	1.9	1.8	---	-.4	1.8
	2	1.9	2.6	2.8	.7	-1.3	2.5
G-1	1	1.6	1.0	2.5	-.2	-.8	-1.1
	2	1.3	1.8	2.2	-1.4	-.7	1.2
I	1	1.6	-.2	4.0	-.9	.5	.3
	2	1.5	1.2	3.0	.1	.2	-.9
I-1	1	1.3	1.7	2.9	-.5	4.5	1.1
H	1	2.5	1.7	3.3	.0	1.5	3.0
	2	1.9	1.6	3.5	-.8	-1.2	-.2
	3	2.4	2.3	3.0	-.6	.8	1.9
M	1	---	1.6	2.5	---	2.9	.8
	2	.8	2.4	3.4	-1.4	-1.8	2.2
L	1	1.4	1.9	---	.4	2.8	---
	2	2.8	2.2	1.0	.3	3.0	.9
Averages		1.7	1.7	2.6	-.38	1.03	.84

TABLE 10.- AVERAGED NOISE MEASUREMENT DATA

Station	Profile	Max dB(c), dB	PNLP, PNdB	PNLM, PNdB	PNLTM (FAA), PNdB	Integrated EPNL (FAA), EPNdB	Approximated EPNL (FAA), EPNdB	Integrated EPNL variation, EPNdB
1	A*	106.5	122.5	121.0	125.5	120.0	121.7	1.4
	A-1	106.5	122.7	120.7	124.6	117.9	119.3	1.7
	G*	104.1	118.9	117.9	121.4	115.5	117.4	---†
	G-1	108.3	123.2	122.5	127.2	120.0	121.5	.0
	I	106.7	122.0	120.6	125.9	120.4	121.9	1.9†
	I-1	106.7	121.8	120.6	124.1	118.5	119.8	---†
	H	93.9	110.1	106.3	112.3	108.5	110.8	7.4†
	M*	103.1	118.6	117.2	120.2	116.6	117.4	---
	L	95.3	111.4	108.2	114.0	110.7	112.8	.8
2	A*	94.5	110.4	109.0	114.3	111.4	113.5	.5
	A-1	92.7	109.0	106.9	111.9	109.3	110.7	3.3†
	G	84.0	97.6	94.4	100.4	95.2	97.5	7.0†
	G-1	76.7	91.9	88.1	94.5	90.7	92.1	3.3
	I	83.7	97.5	95.6	100.5	100.5	101.5	.2
	I-1	76.5	93.0	89.1	94.7	90.8	92.5	---
	H	81.7	97.1	94.0	100.1	95.8	97.6	.9†
	M	83.2	99.8	96.8	102.6	98.9	100.9	3.0
	L	85.3	101.7	98.7	104.2	102.6	104.7	.0
3	A*	87.7	103.4	101.3	106.7	103.2	105.2	1.6
	A-1	87.8	103.7	101.8	107.6	100.8	103.2	2.3†
	G	84.7	97.3	95.4	101.1	99.5	101.8	.6
	G-1	83.9	96.4	95.2	101.5	94.9	97.2	3.5
	I	84.6	97.8	96.1	102.2	96.9	100.4	.2
	I-1	82.2	94.1	92.8	99.4	95.7	98.6	---
	H	85.6	98.0	96.3	102.8	97.0	100.2	6.7†
	M	86.4	100.6	99.4	105.1	100.8	103.8	2.2
	L*	83.8	98.3	96.4	100.6	99.8	100.8	---

\*Profiles for which some data were disregarded.

†Data taken during unsteady throttle activity.

TABLE 11.- AVERAGED NOISE REDUCTION DATA

Station	Profile	Max dB(c), dB	PNLP, PNdB	PNLM, PNdB	PNLTM (FAA), PNdB	Integrated EPNL (FAA), EPNdB	Approximated EPNL (FAA), EPNdB
1	A	---	---	---	---	---	---
	A-1	---	---	---	---	---	---
	G	-2.4	-3.6	-3.1	-4.1	-4.5	-4.3
	G-1	1.8	.5	1.8	2.6	2.1	2.2
	I	.2	-.5	-.4	.4	.4	.2
	I-1	.2	-.9	-.1	-.5	.6	.5
	H	-12.6	-12.4	-14.7	-13.2	-11.5	-10.9
	M	-3.4	-3.9	-3.8	-5.3	-3.4	-4.3
	L	-12.2	-11.1	-12.8	-11.5	-9.3	-8.9
2	A	---	---	---	---	---	---
	A-1	---	---	---	---	---	---
	G	-10.5	-12.8	-14.6	-13.9	-16.2	-16.0
	G-1	-16.0	-17.1	-18.8	-17.4	-18.6	-18.6
	I	-10.8	-12.9	-13.4	-13.8	-10.9	-12.0
	I-1	-16.2	-16.0	-17.8	-17.2	-18.5	-18.2
	H	-12.8	-13.3	-15.0	-13.2	-15.6	-15.9
	M	-11.3	-10.6	-12.2	-11.7	-12.5	-12.6
	L	-9.2	-8.7	-10.3	-10.1	-8.8	-8.8
3	A	---	---	---	---	---	---
	A-1	---	---	---	---	---	---
	G	-3.0	-6.1	-5.9	-5.6	-3.7	-3.4
	G-1	-3.9	-7.3	-6.6	-6.1	-5.9	-6.0
	I	-3.1	-5.6	-5.2	-4.5	-6.3	-4.8
	I-1	-5.6	-9.6	-9.0	-8.2	-5.1	-4.6
	H	-2.1	-5.4	-5.0	-3.9	-6.2	-5.0
	M	-1.3	-2.8	-1.9	-1.6	-2.4	-1.4
	L	-3.9	-5.1	-4.9	-6.1	-3.4	-4.4





Figure 1.- Boeing 367-80 airplane.



Figure 2.- Boeing 367-80 airplane cockpit.

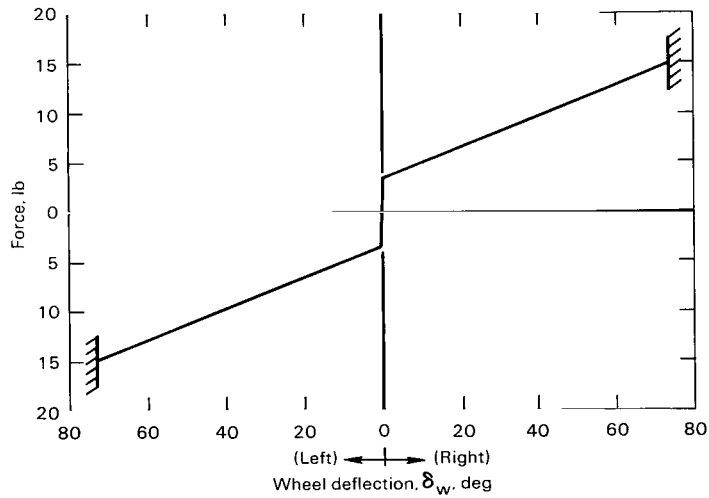
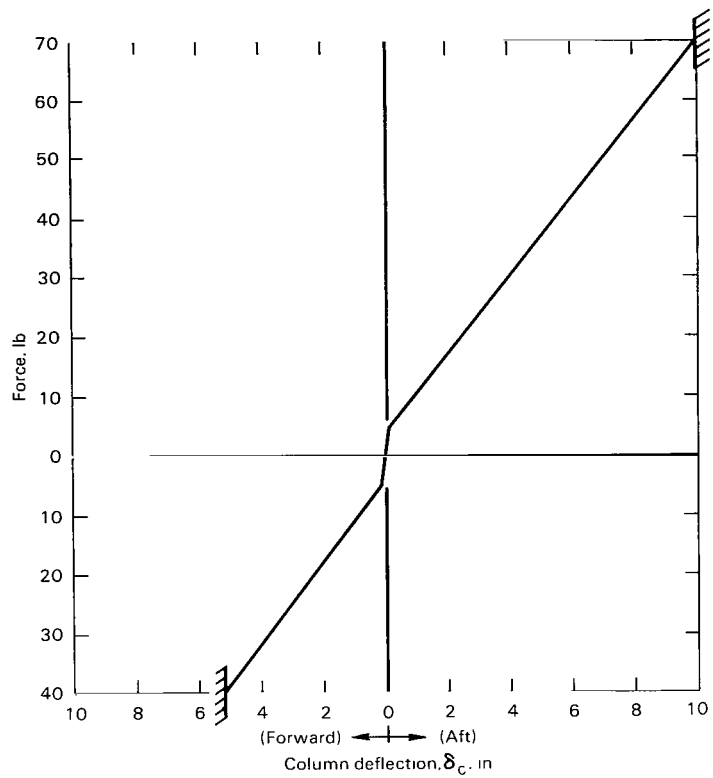


Figure 3.- Control force variation with deflection.

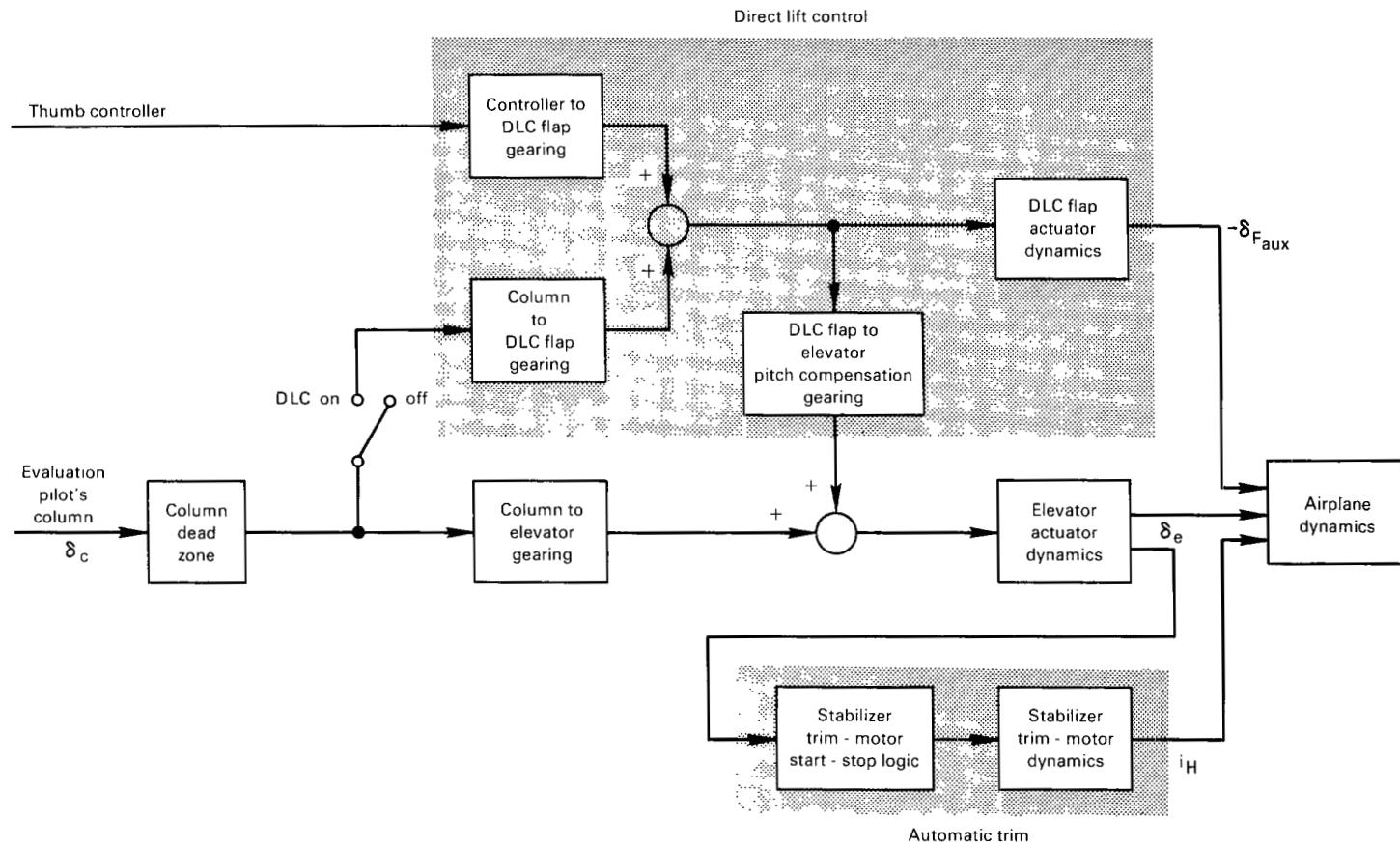


Figure 4.- Block diagram of basic airplane, direct lift control, and automatic trim systems.



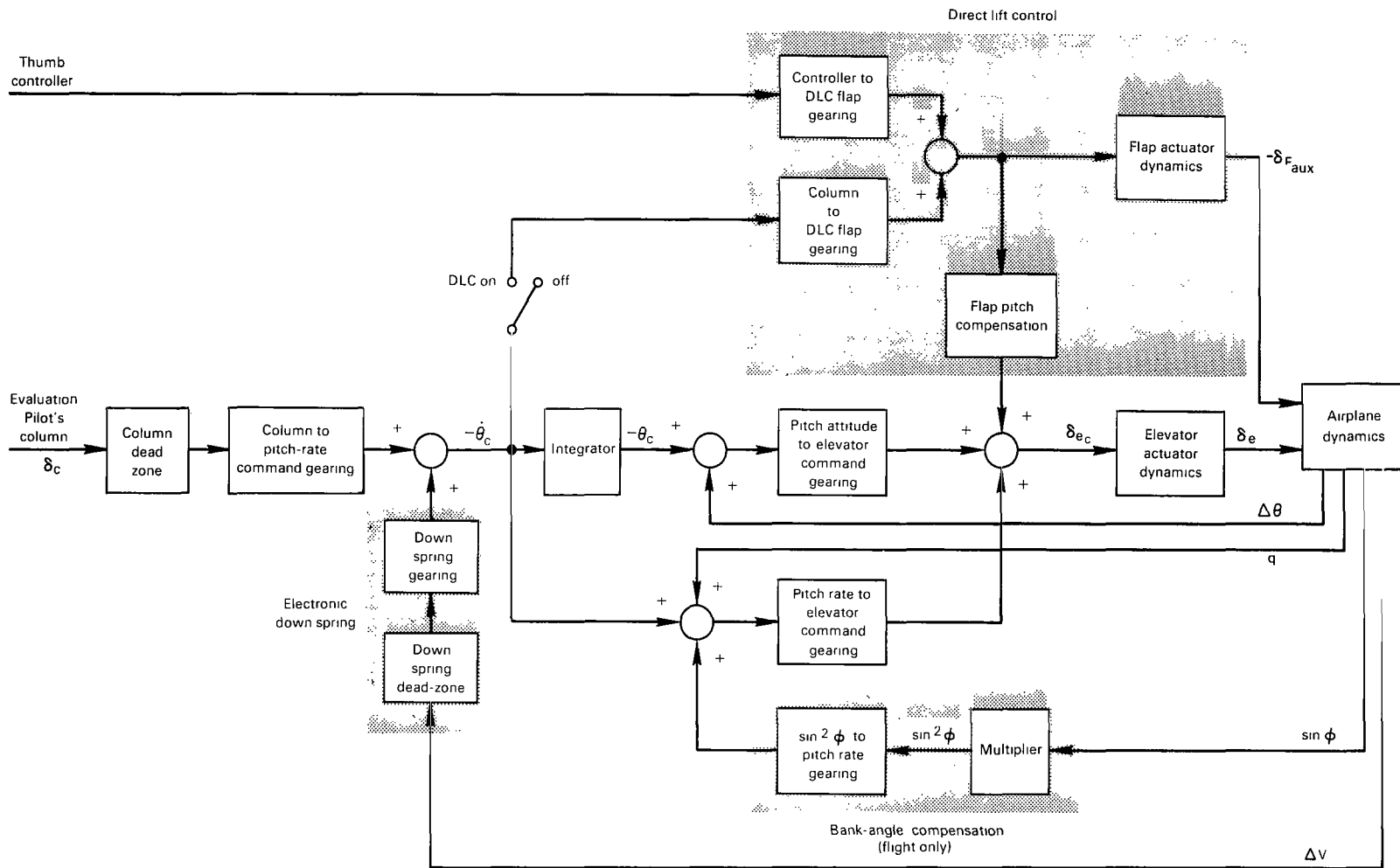
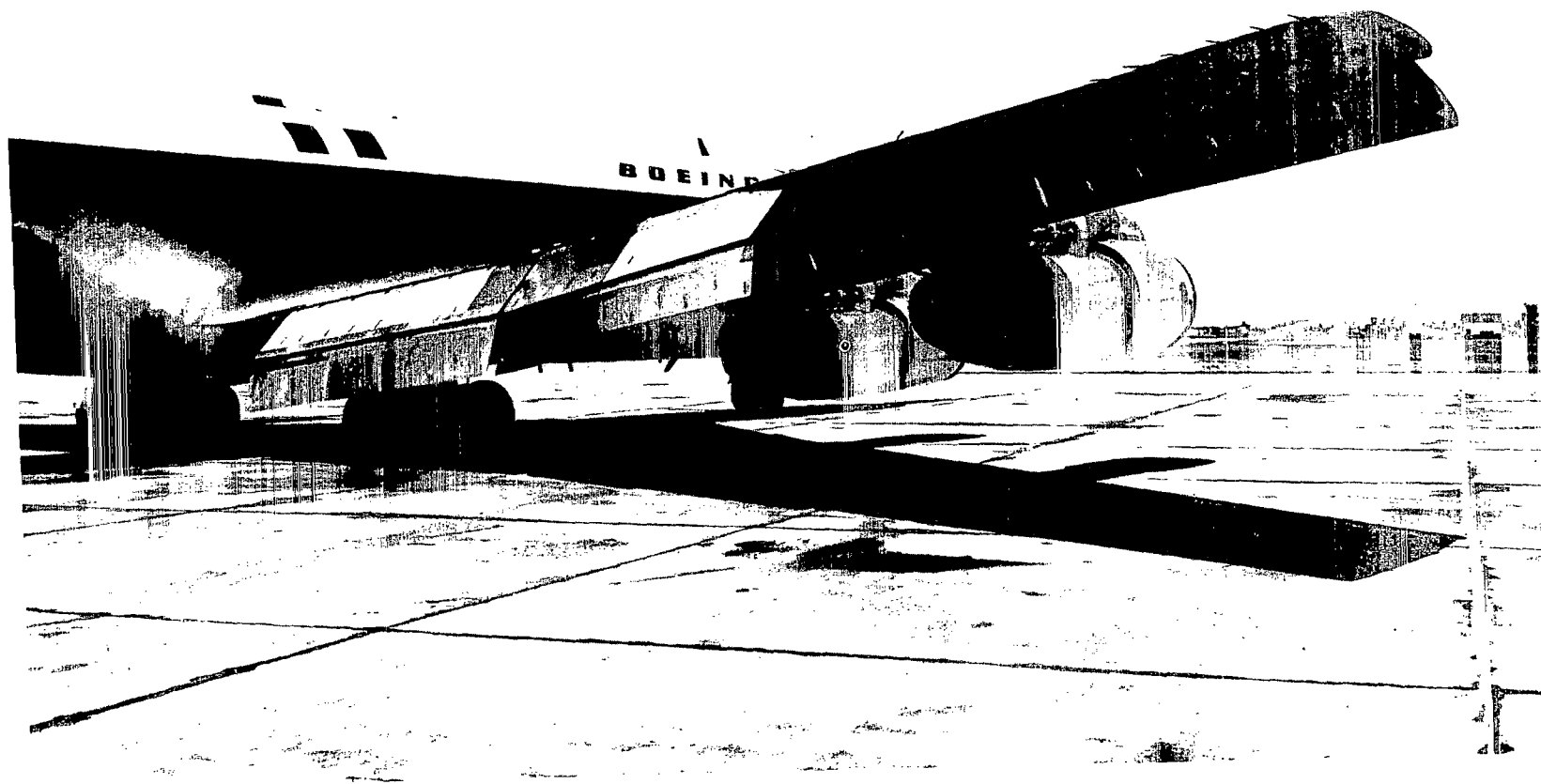
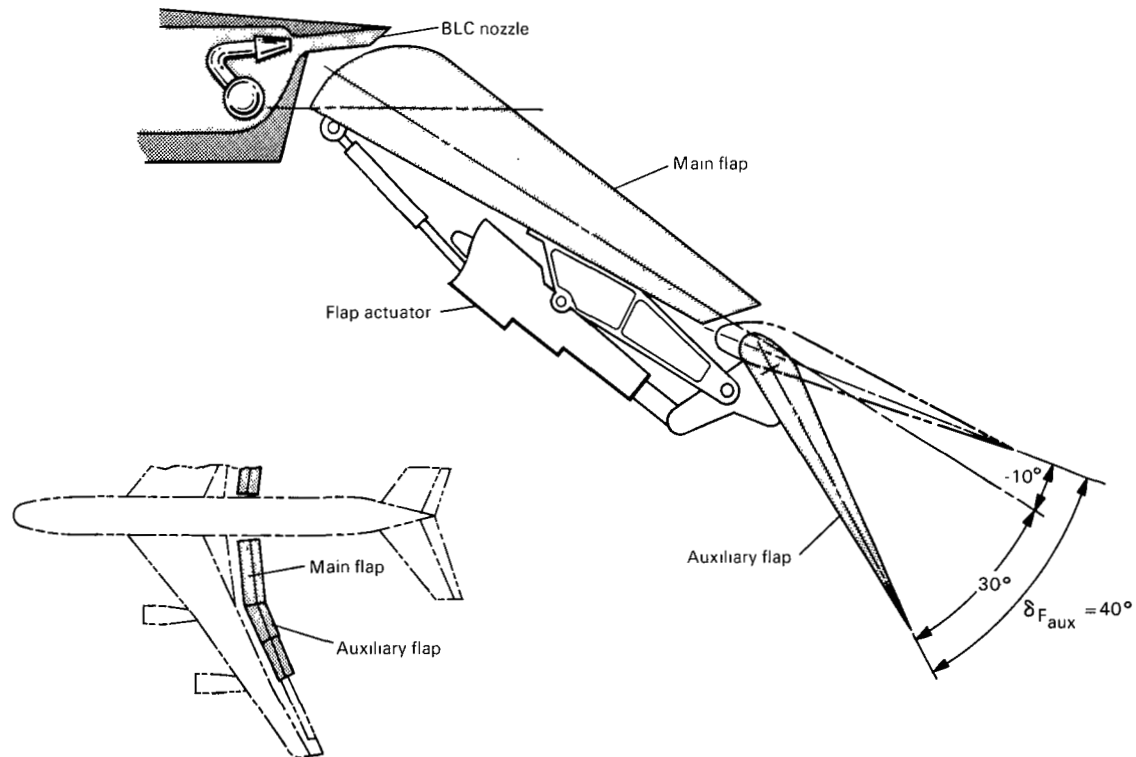


Figure 5.- Block diagram of direct lift control system and pitch rate — command system with attitude hold.



(a) Flap installation.

Figure 6.- Modified flap system.



(b) Flap details.

Figure 6.- Concluded.

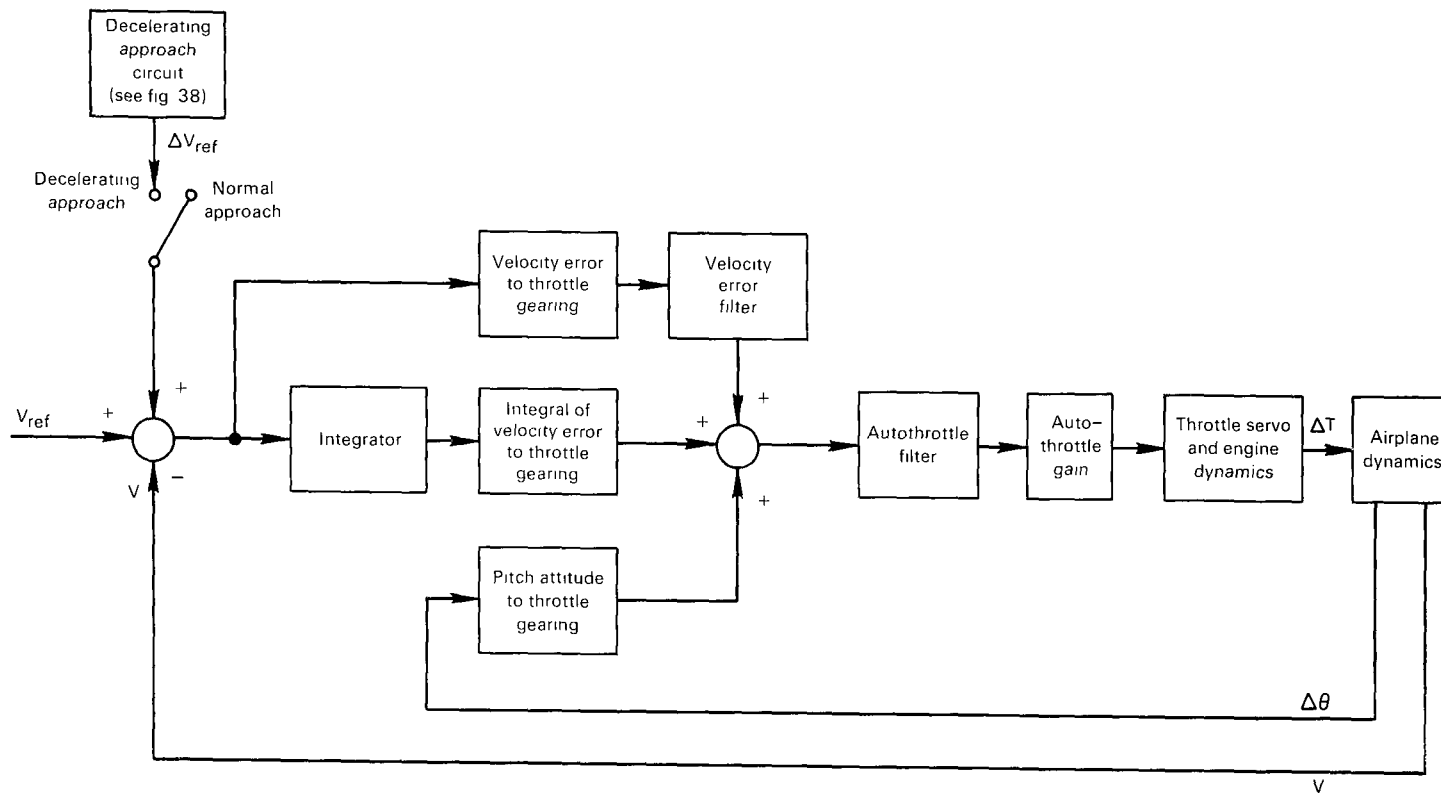


Figure 7.- Block diagram of autothrottle.



Figure 8.- Airplane cockpit showing EADI installation.

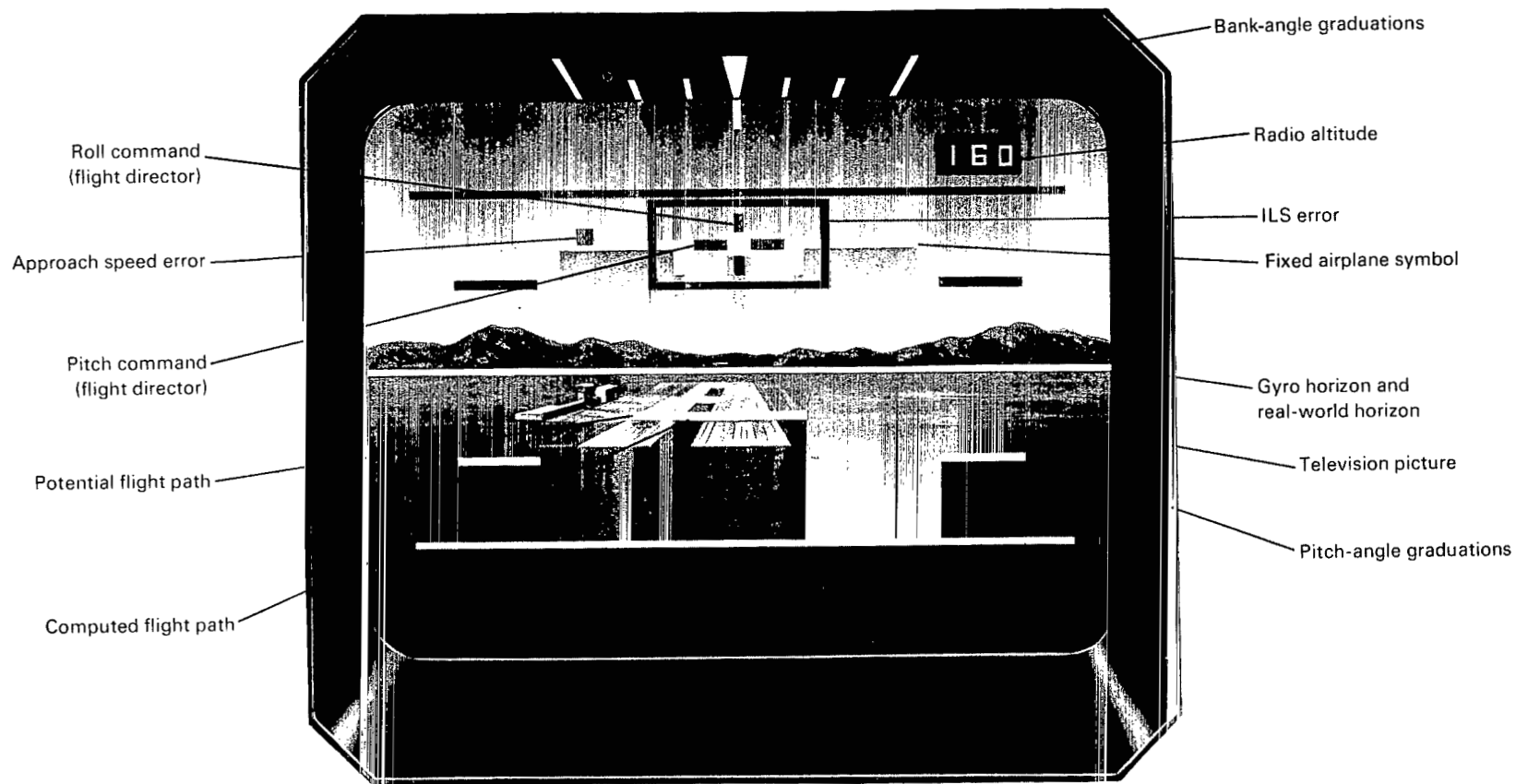
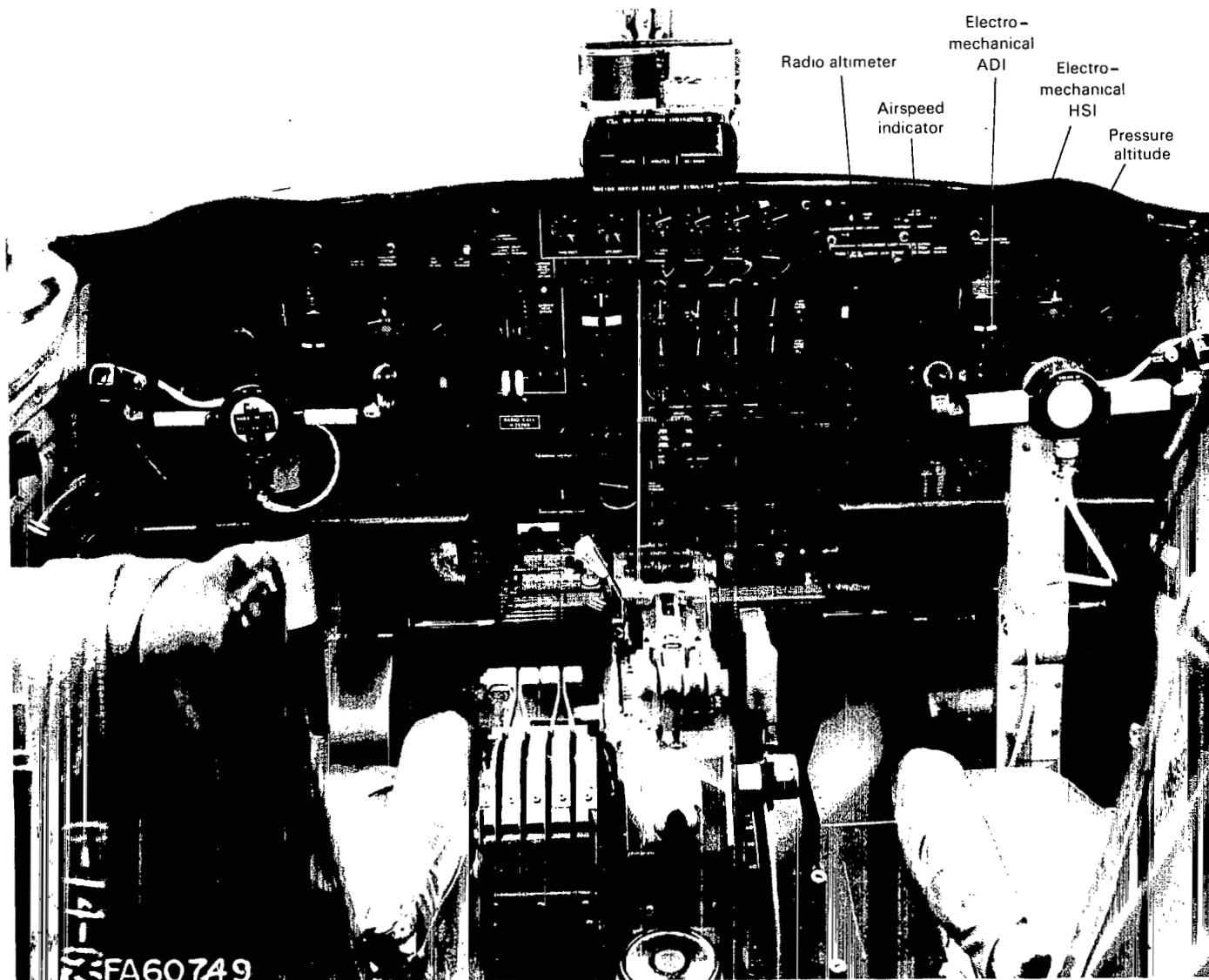


Figure 9.- Electronic attitude director indicator.



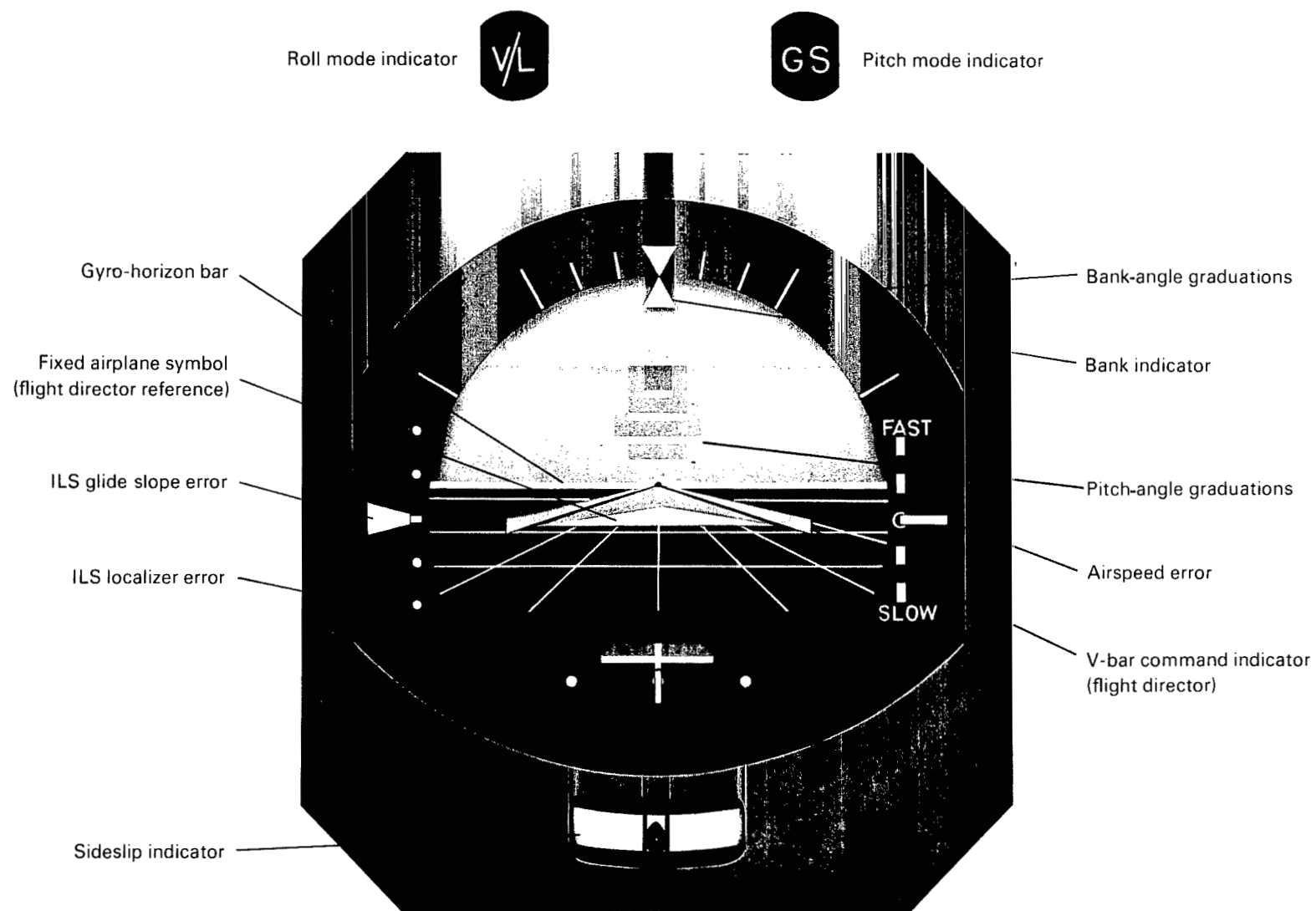
Figure 10.- Closed-circuit television camera on airplane.



(a) Cockpit installation.

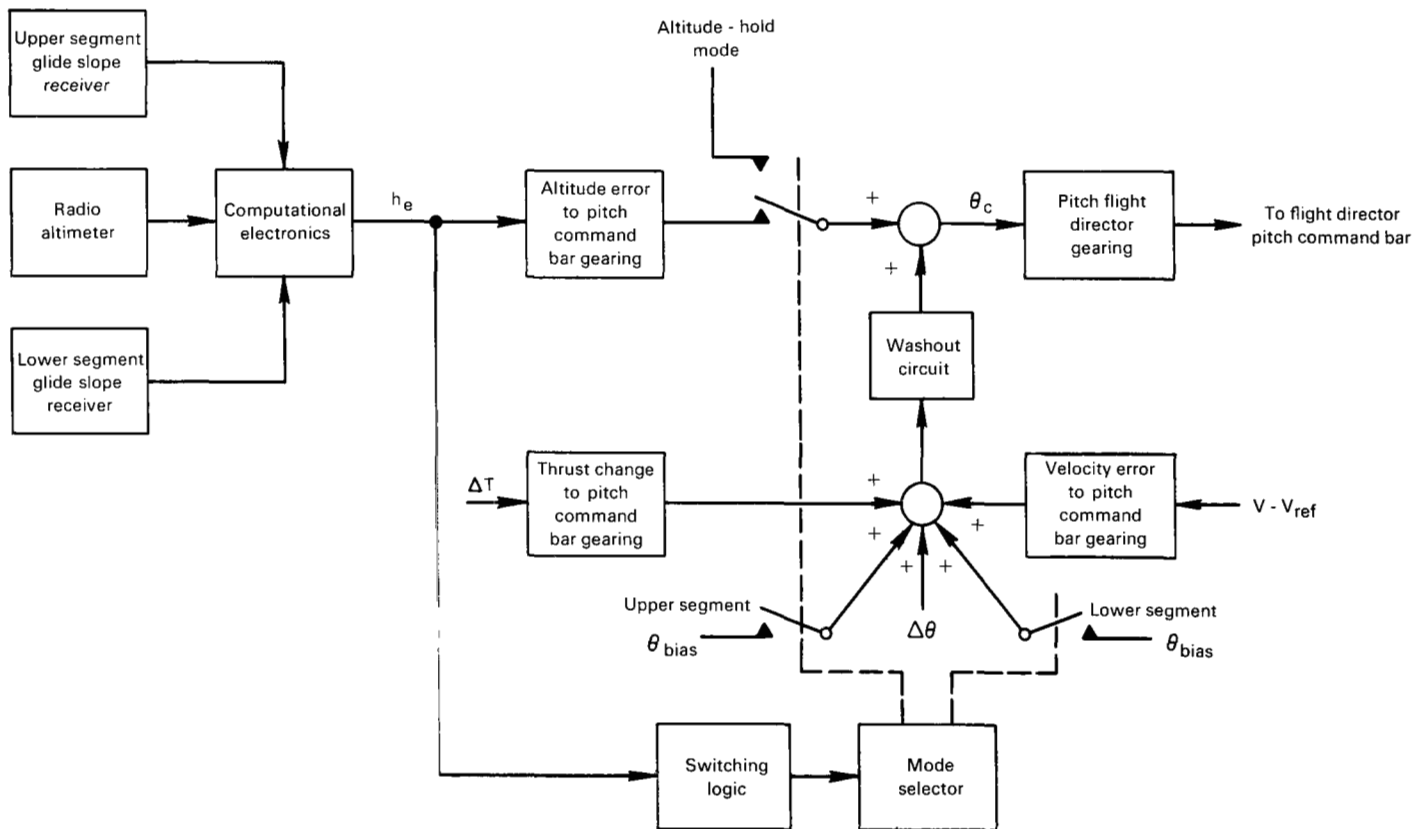
Figure 11.- Electromechanical attitude director indicator.





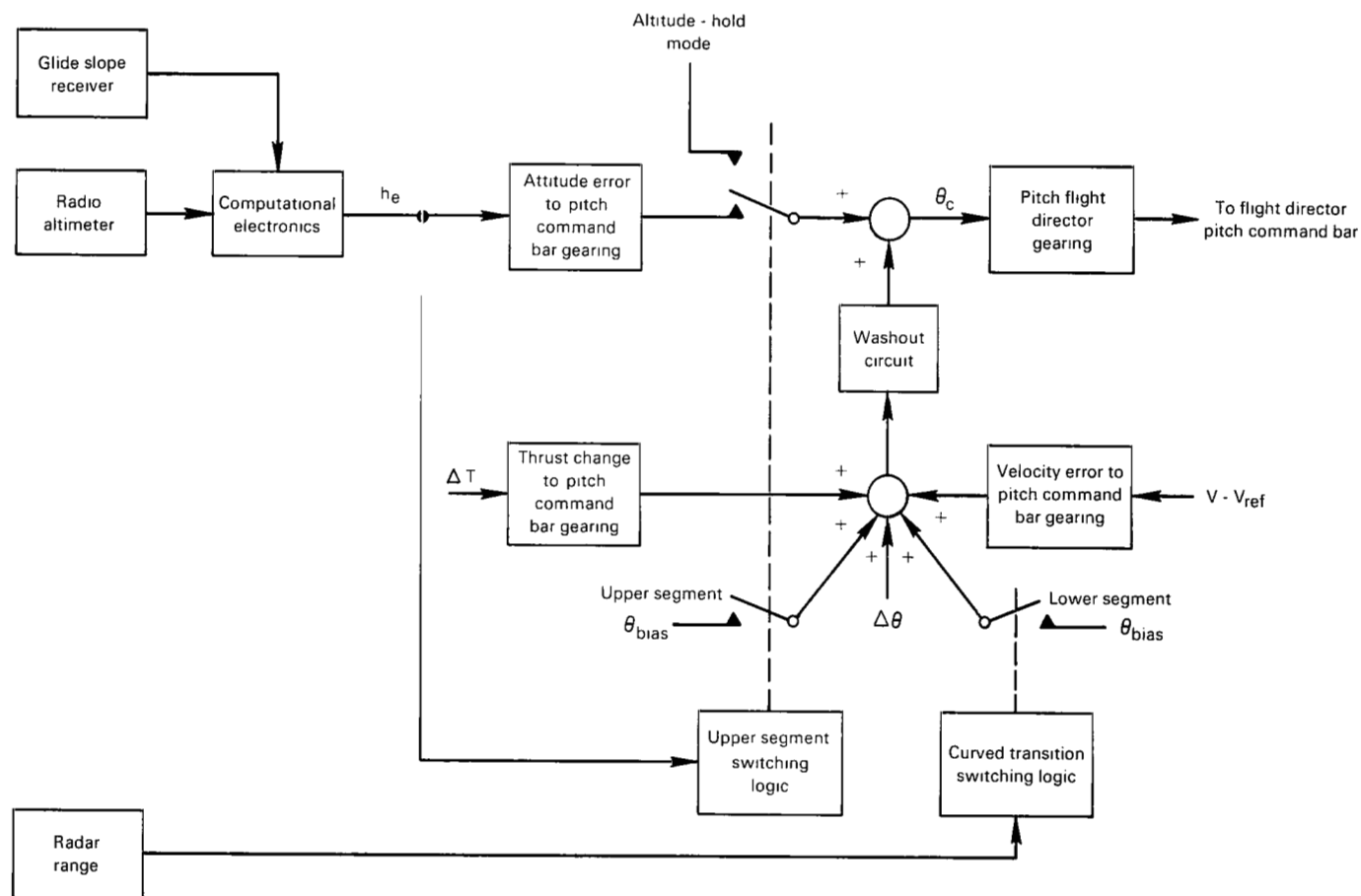
(b) Details of electromechanical ADI.

Figure 11.- Concluded.



(a) Two ILS beam guidance system.

Figure 12.- Block diagram of pitch axis flight director.



(b) Single ILS beam guidance system.

Figure 12.- Concluded.

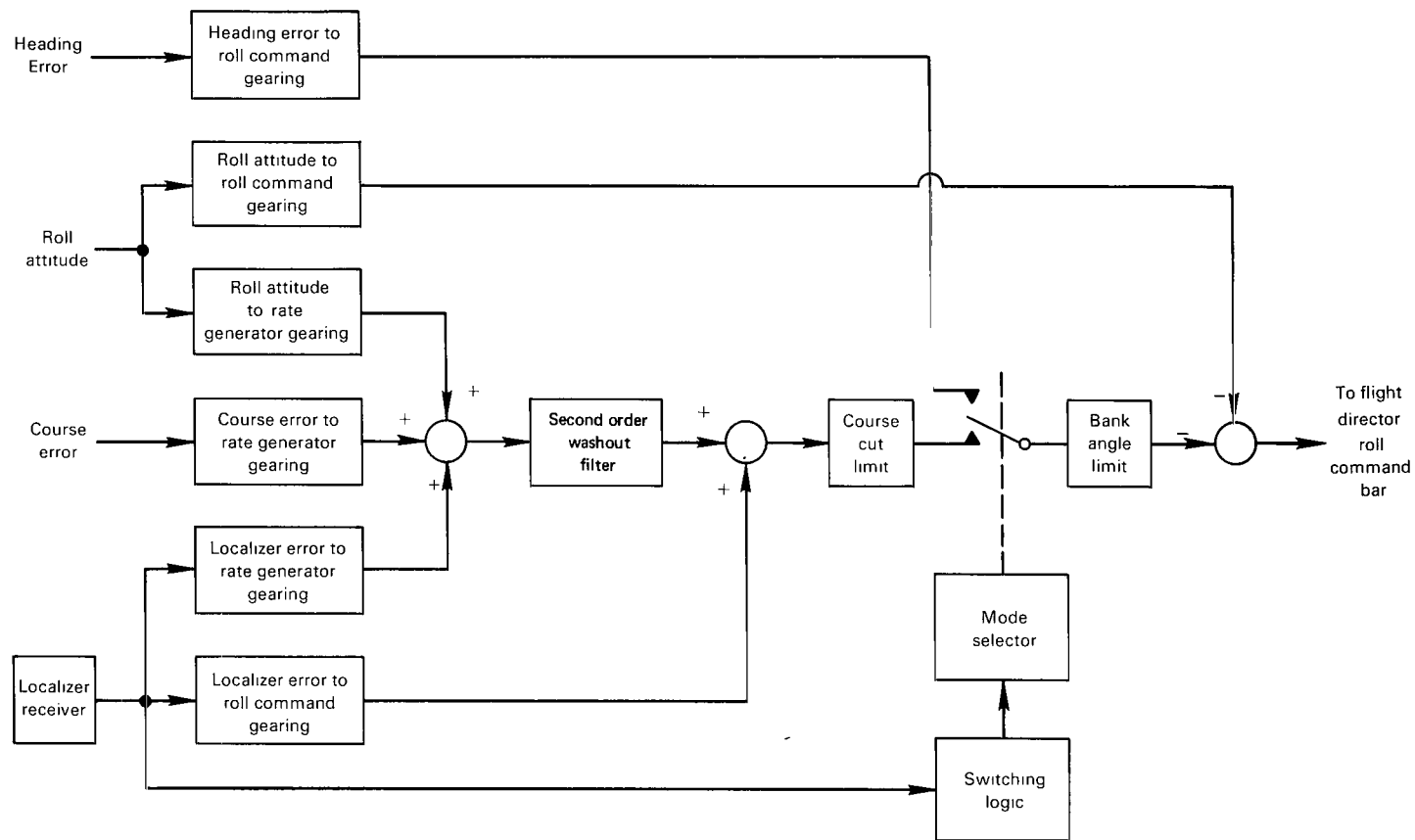


Figure 13.- Block diagram of lateral flight director.

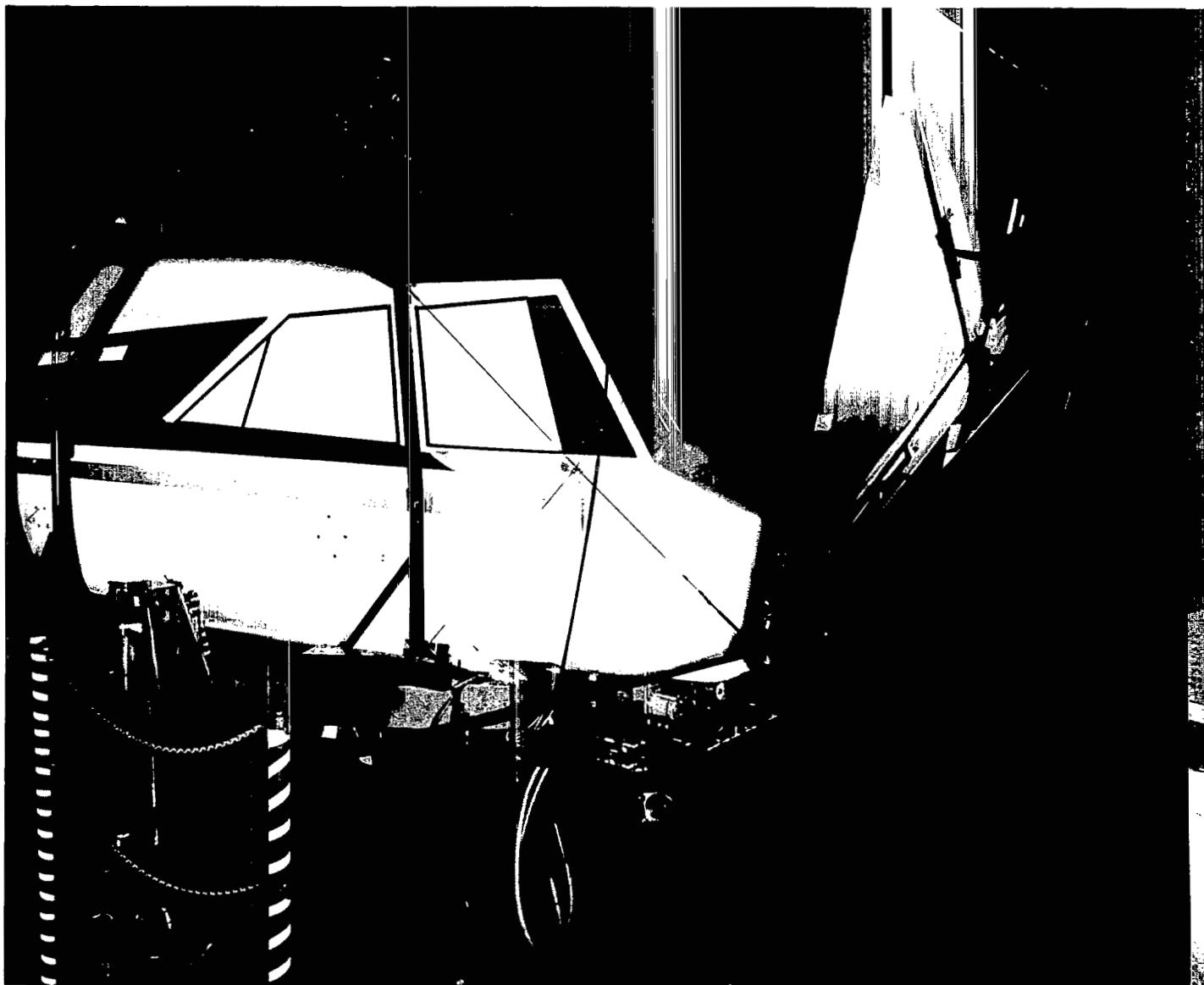


Figure 14.- Ground-based simulator.

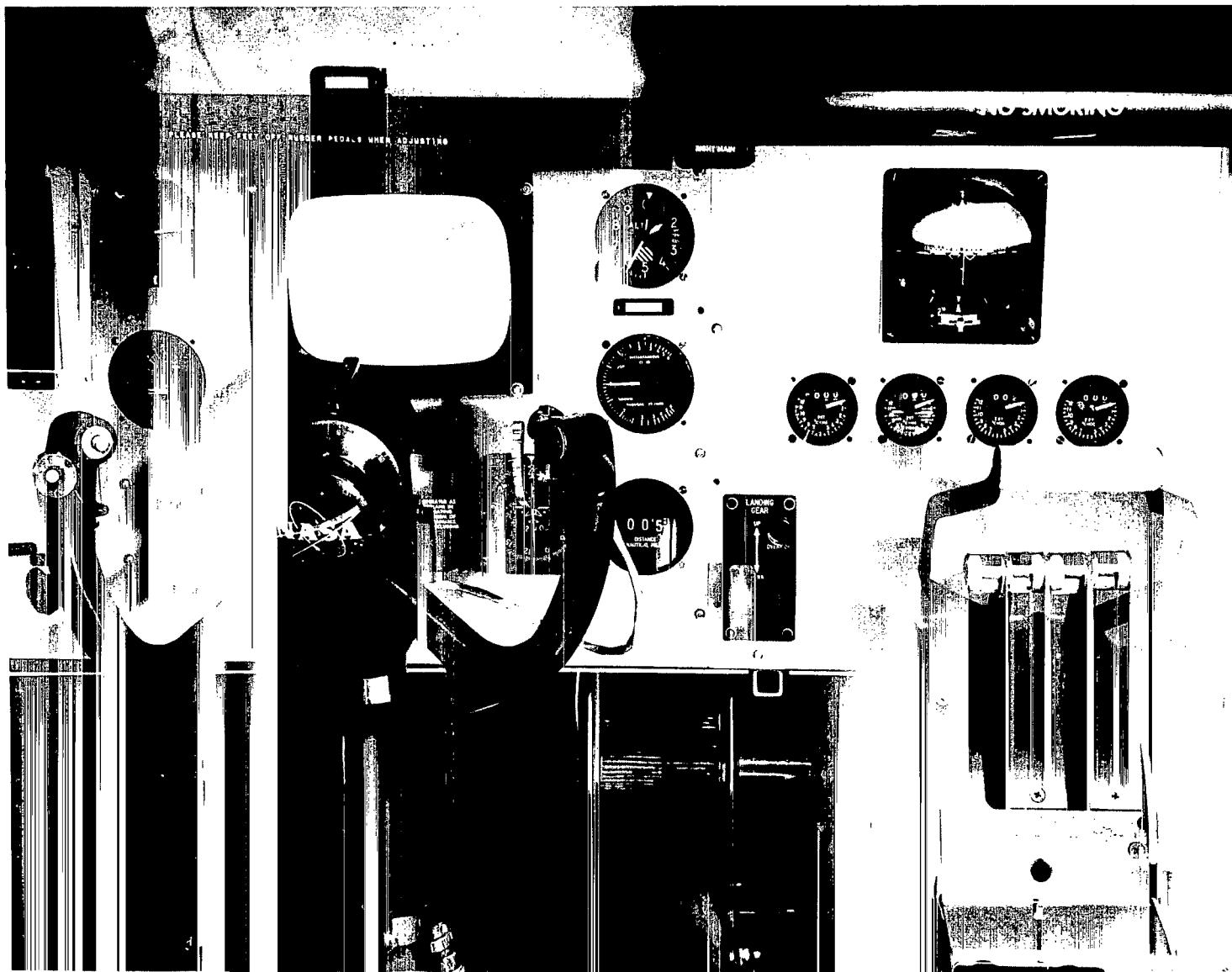


Figure 15.- Ground-based simulator cockpit.

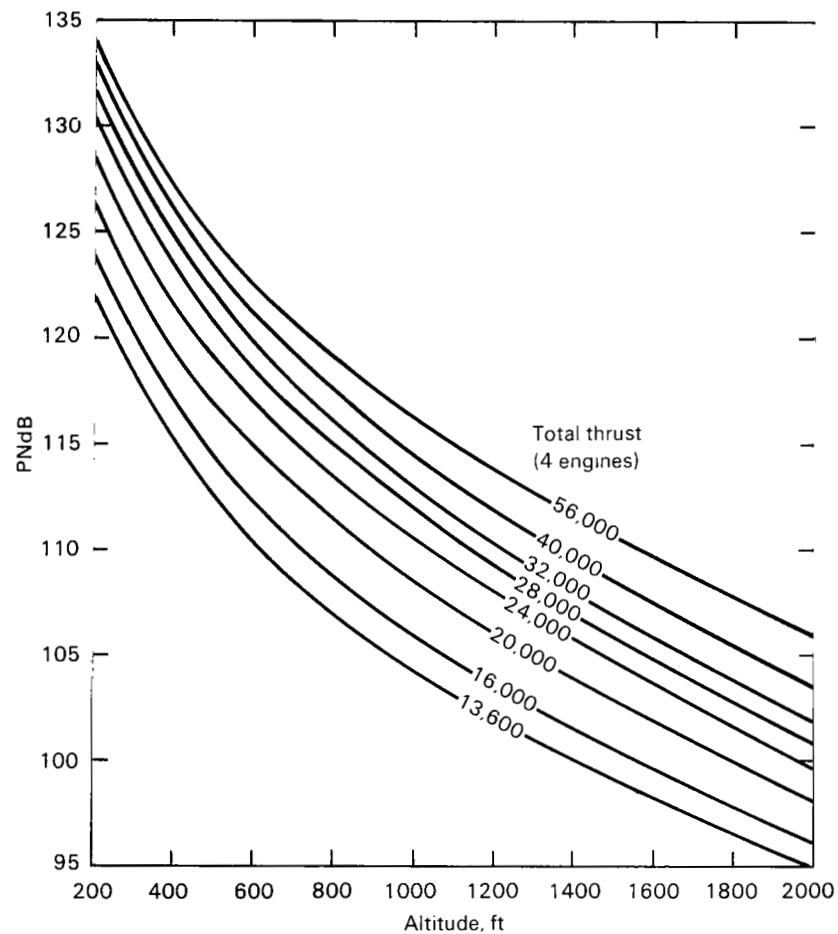


Figure 16.- Noise data for fan-jet engine simulation.

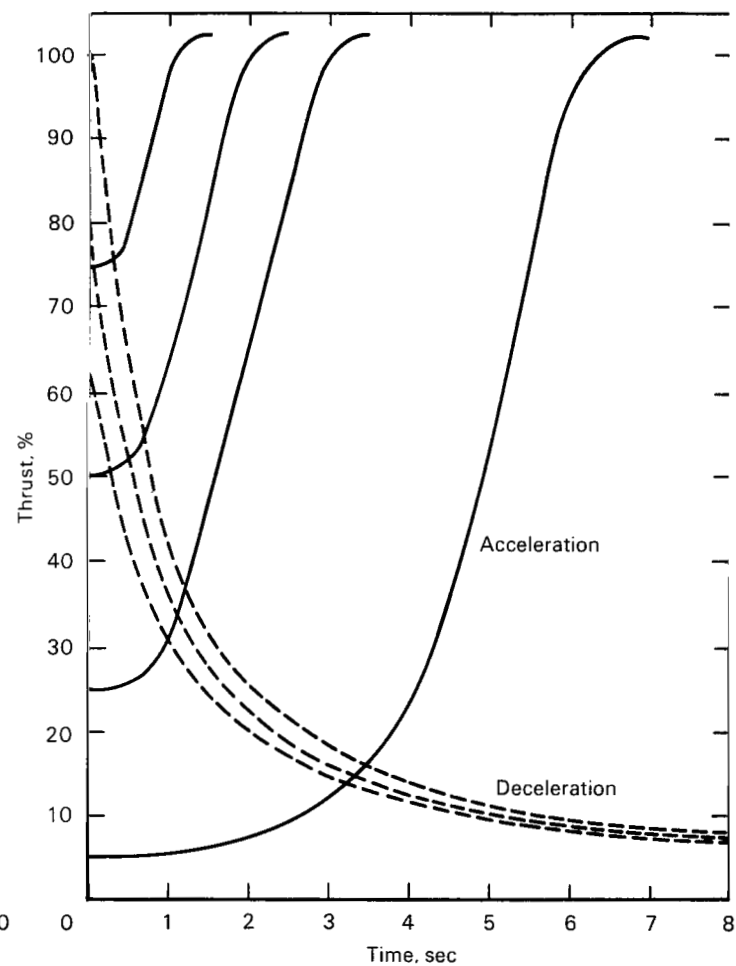


Figure 17.- Simulated fan-jet engine response to step throttle commands.

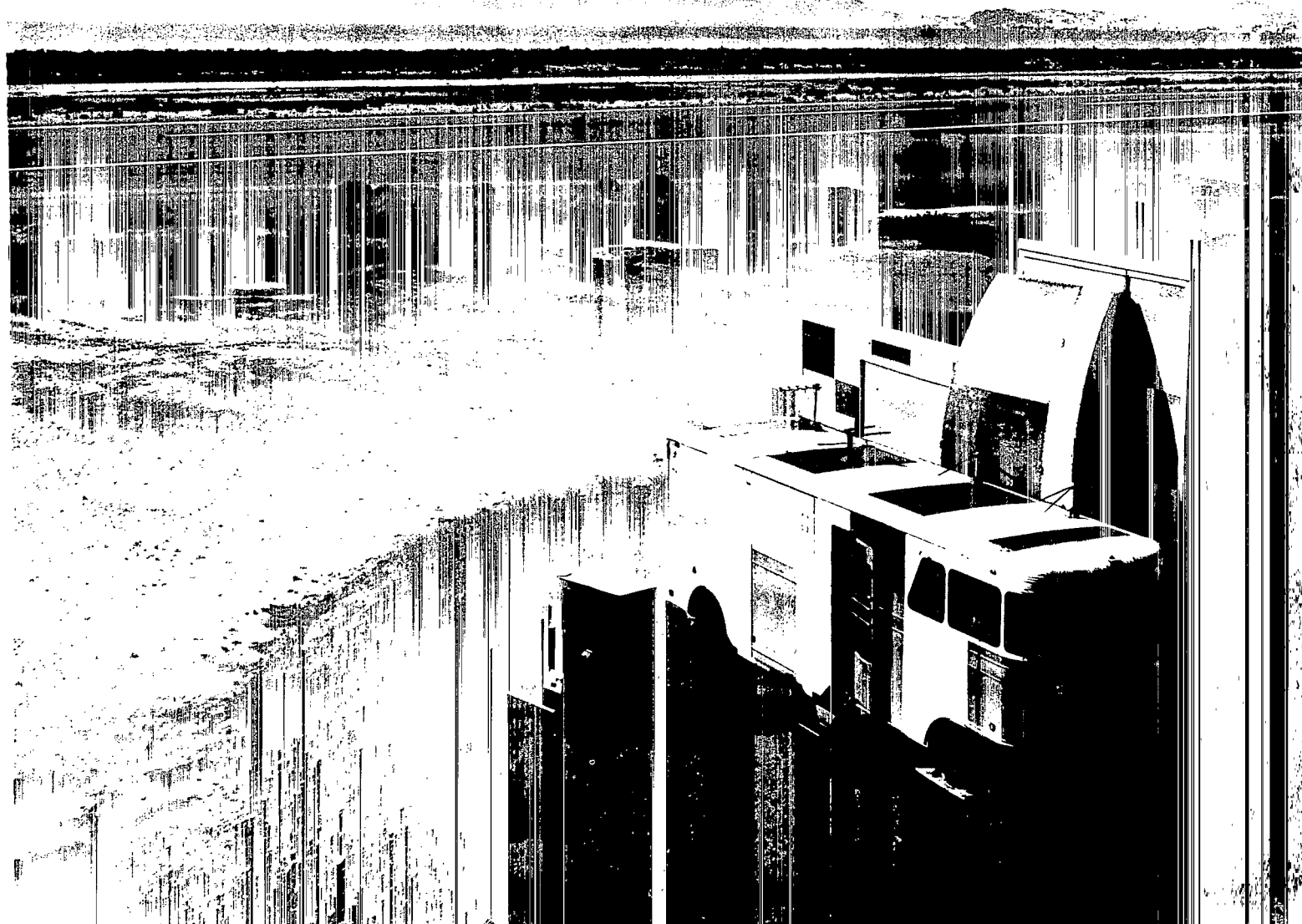


Figure 18.- Radar landing approach system installation.



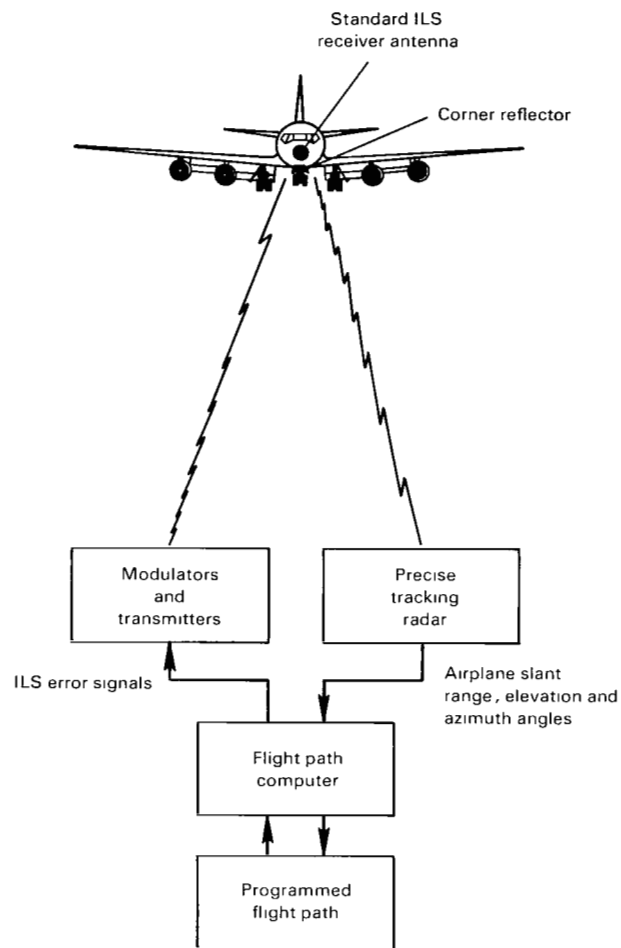


Figure 19.- Sketch of radar approach landing system.

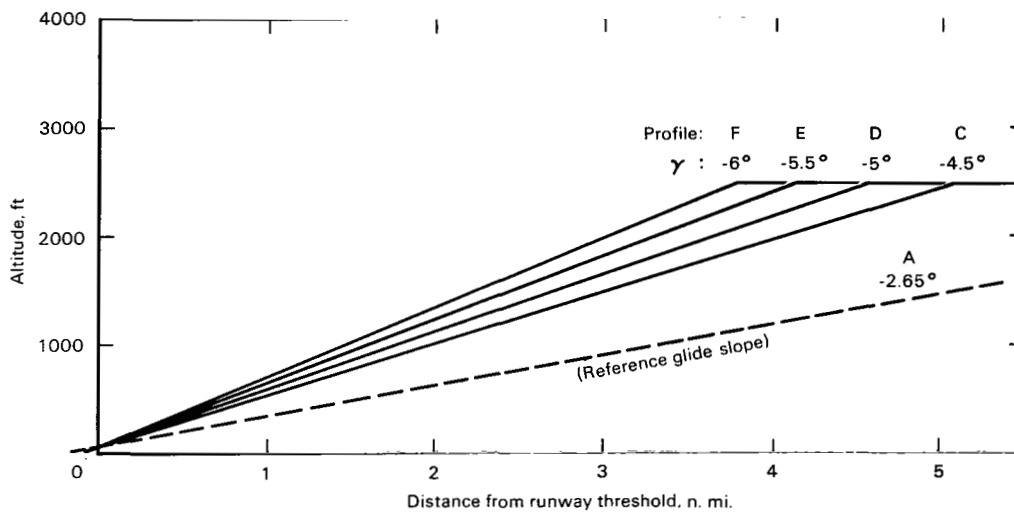


Figure 20.- Single-segment approach profiles.

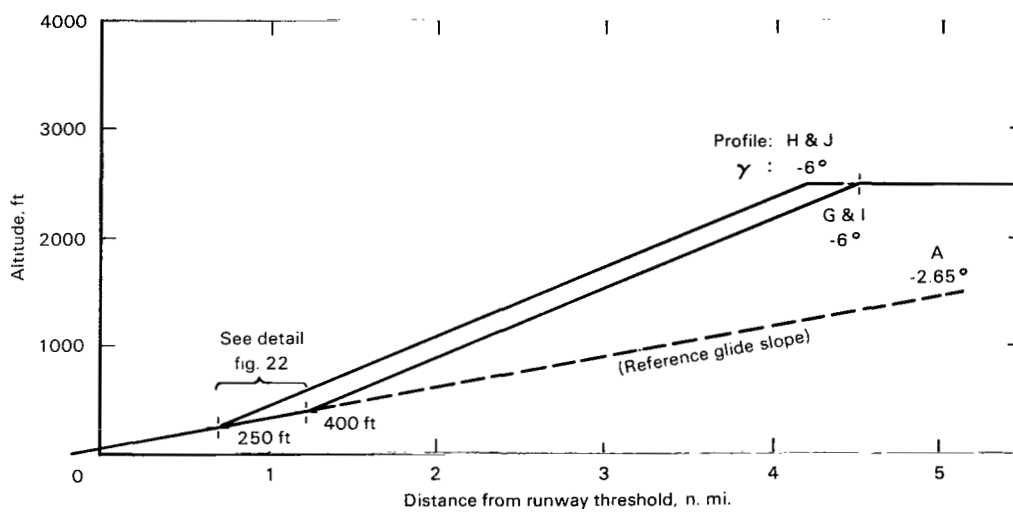
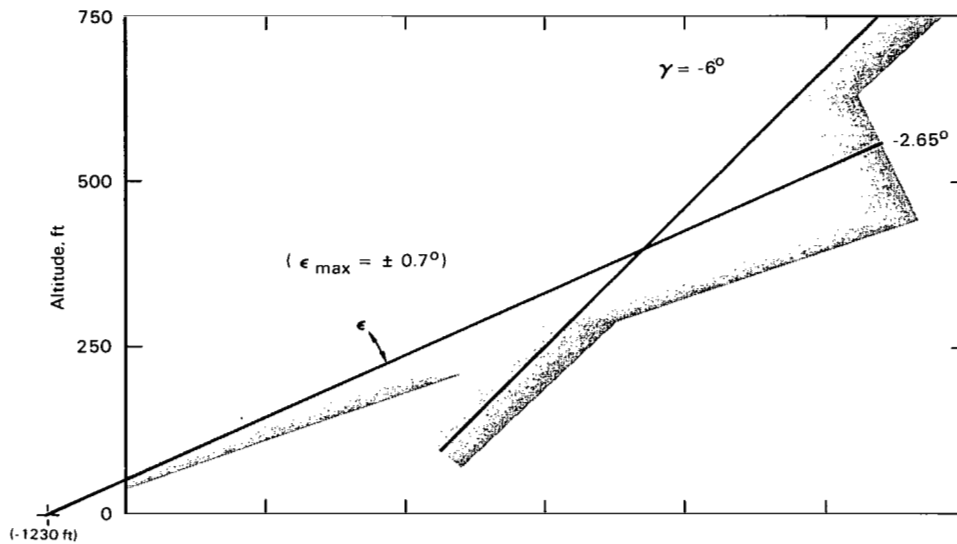
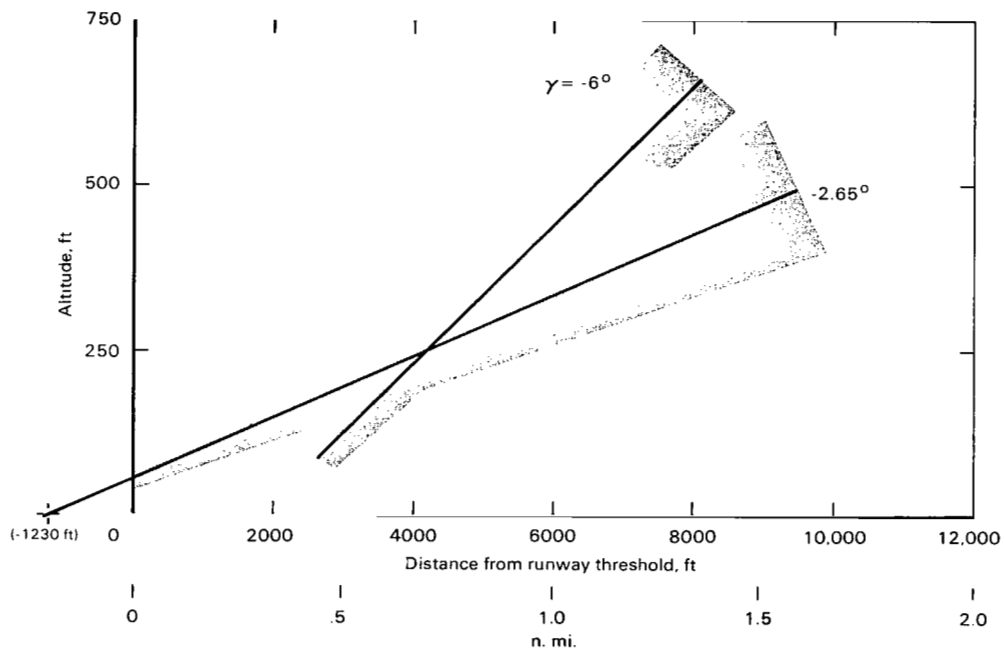


Figure 21.- Two-segment approach profiles.

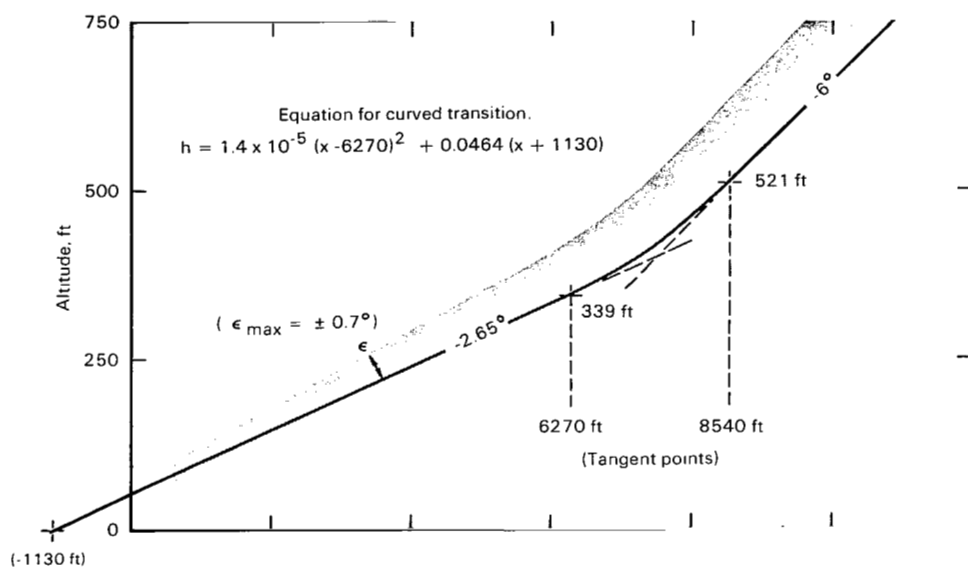


(a) Intercept altitude 400 ft, profile G.

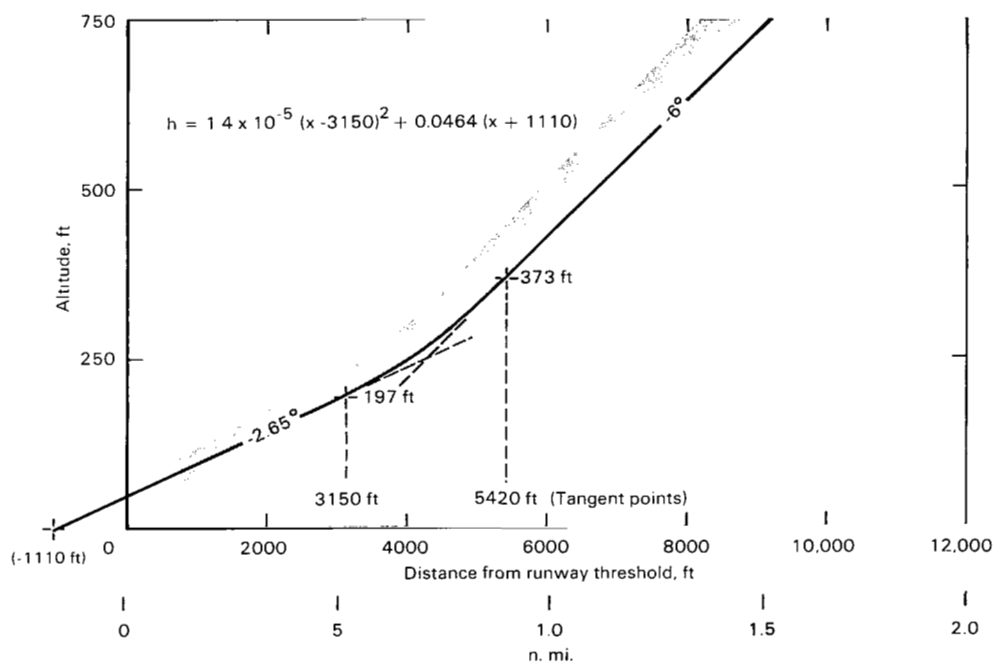


(b) Intercept altitude 250 ft, profile H.

Figure 22.- Guidance system for two-segment profiles using two ILS glide-slope beams.



(a) Intercept altitude 400 ft, profile I.



(b) Intercept altitude 250 ft, profile J.

Figure 23.- Guidance system for two-segment profiles using a single glide-slope beam with curvilinear transition.

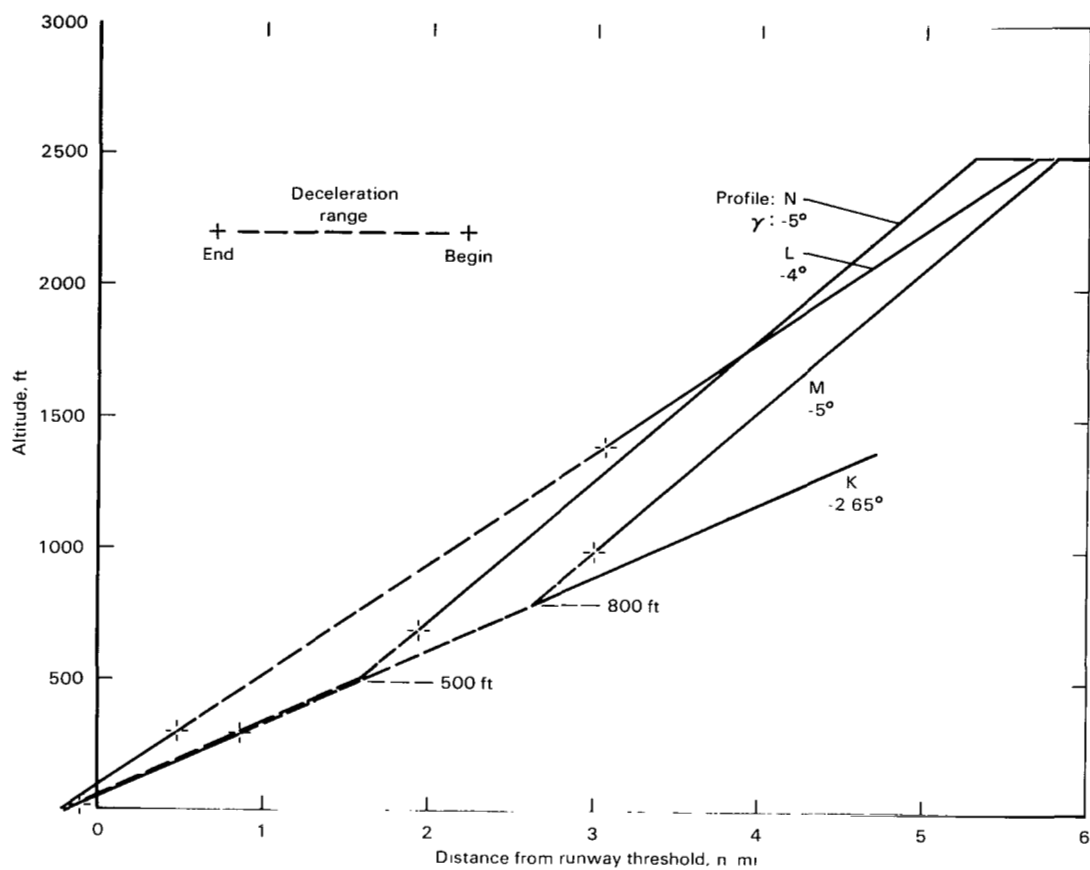


Figure 24.- Decelerating approach profiles.

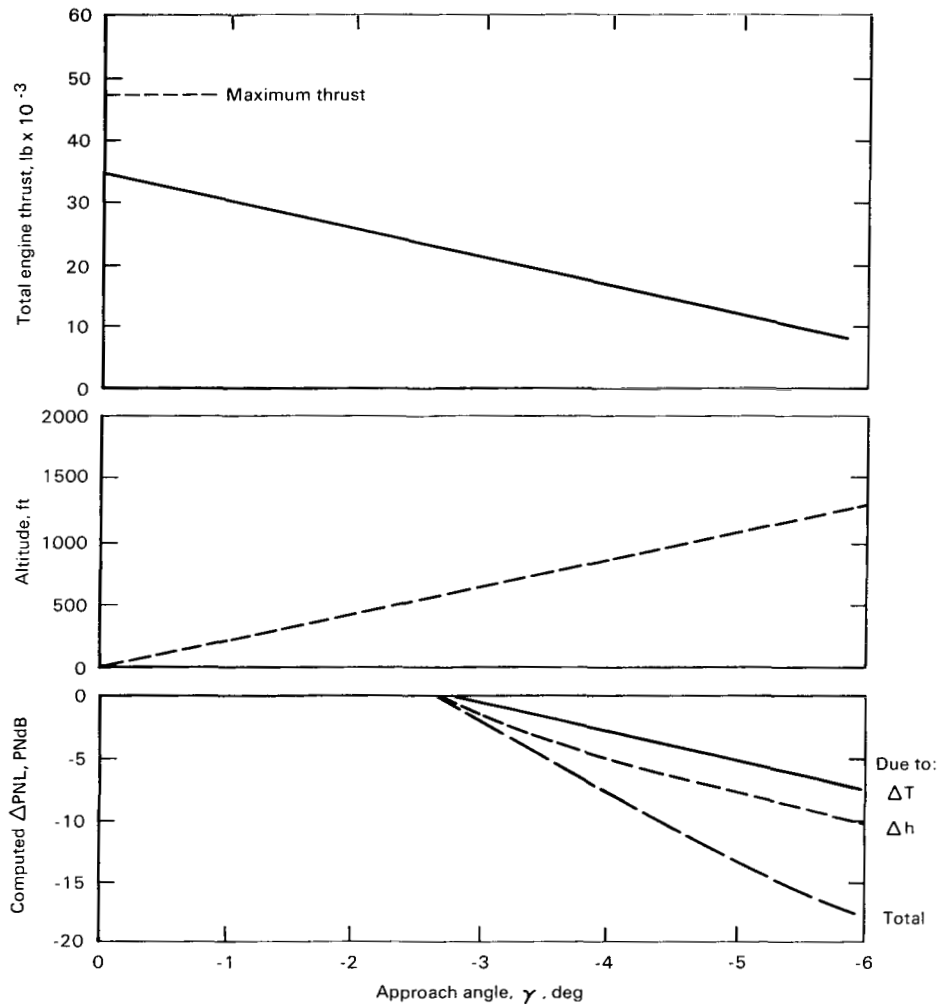


Figure 25.- Noise reduction due to thrust and altitude changes with steepened approach angle; range 2 n.mi,  $\delta_F = 40/10$ ,  $V_{APP} = 115$  knots.

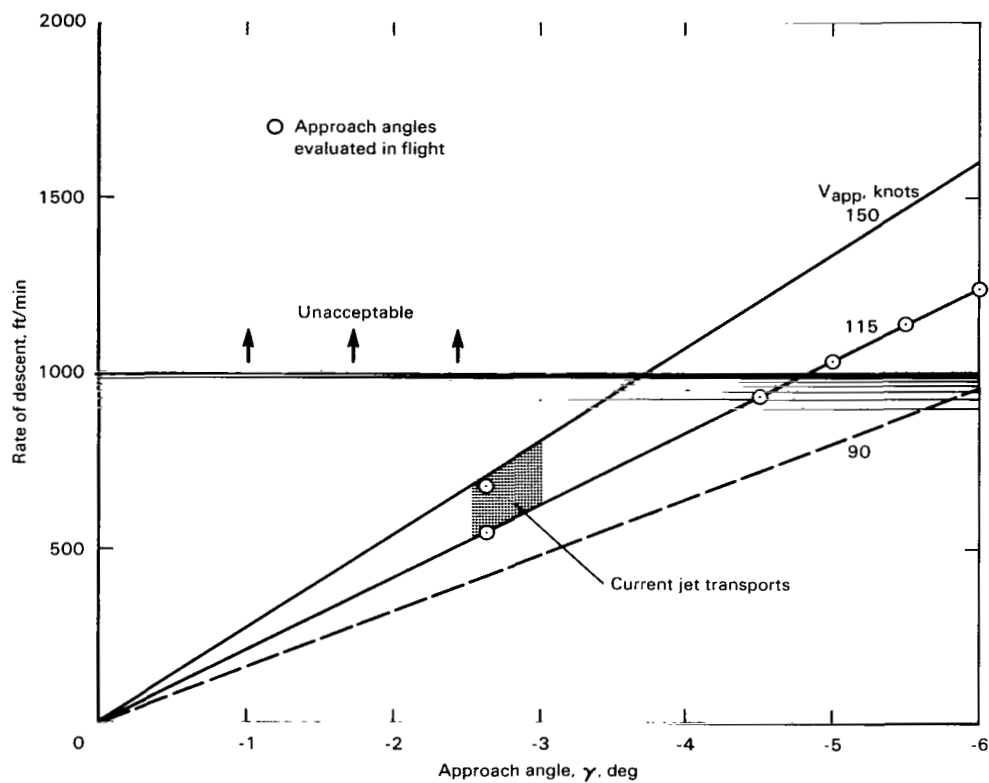


Figure 26.- Variation of rate of descent with approach angle.

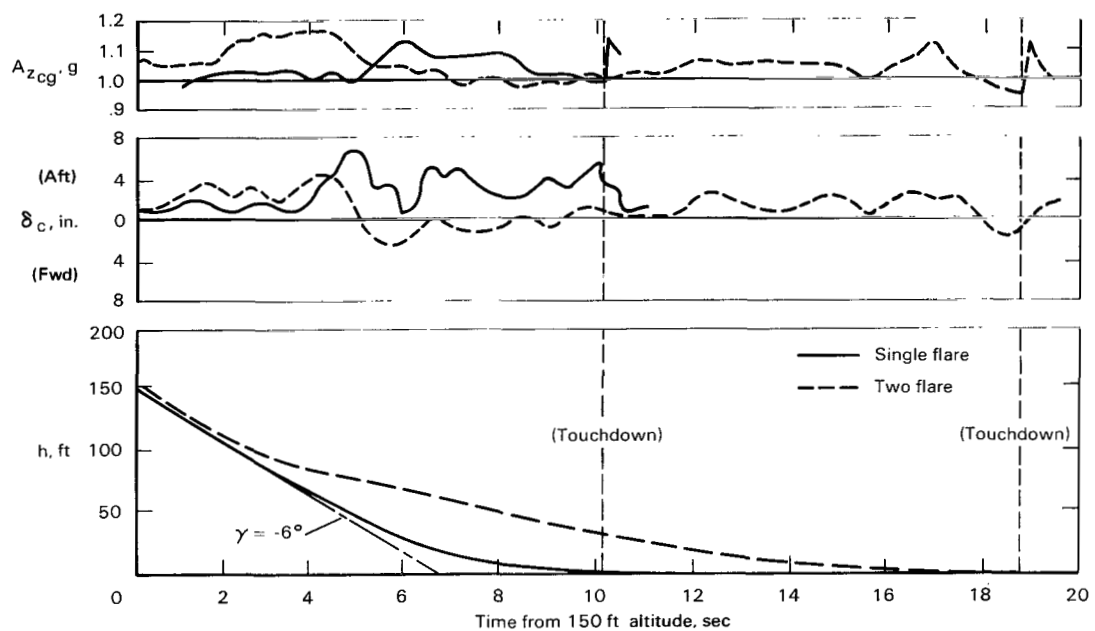
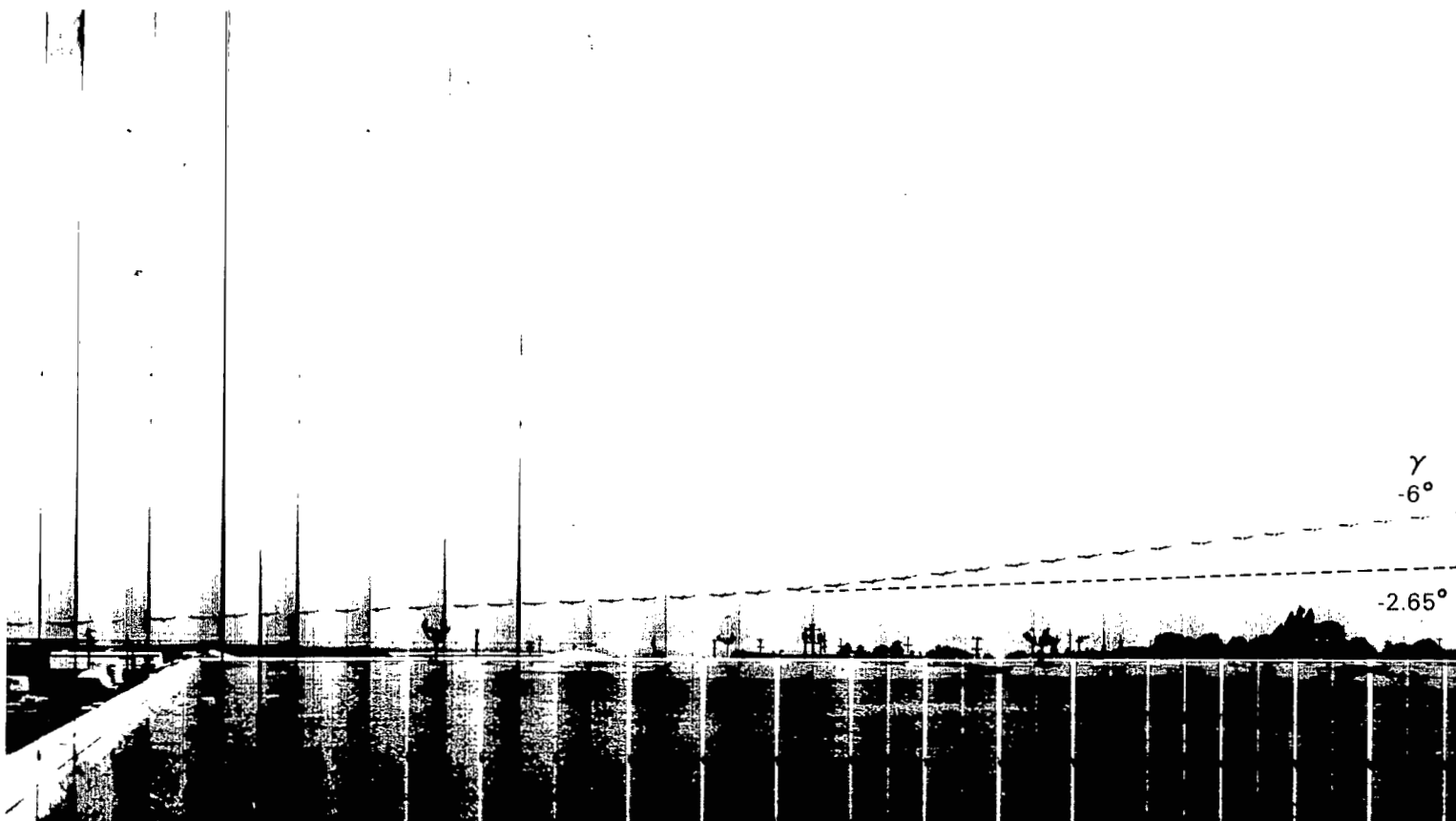


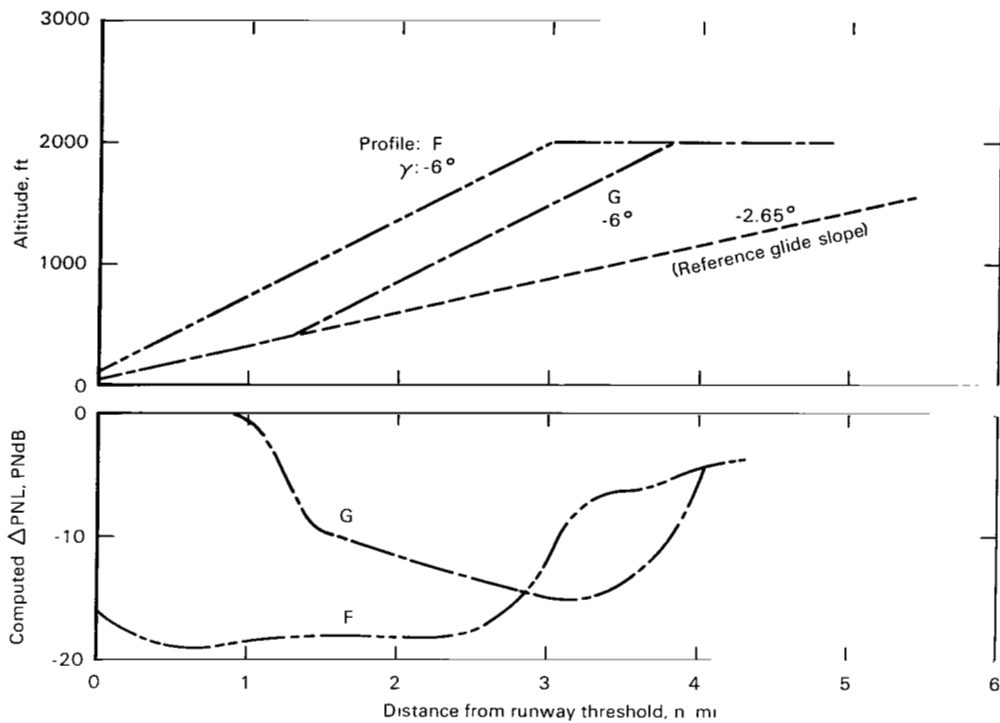
Figure 27.- Flare technique for  $6^\circ$  single-segment approach.





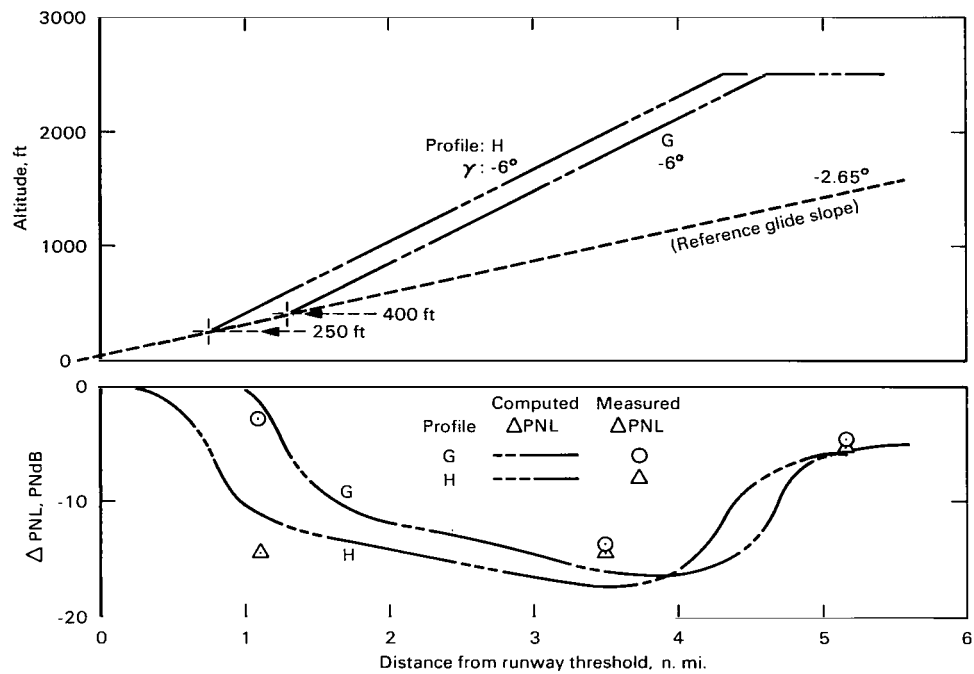
(a) Multiple exposure photograph of the Boeing 367-80 making a two-segment approach.

Figure 28.- Two-segment landing approach profile.



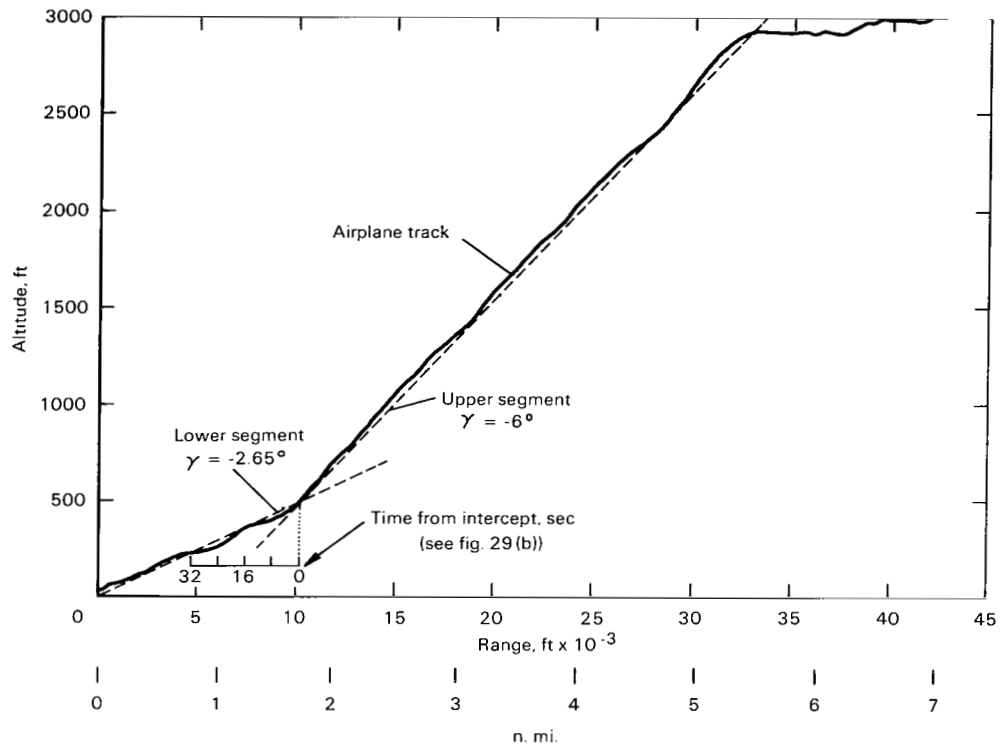
(b) Comparison of noise reduction with two-segment and single-segment approaches.

Figure 28.- Continued.



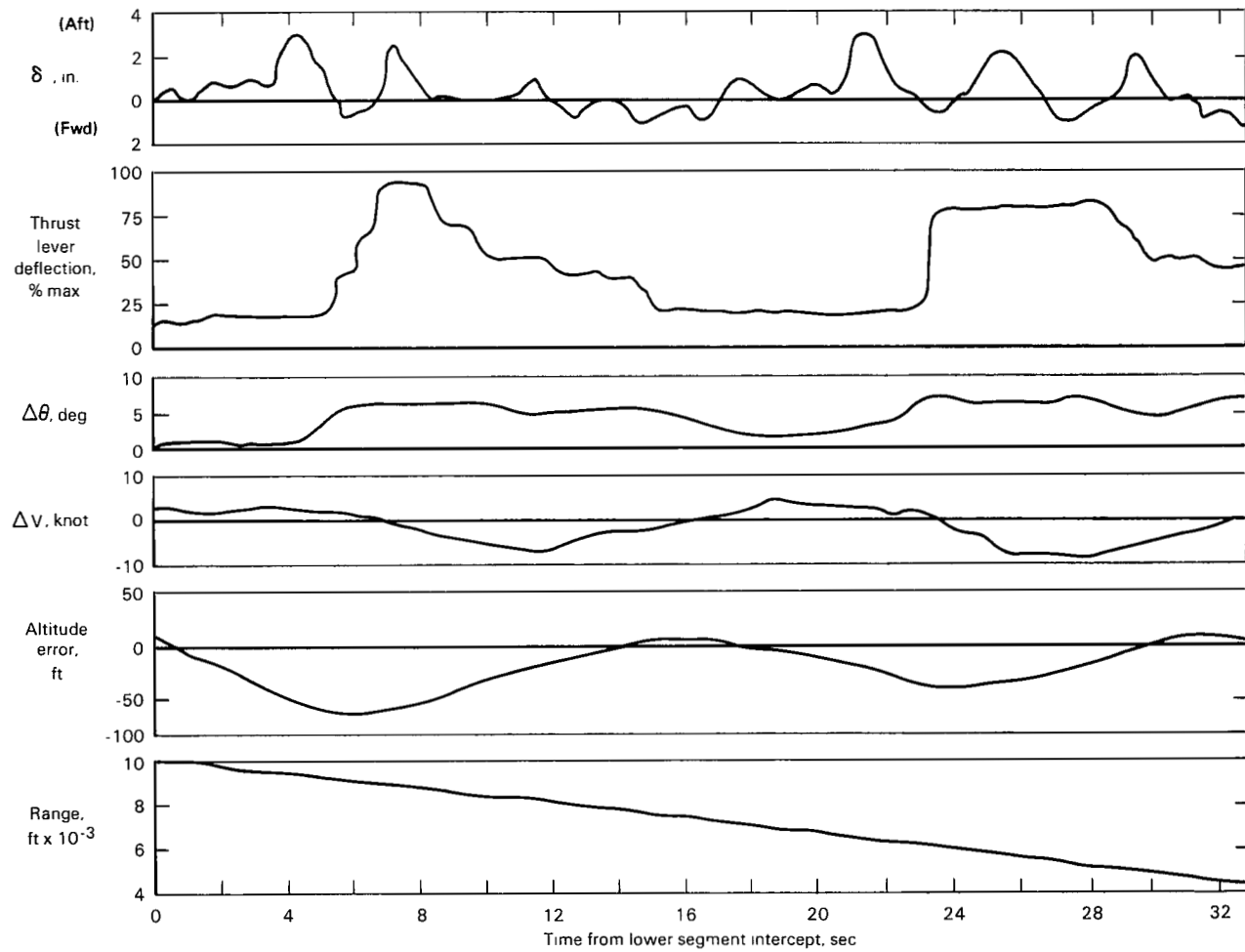
(c) Noise reduction with 250- and 400-ft intercept altitudes.

Figure 28.- Concluded.



(a) Comparison of airplane track with two-beam ILS.

Figure 29.- Two-segment approach with standard flight director guidance.



(b) Time history of transition to lower segment.

Figure 29.- Concluded.

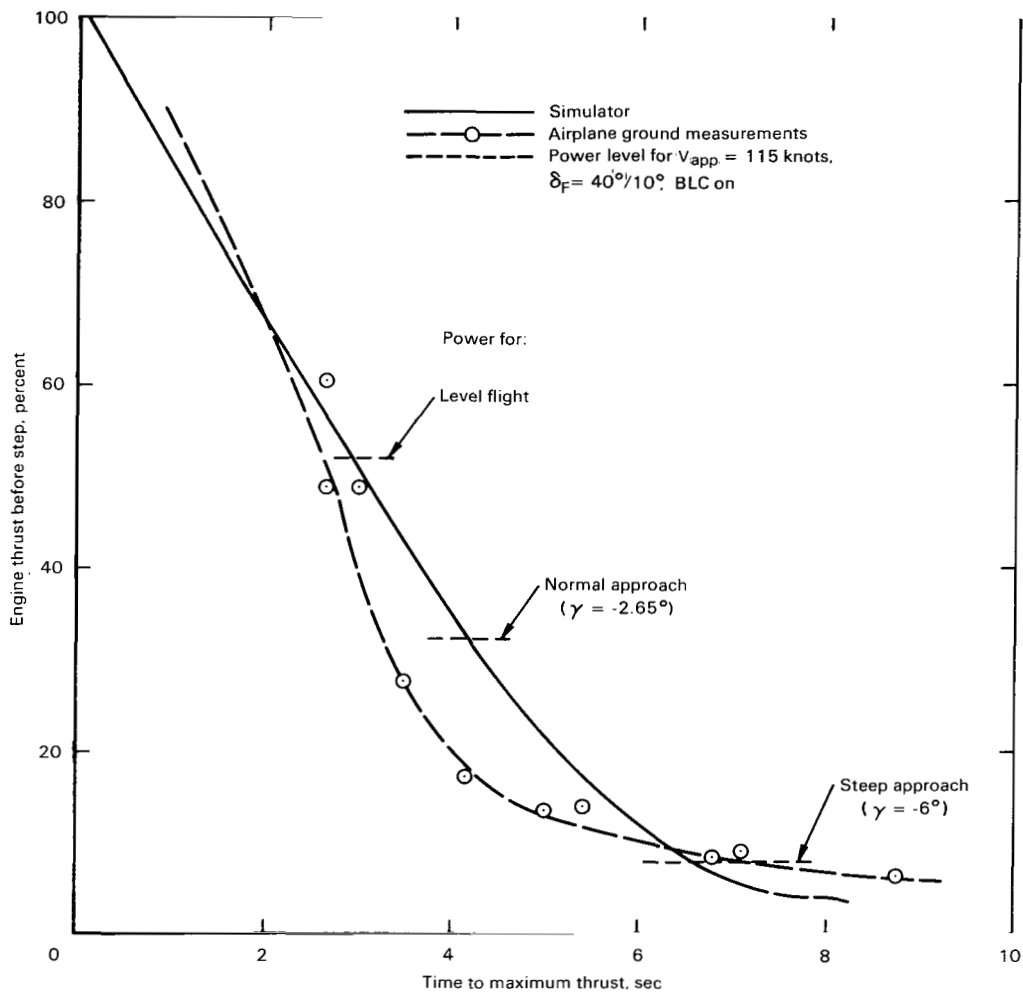


Figure 30.- Time to maximum thrust from approach thrust for step throttle.

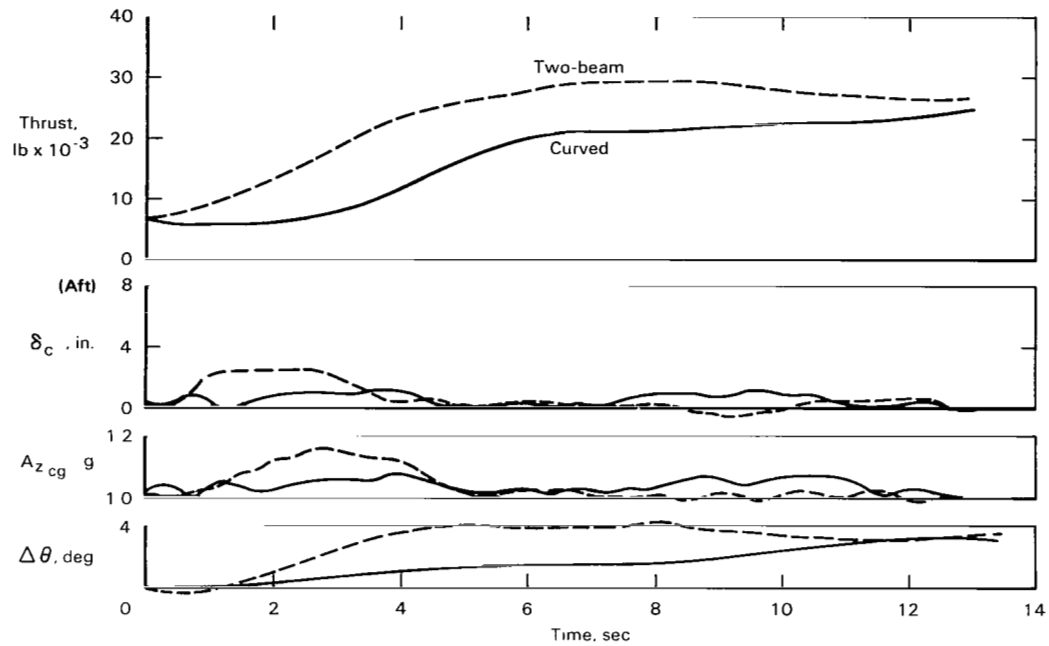
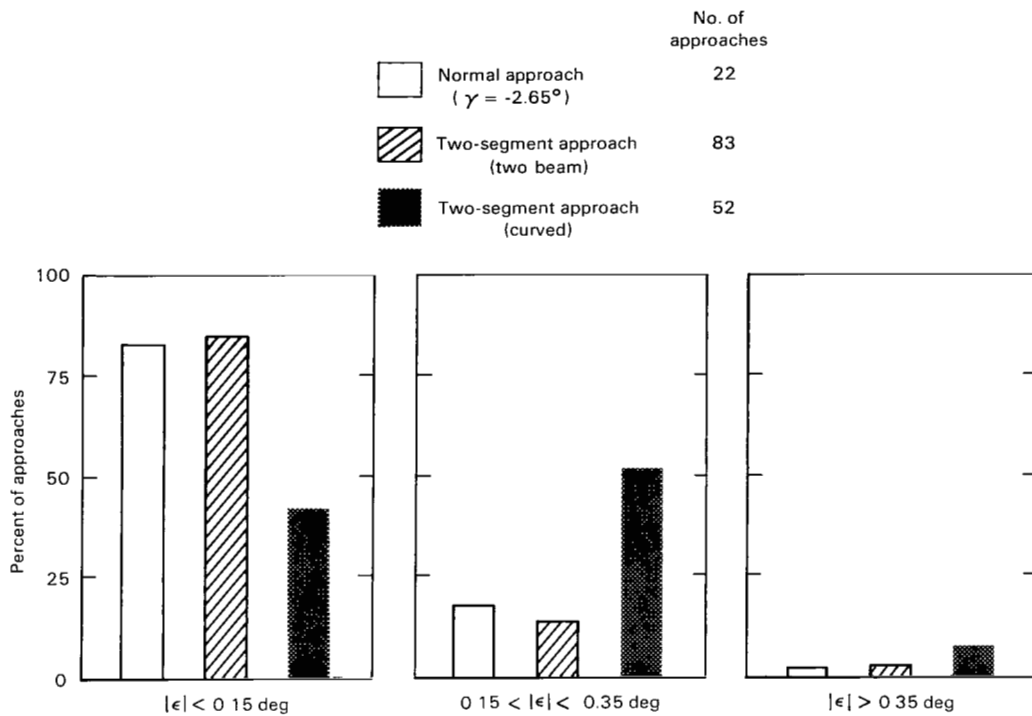
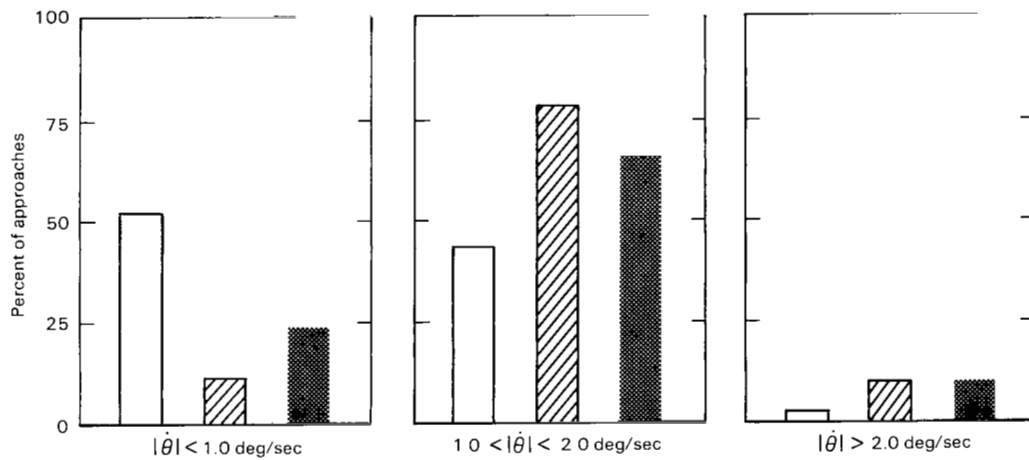


Figure 31.- Time histories of transitions; 400-ft intercept.



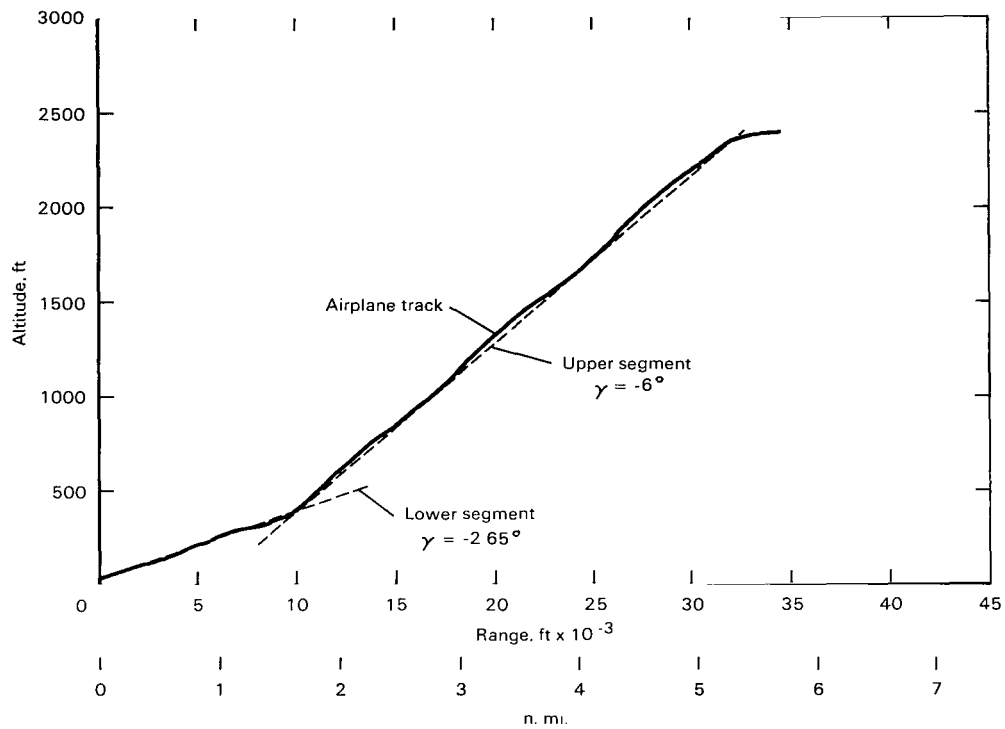
(a) ILS glide-slope errors.



(b) Airplane pitch rate.

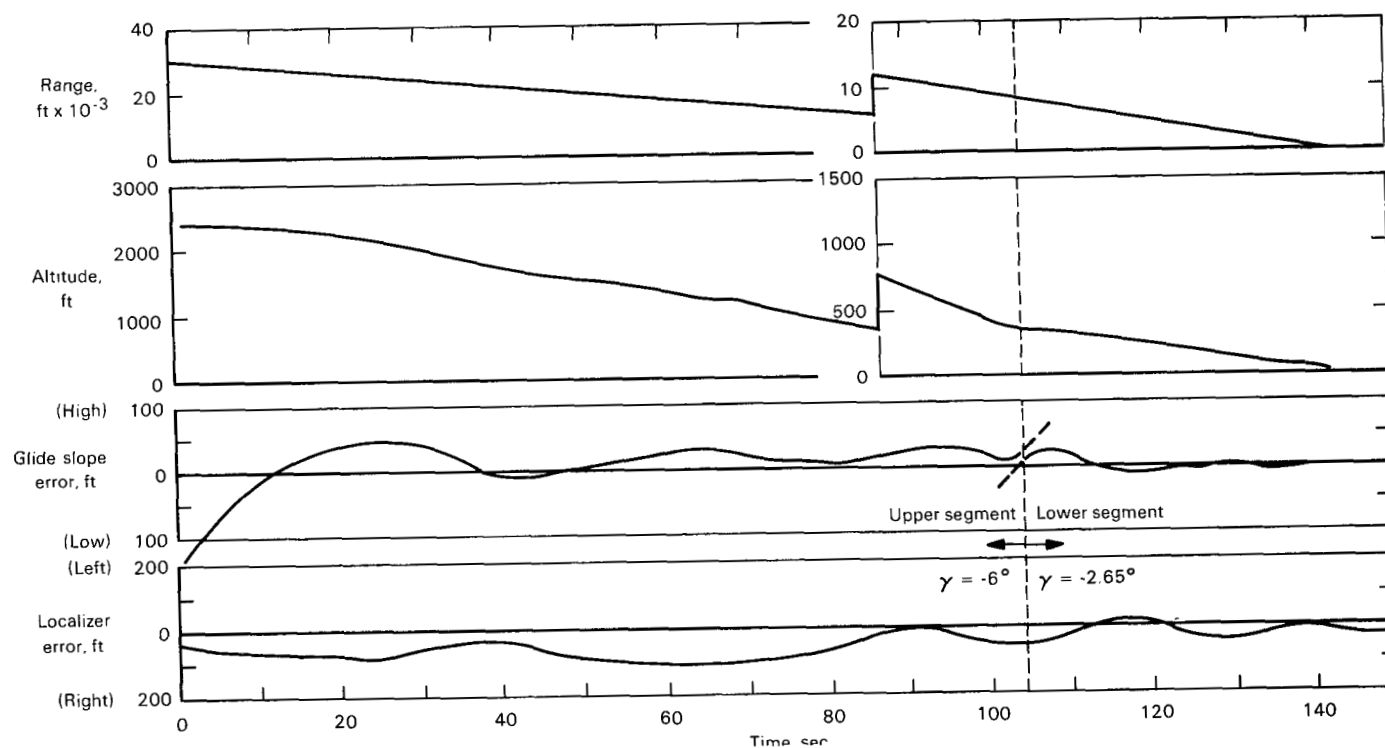
Figure 32.- ILS glide-slope errors and airplane pitch rate during two-segment transitions compared with normal approaches between 200- and 300-ft altitude.





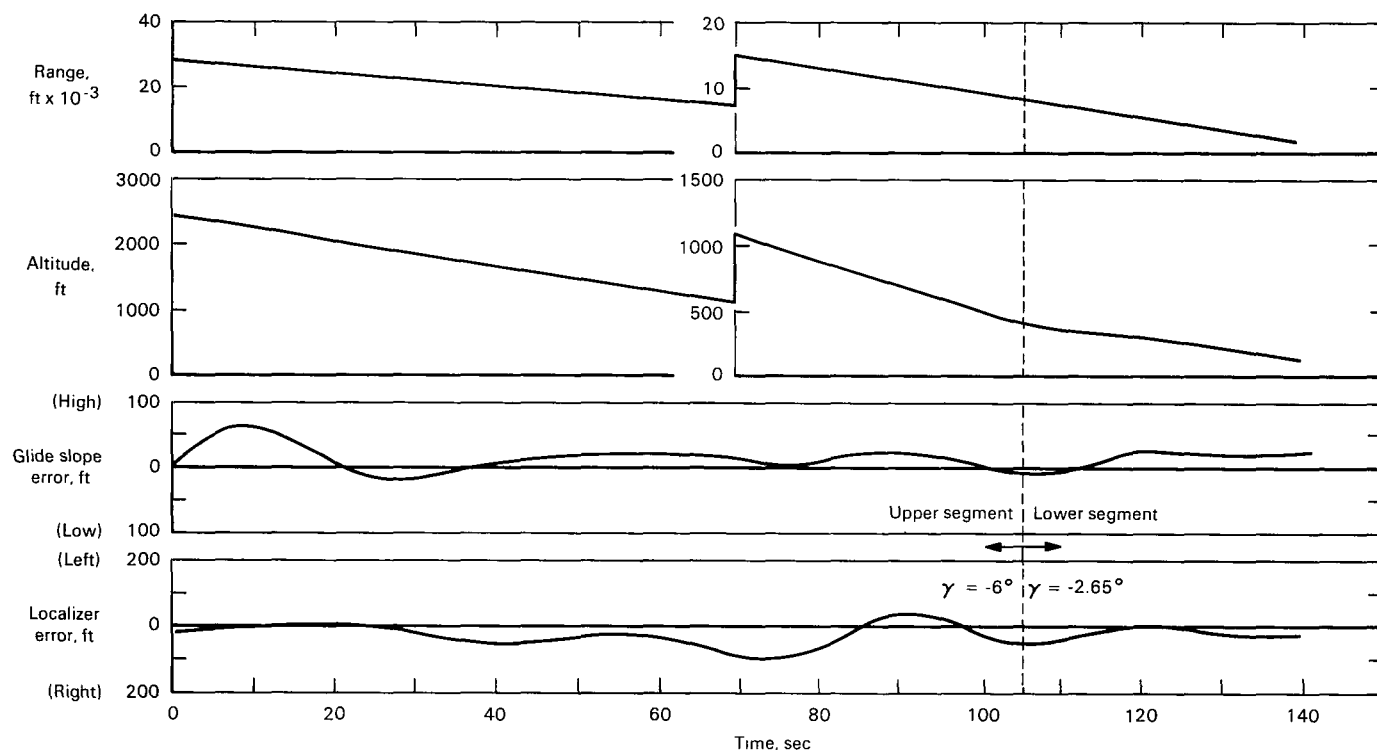
(a) Airplane track as measured by radar compared to two-beam guidance system.

Figure 33.- Typical two-segment approaches.



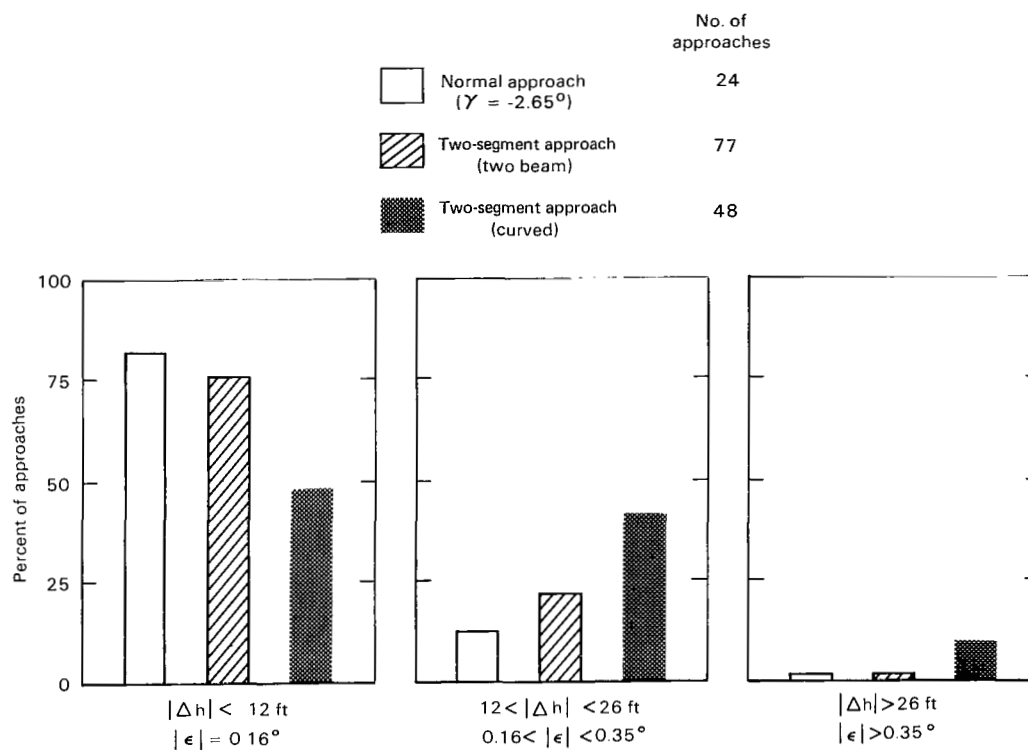
(b) Typical time history of approach with two-beam ILS guidance.

Figure 33.- Continued.

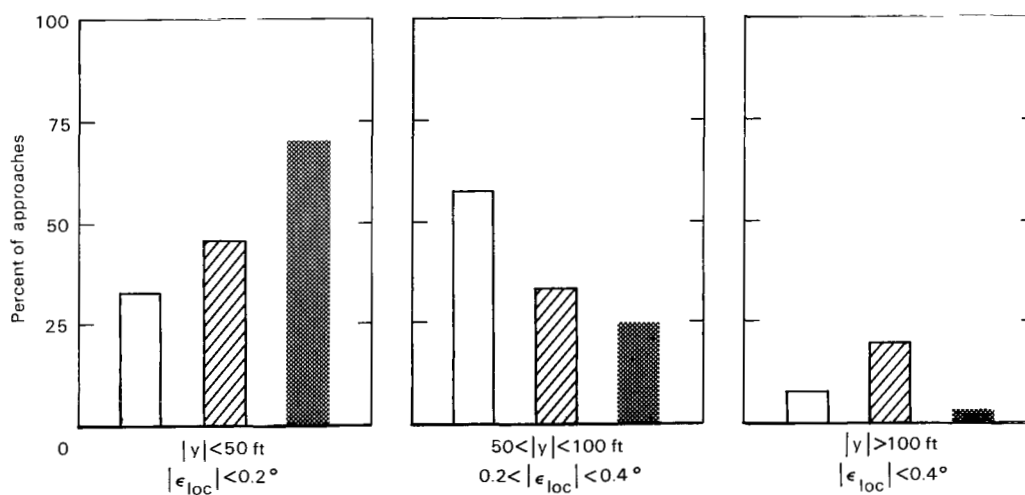


(c) Time history of approach with single beam with curved transition guidance.

Figure 33.- Concluded.

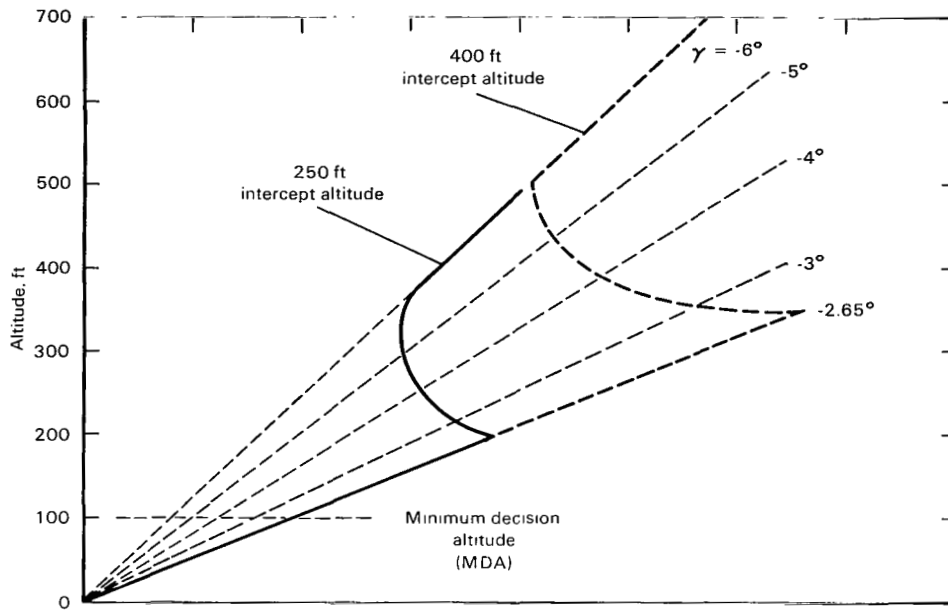


(a) Altitude error from ILS glide slope.

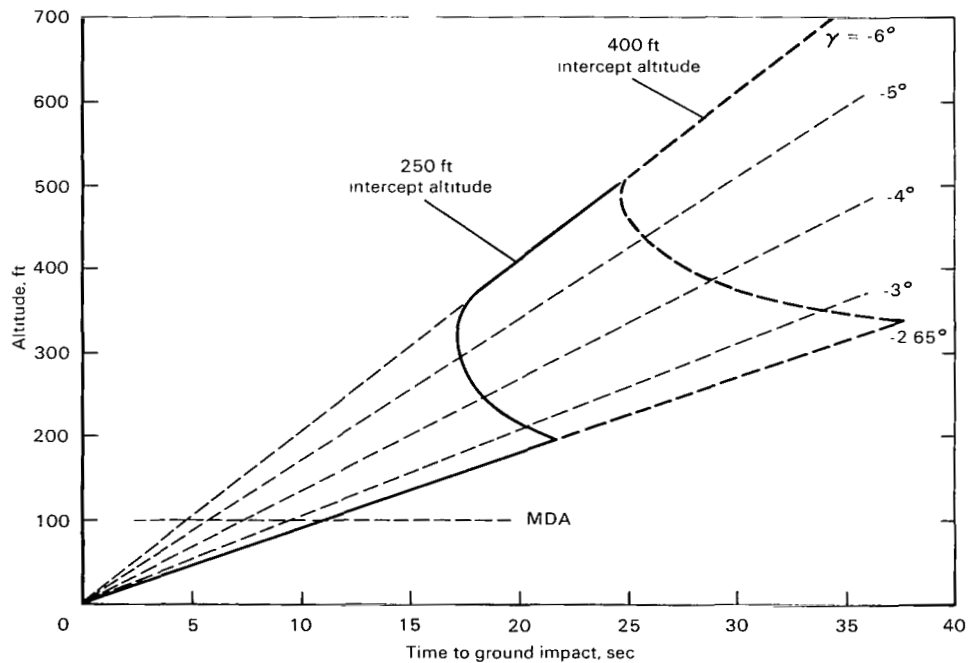


(b) Lateral error from ILS localizer.

Figure 34.- Error from the ILS at an altitude of 200 ft.



(a) 115-knot approach speed.



(b) 135-knot approach speed.

Figure 35.- Variation of time-to-ground impact with altitude for two-segment approaches with curved transitions.

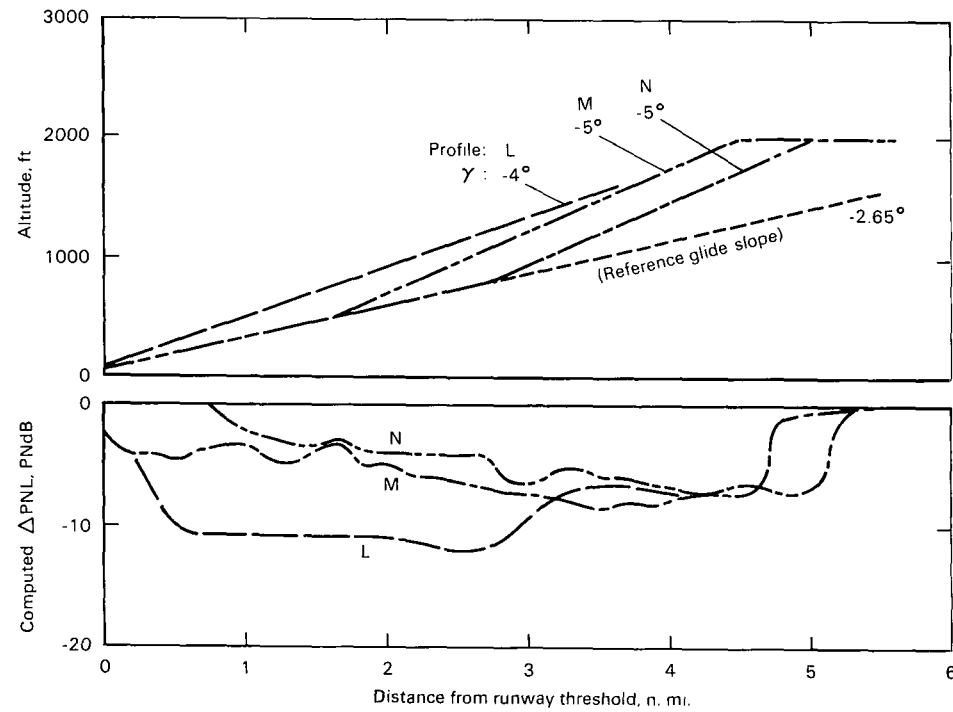


Figure 36.- Computed noise reduction with decelerating approaches ( $V = 150$  to  $118$  knots) referenced to  $2.65^\circ$  approach;  $\delta_F = 30/10$ , BLC on,  $V = 118$  knots.

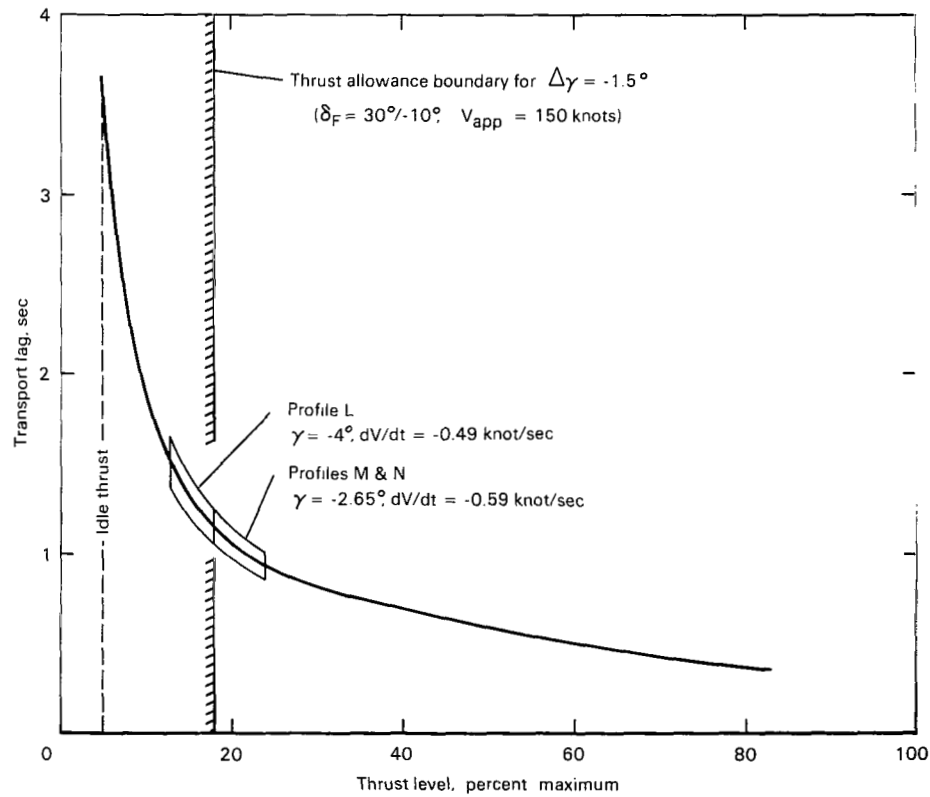
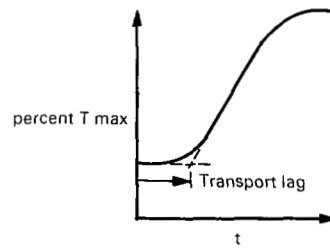


Figure 37.- Engine transport lag and thrust margins for the decelerating approach flight conditions.

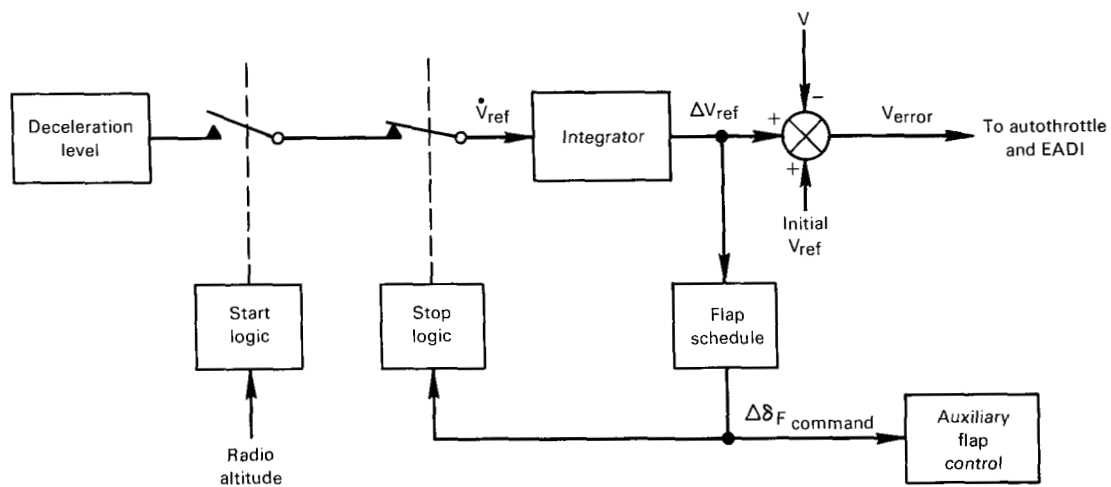
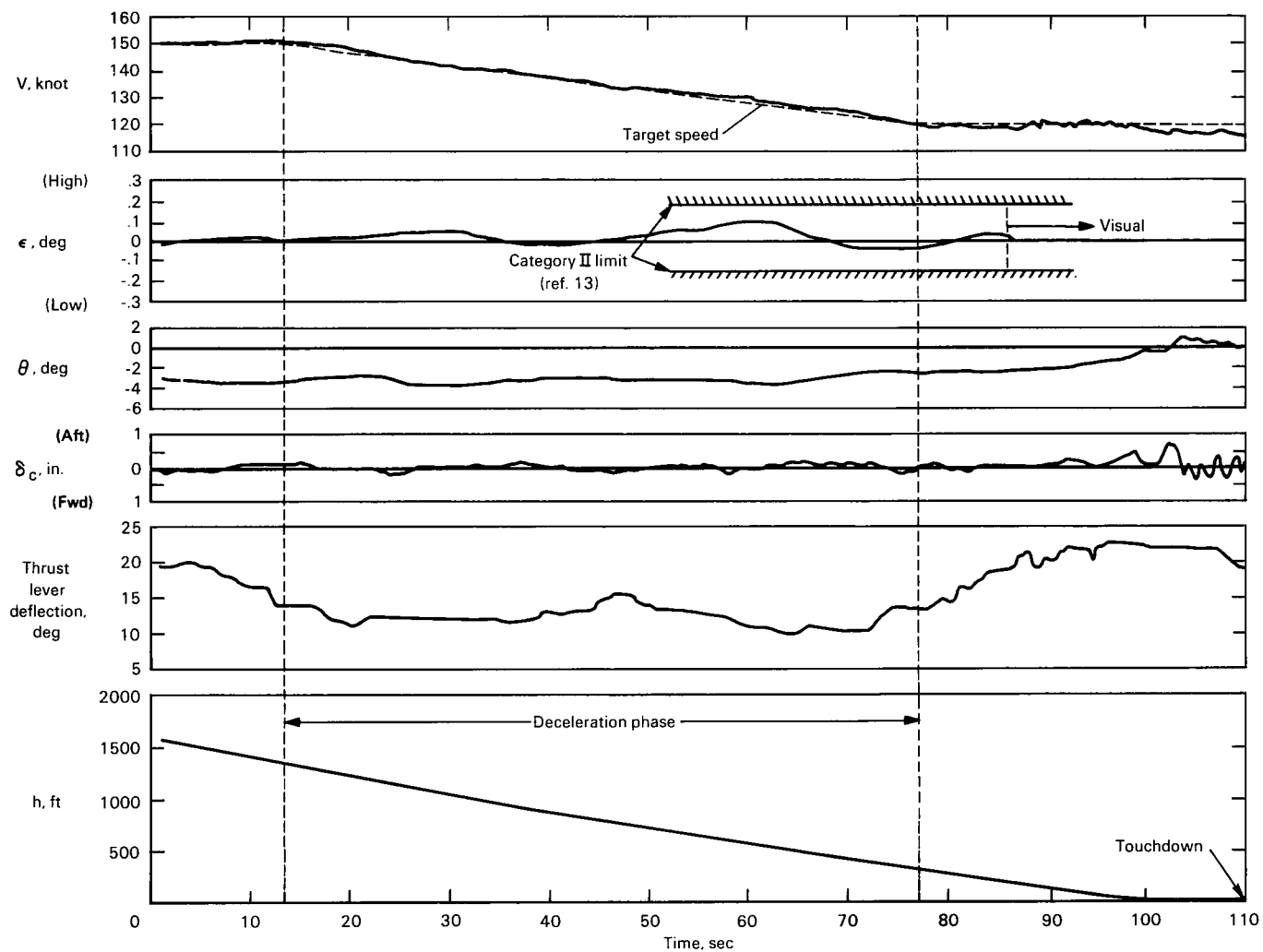


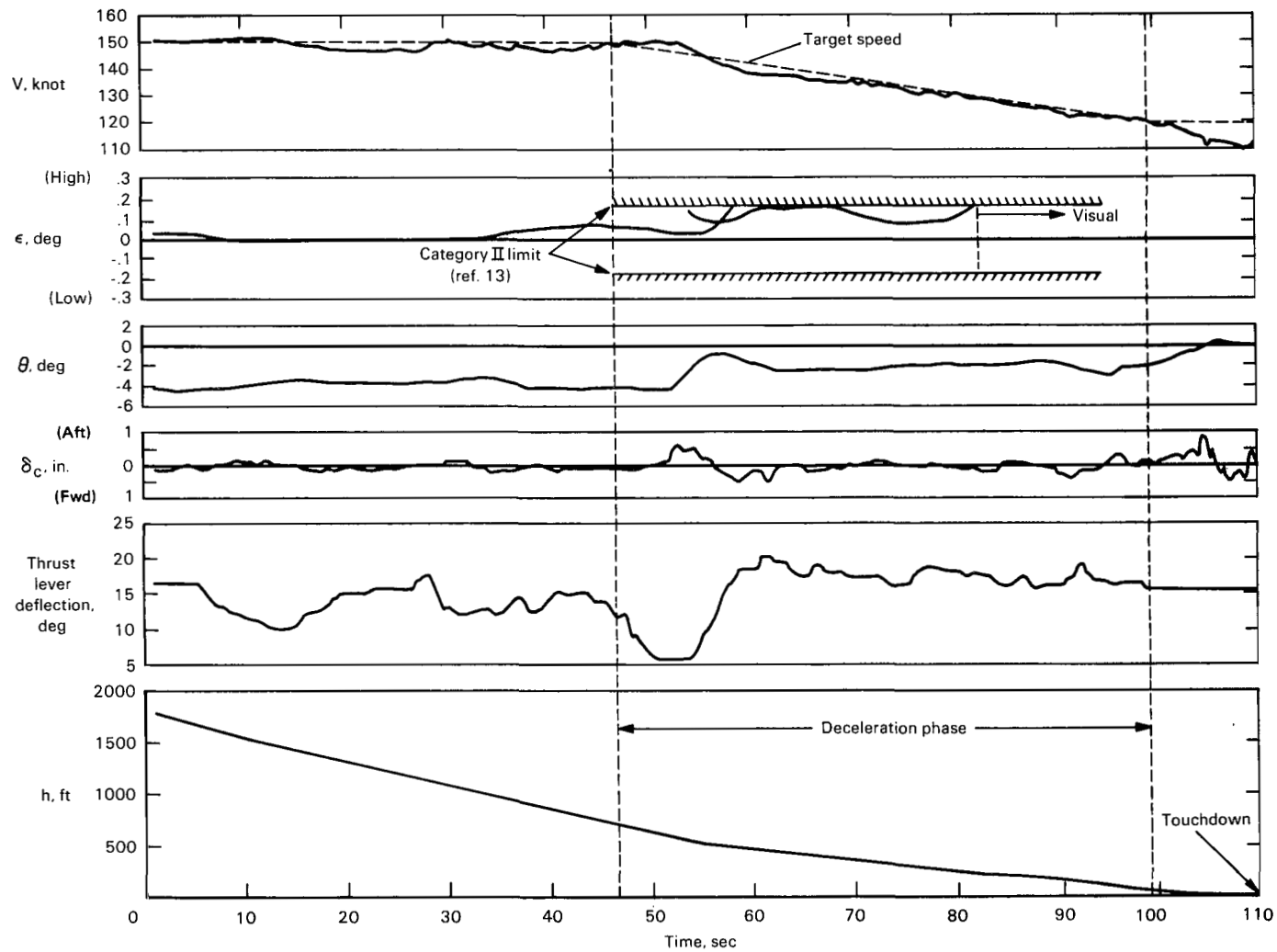
Figure 38.- Deceleration programming to airspeed and auxiliary flaps.





(a)  $4^\circ$  decelerating approach; auxiliary flap rate  $0.31^\circ/\text{sec}$ .

Figure 39.- Time history of decelerating approaches; initial flap position  $30^\circ/-9.4^\circ$ , final position  $50^\circ/10^\circ$ .



(b) Two-segment decelerating approach ( $5^\circ/2.65^\circ$ ); auxiliary flap rate  $0.37^\circ/\text{sec}$ .

Figure 39.- Concluded.

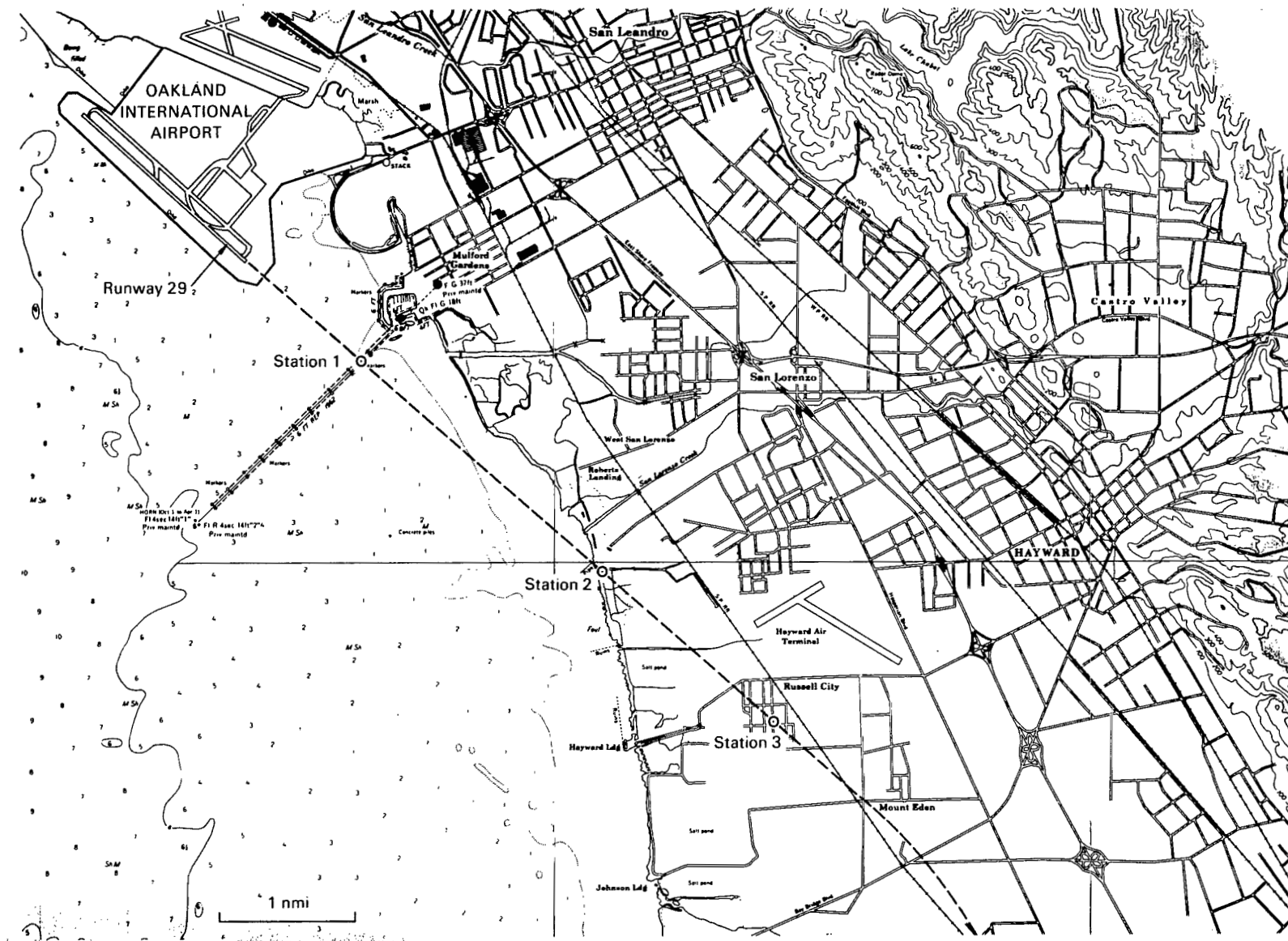


Figure 40.- Chart of test area.

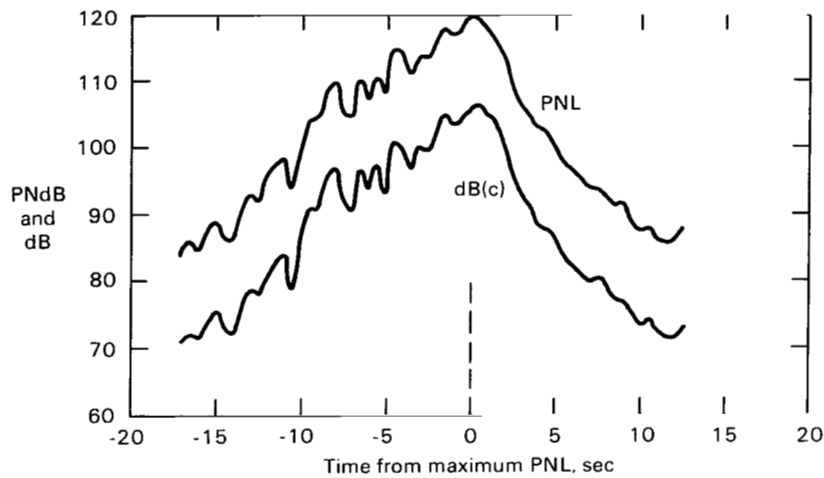


Figure 41.- Comparison of perceived noise level and dB(c) for typical flyover (profile A, run 3, station 1).

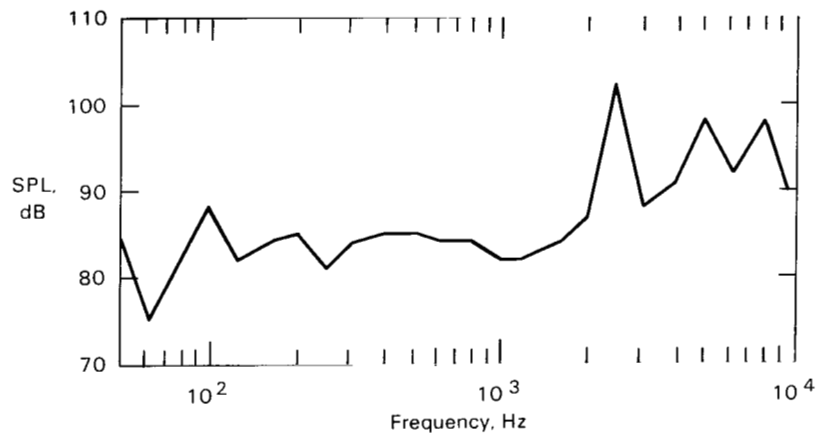


Figure 42.- Frequency characteristics of flyover noise at time of PNLT (profile A, run 3, station 1).

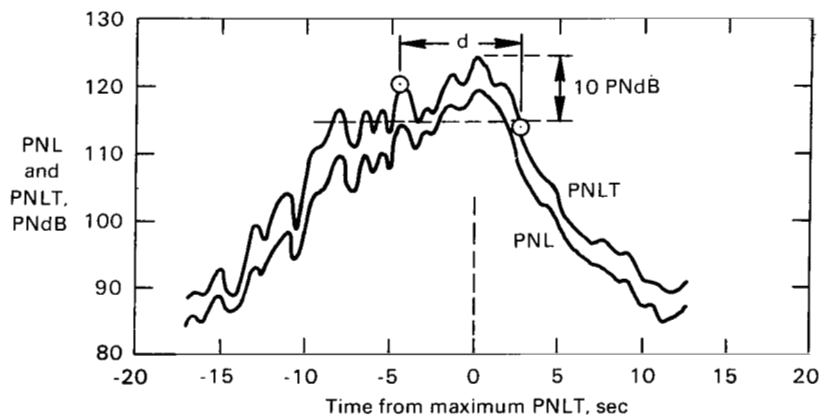
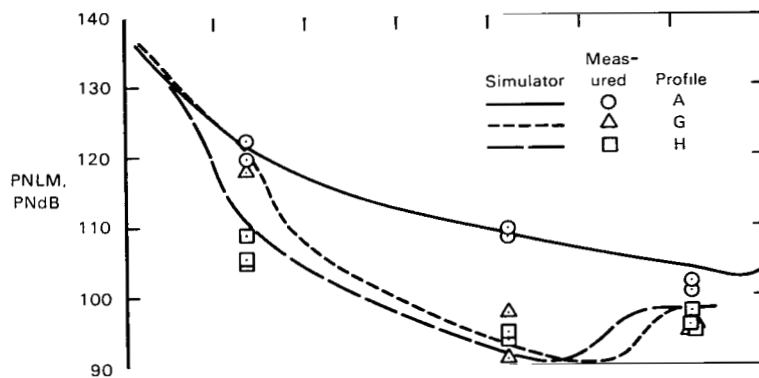
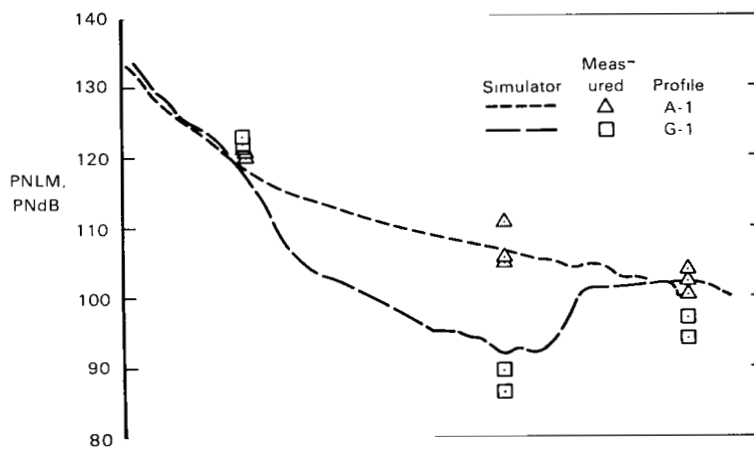


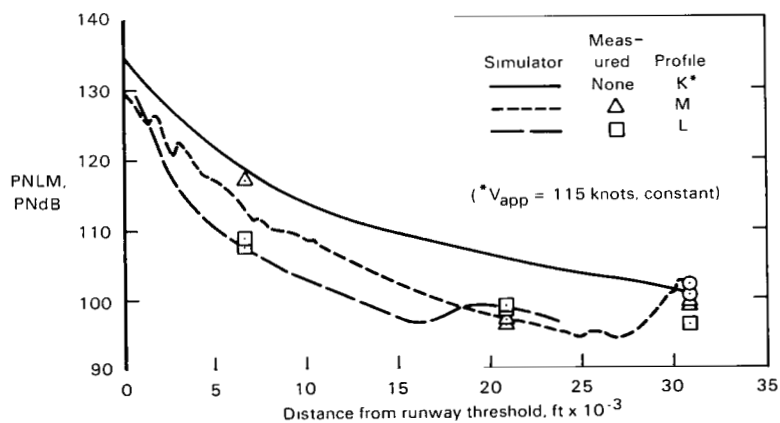
Figure 43.- Comparison of tone corrected perceived noise level and perceived noise level for a typical flyover (profile A, run 3, station 1).



(a) 40°/10° flap configuration.

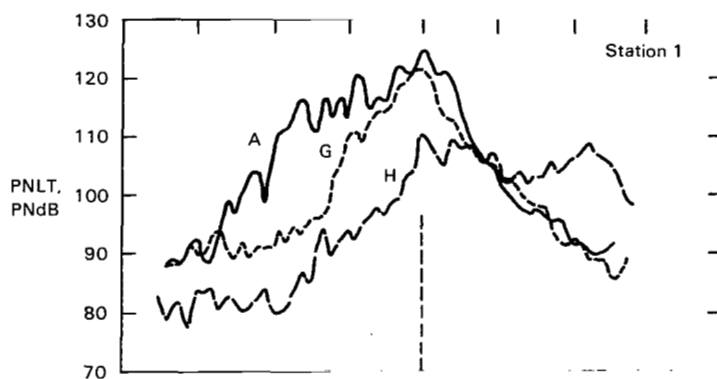


(b) 30°/10° flap configuration.

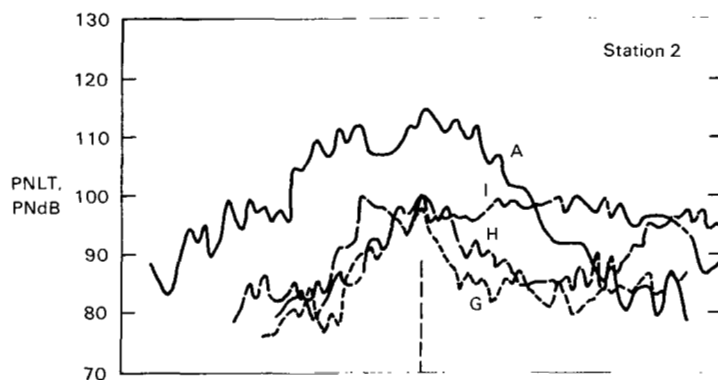


(c) Decelerating approaches.

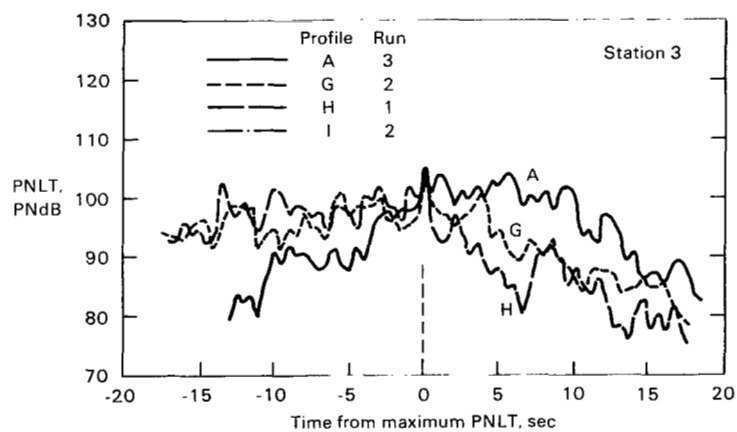
Figure 44.- Comparison of simulator (continuous) and measured (points) noise data.



(a) Station 1

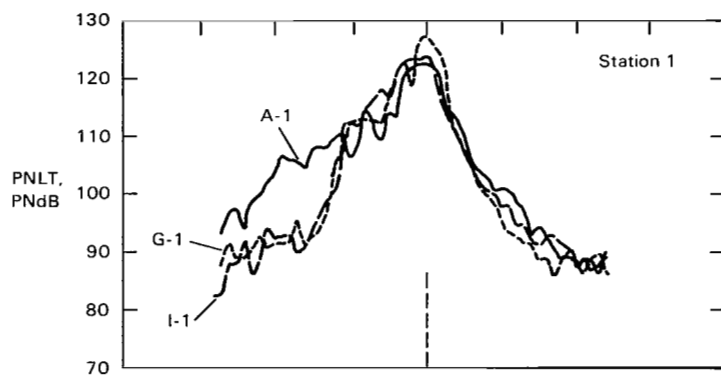


(b) Station 2.

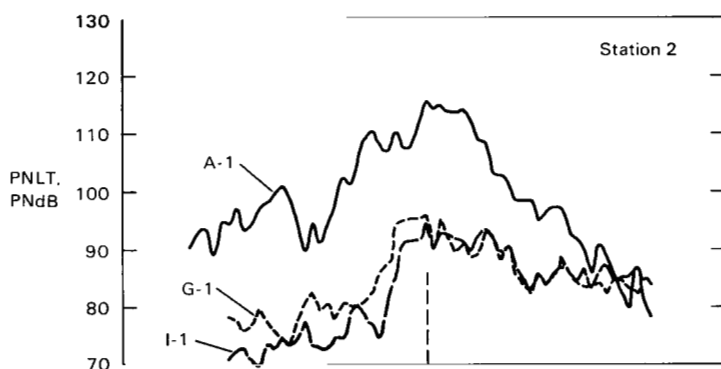


(c) Station 3.

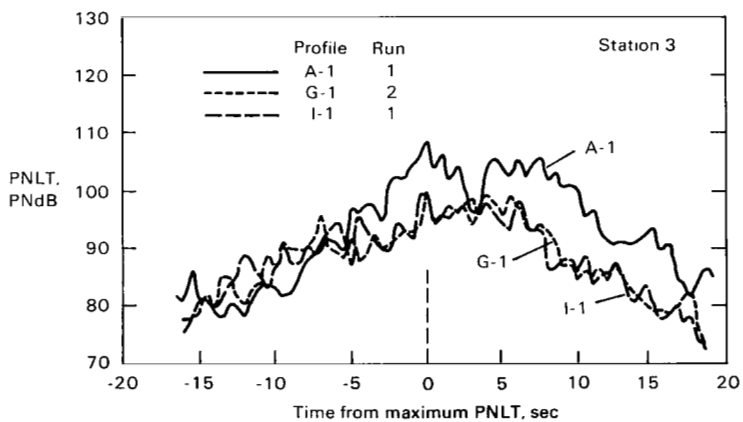
Figure 45.- Comparison of tone corrected perceived noise levels for noise abatement approaches with 40°/10° flap configuration.



(a) Station 1.

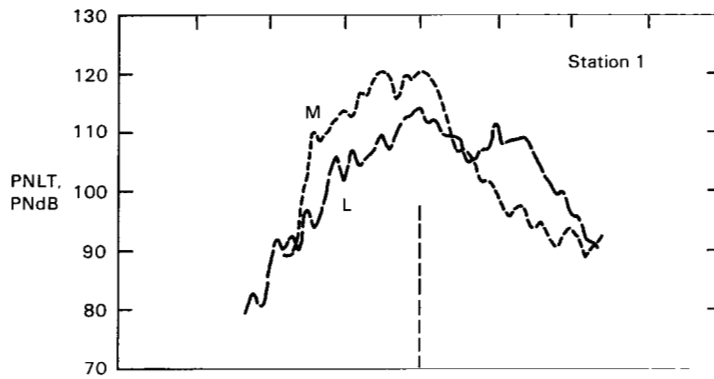


(b) Station 2.

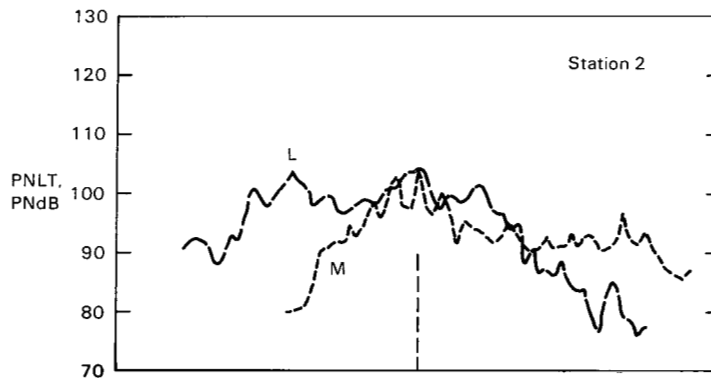


(c) Station 3.

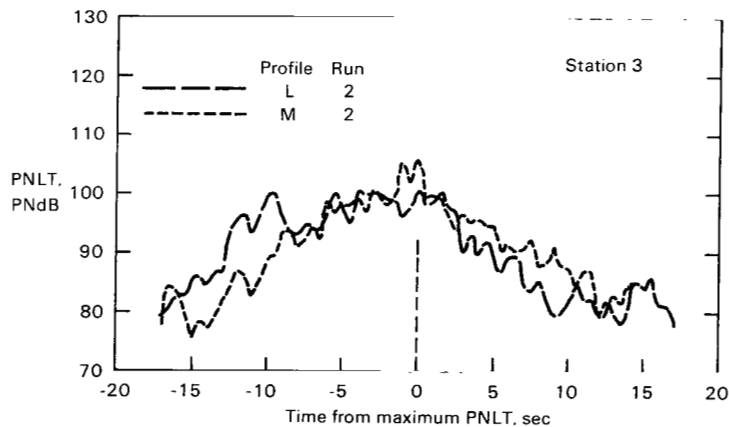
Figure 46.- Comparison of tone corrected perceived noise levels for noise abatement approaches with 30°/10° flap configuration.



(a) Station 1.



(b) Station 2.



(c) Station 3.

Figure 47.- Comparison of tone corrected perceived noise levels for noise abatement decelerating approaches.



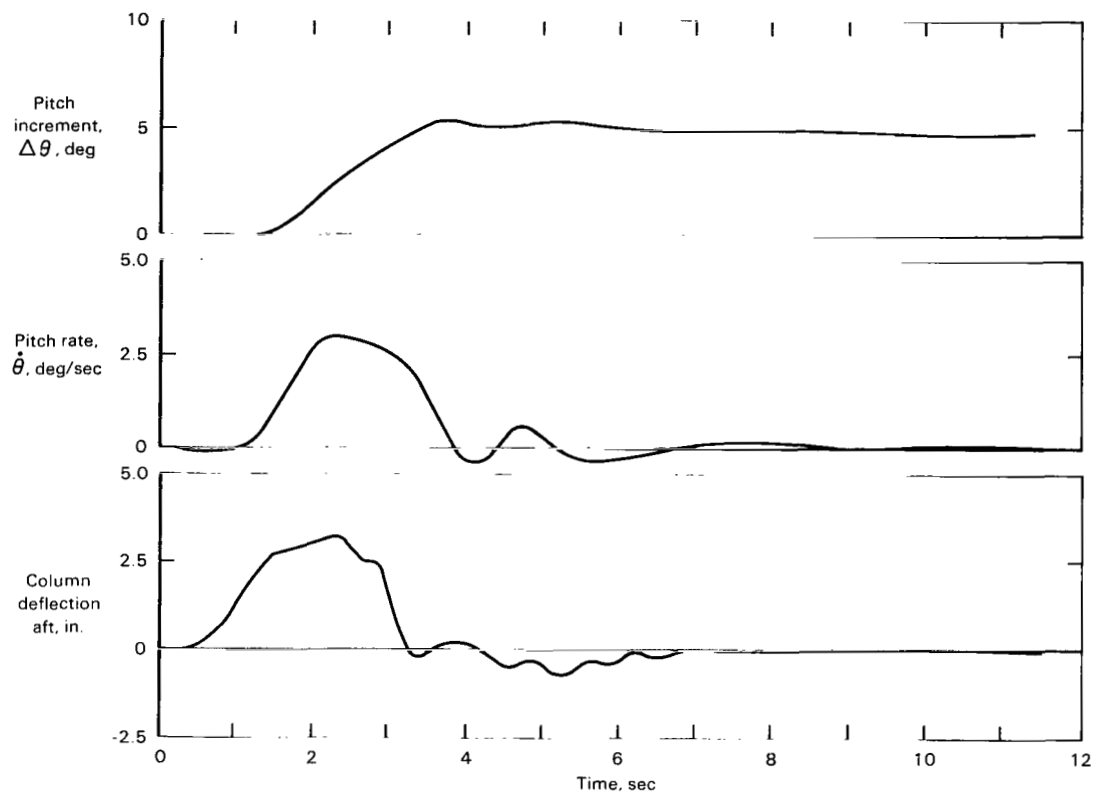


Figure 48.- Pitch attitude change of  $5^\circ$  with SAS on, DLC on,  $V = 130$  knots, and  $W = 173,000$  lb.

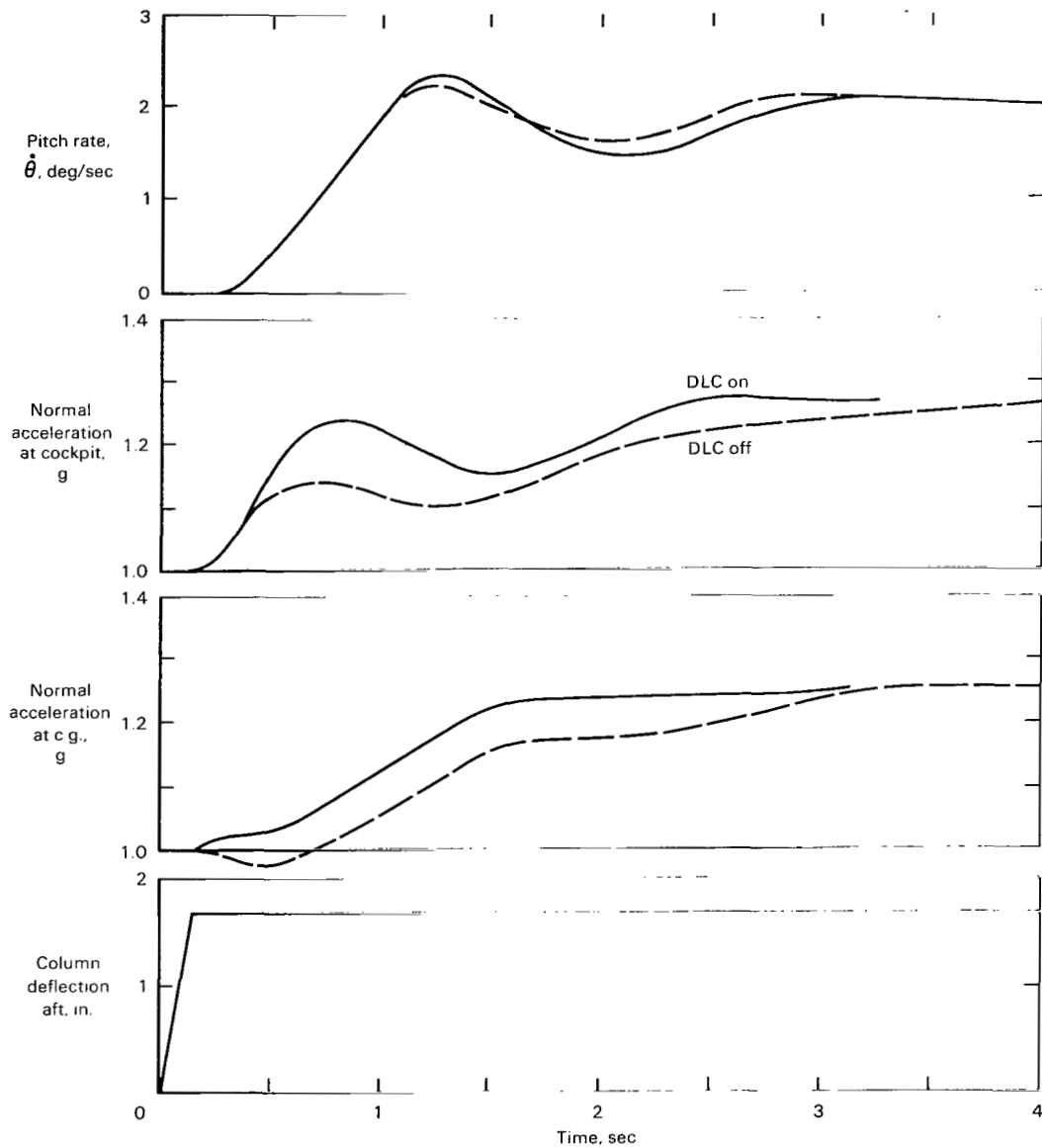


Figure 49.- Pitch response to step column input with and without direct lift control; SAS on, autothrottle on, V = 120 knots, and W = 175,000 lb.

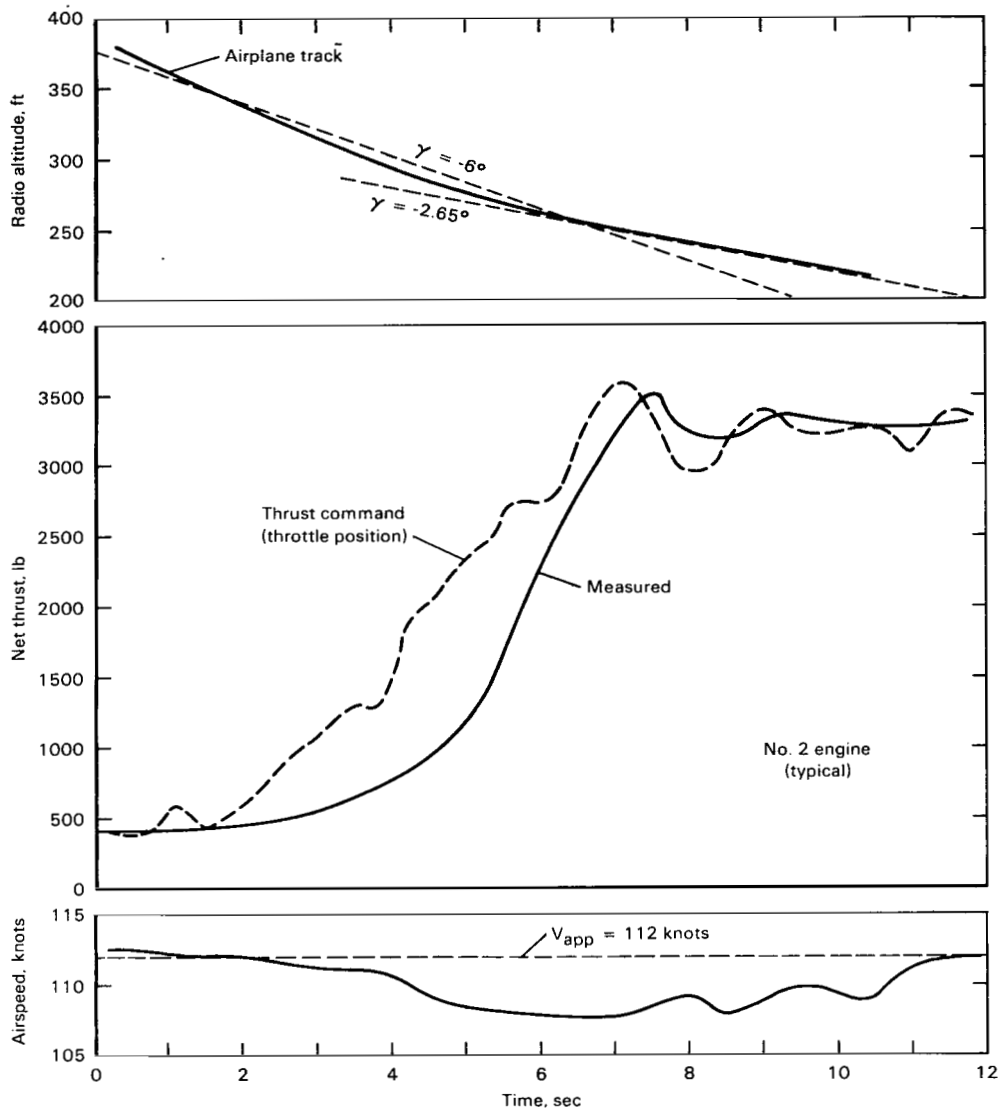


Figure 50.- Time history of transition on two-segment landing approach.

FIRST CLASS MAIL



POSTAGE AND FEES PAID  
NATIONAL AERONAUTICS AND  
SPACE ADMINISTRATION

Section 158  
Not Return

*"The aeronautical and space activities of the United States shall be conducted so as to contribute . . . to the expansion of human knowledge of phenomena in the atmosphere and space. The Administration shall provide for the widest practicable and appropriate dissemination of information concerning its activities and the results thereof."*

— NATIONAL AERONAUTICS AND SPACE ACT OF 1958

## NASA SCIENTIFIC AND TECHNICAL PUBLICATIONS

**TECHNICAL REPORTS:** Scientific and technical information considered important, complete, and a lasting contribution to existing knowledge.

**TECHNICAL NOTES:** Information less broad in scope but nevertheless of importance as a contribution to existing knowledge.

**TECHNICAL MEMORANDUMS:** Information receiving limited distribution because of preliminary data, security classification, or other reasons.

**CONTRACTOR REPORTS:** Scientific and technical information generated under a NASA contract or grant and considered an important contribution to existing knowledge.

**TECHNICAL TRANSLATIONS:** Information published in a foreign language considered to merit NASA distribution in English.

**SPECIAL PUBLICATIONS:** Information derived from or of value to NASA activities. Publications include conference proceedings, monographs, data compilations, handbooks, sourcebooks, and special bibliographies.

**TECHNOLOGY UTILIZATION PUBLICATIONS:** Information on technology used by NASA that may be of particular interest in commercial and other non-aerospace applications. Publications include Tech Briefs, Technology Utilization Reports and Technology Surveys.

*Details on the availability of these publications may be obtained from:*

SCIENTIFIC AND TECHNICAL INFORMATION DIVISION  
NATIONAL AERONAUTICS AND SPACE ADMINISTRATION  
Washington, D.C. 20546